

Bonded FRP/steel deck-to-girder connections

Renovation of movable bridges

J.U. de Jong

Technische Universiteit Delft

Bonded FRP/steel deck-to-girder connections

Renovation of movable bridges

by

J.U. de Jong

to obtain the degree of Master of Science
at the Delft University of Technology,
to be defended publicly on Friday December 14, 2018 at 11:30 AM.

Thesis committee: Prof. dr. ir. M. Veljković, TU Delft
Dr. M. Pavlović, TU Delft
ing. M. Zewald, Iv-Infra
Dr. S. Teixeira De Freitas, TU Delft

An electronic version of this thesis is available at <http://repository.tudelft.nl/>.



Iv-Infra

Preface

The work presented in this thesis focuses on stress analysis of adhesively bonded FRP/steel deck-to-girder connections and its strength performance. The project was carried out at the Faculty of Civil Engineering and Geosciences, Division of Structural Engineering, Steel and Composite Structures, Delft University of Technology.

In the first place, I would like to express my sincere gratitude to my university supervisor, Dr. Marko Pavlović for guiding and helping me throughout this thesis. I would like to express my appreciation to Merlijn Zewald, my company supervisor, for the time and energy, that he dedicated to reviewing my report, and guidance throughout this thesis. I would like to show gratitude to my thesis committee, to Prof. dr. Milan Veljković and Dr. Sofia Teixeira De Freitas for their professional guidance and critical view, helping me to improve the quality of the work. I also owe gratitude to all of the employees of the Steel and Movable Structures department of Iv-Infra who were always open to my questions.

*J.U. de Jong
Delft, December 2018*

Summary

Many movable bridges, built in the 1950's and 1960's, reach their end of service life or do not meet future traffic demands. Renovation of those bridge, if possible, is preferred over newly built from an economical point of view. Fibre-reinforced polymer (FRP) decks prove to be excellent for retrofitting bridge decks compared to traditional decks, mainly due to its high strength-to-weight ratio. Lightweight bridge decks are advantageous in movable bridges considering the savings on foundation, counterweights and mechanical equipment, not to mention, reduced transportation costs, installation time and traffic hindrance during execution.

Connecting FRP decks to the steel girders can either be done mechanically (bolts), chemically (bonded) or in a hybrid fashion. Adhesively bonded connections do not require drilling in the FRP deck, thereby increasing its durability, have a more uniform stress distribution and fabrication costs are lower compared to bolted connections. Complex stress states and strength prediction of a bonded joints are yet not fully understood, therefore rarely being applied in primary load bearing structures like bridges.

This thesis focuses on the stress analysis and strength prediction of adhesively bonded connection between FRP decks and steel girders. An existing bridge, representative for renovation projects, is considered as case study. Its former bridge deck is replaced by a FRP deck and adhesively bonded to the steel girders. Structural analysis of the bridge deck performed with a global and local numerical model, focuses on the stress states in the bonded deck-to-girder connections. Traffic and thermal loads are the governing load cases, which show the largest stress concentrations. Peak stress levels are obtained along the edges and ends of the bonded connection between the FRP deck and secondary girders.

Comparison of results from the global and local model showed significant difference in stress levels and was further investigated. Stress concentration factors are determined to relate the (peak) stresses from the global and local model for different adhesive thickness and elastic modulus. Stress results from the global model are tweaked with the stress concentration factors and compared with strength values from literature. It can be concluded that bonded FRP/steel deck-to-girder connections are critical details in movable bridges.

Contents

Summary	v
1 Introduction	1
1.1 Project motivation	1
1.2 Problem statement	1
1.3 Aim and objectives	2
1.4 Methodology	2
1.5 Limitations	2
1.6 Outline	2
2 State-of-the-art	3
2.1 Composite FRP/steel girders	3
2.2 Adhesively bonded FRP/steel connections	4
2.2.1 Stress analysis	4
2.2.2 Strength performance	5
2.2.3 Thickness effect	6
2.2.4 Fatigue strength	6
2.2.5 Environmental effects	7
2.2.6 Surface pretreatment	8
2.3 Summary	8
3 Case study	9
3.1 Background	9
3.2 Structural design	9
3.3 Renovation project	10
3.4 Design proposal	10
3.4.1 Deck type	10
3.4.2 Geometry	12
3.4.3 Stiffness properties	12
3.4.4 Thermal properties	13
3.4.5 Adhesive properties	13
3.5 Considered loads	13
3.5.1 Permanent loads	13
3.5.2 Traffic load model 1	13
3.5.3 Load model 2	14
3.5.4 Fatigue load model 4b	14
3.5.5 Thermal loads	15
3.6 Summary	16
4 Numerical models and methods	17
4.1 Global model	17
4.1.1 Boundary conditions	18
4.1.2 Element types	18
4.1.3 Orthotropic stiffness GFRP	18
4.1.4 Deck-to-girder connections	18
4.1.5 Stress state bonded deck-to-girder connection	18
4.1.6 Limitations	19

4.2	Local model	19
4.2.1	Dimensions	19
4.2.2	Boundary conditions	19
4.2.3	Element types	20
4.2.4	Modelling GFRP laminates.	21
4.2.5	Modelling adhesive layer.	21
4.2.6	Stress state bonded deck-to-girder connection	21
4.3	Validation methods	21
4.4	Summary	22
5	Structural analysis	23
5.1	Composite action	23
5.2	Bonded deck-to-girder connections	23
5.3	Permanent loads	24
5.3.1	Opening/closing	24
5.4	Traffic loads	26
5.4.1	Global analysis	26
5.4.2	Local analysis.	27
5.4.3	Fatigue analysis	30
5.4.4	Effect of main girder	31
5.5	Thermal loads	33
5.5.1	Global analysis	34
5.5.2	Local analysis.	34
5.5.3	Thermal cycles	36
5.5.4	Effect of main girder	37
5.5.5	Deformation.	37
5.6	Conclusions.	38
6	Comparison of results	39
6.1	Deck-to-secondary girder	39
6.2	Deck-to-main girder	41
6.3	Conclusions.	42
7	Parametric study	43
7.1	Shear stiffness	43
7.2	Effect of adhesive thickness	43
7.3	Effect of adhesive elastic modulus.	44
7.4	Extreme cases	45
7.5	Parametric relations	46
7.6	Stress concentration factors	47
7.7	Composite action	50
7.8	Conclusions.	51
8	Strength performance	53
8.1	Required strength	53
8.2	Strength prediction	54
8.3	Recommendation for experimental program	55
8.4	Conclusions.	55
9	Conclusions and recommendations	57
9.1	Main conclusions	57
9.2	Recommendations	58
A	Figures	59
	Bibliography	67

Introduction

1.1. Project motivation

Many movable bridges, built in the 1950's and 1960's, reach their end of service life or do not meet future traffic demands. They typically consists of a steel structure supporting timber bridge decks. Retrofitting those bridges, if possible, is preferred over newly built from an economical point of view.

Usually, the steel structure is still in adequate condition for future service life. Its originally timber deck however, has already been replaced or will be replaced in the near future (Fig. 1.1). Main purpose of the timber deck is to transfer external loads from the deck to the steel girders. Composite action, i.e. the degree in which the deck and girder act together, is mostly not taken into account in the original design. The steel structure has sufficient capacity to bear loads without composite action.



Figure 1.1: Renovation bridge deck of Marebrug, Leiden

Fibre-reinforced polymer (FRP) bridge decks have become a good alternative to traditional timber and steel bridge decks, mainly due to its high strength-to-weight ratio. Lightweight bridge decks are advantageous in movable bridges considering the savings on foundation, counterweights and mechanical equipment, not to mention, reduced transportation costs, installation time and traffic hindrance during execution. Lastly, its freedom in design, good corrosion resistance, high durability and low maintenance make FRP decks excellent for retrofitting movable bridge decks.

Connecting FRP decks to the steel structure can either be done mechanically (e.g. bolts), chemically (e.g. adhesive bonding) or in a hybrid fashion. Bolted connections require drilling holes in the FRP deck, causing local stress concentrations, reduced durability of the deck and possible tolerance problems during execution. Adhesively bonded connections on the other hand, leave the deck unaffected, having a more uniform stress distribution and lower fabrication costs. Main two disadvantages for adhesively bonded connections are the required extensive surface preparation and sensitivity to environmental effects.

1.2. Problem statement

Design of structural bonded joints have been a subject of interest for many years. Stress state and strength prediction of a bonded joints are yet not fully understood, therefore rarely being applied in primary load bearing structures like bridges. Adhesively bonded joints do however provide relative high resistance when loaded in shear. More experimental research on adhesively bonded (FRP/steel) joints suitable for civil engineering structures is necessary to ultimately apply them in structural design.

Failure of bonded deck-to-girder connections during opening of the bridge would be an catastrophic event and should be prevented in any case. In closed position however, vertical loads could still be

transferred from the deck to the girders when the bonded connection has failed. Crack initiation in the bonded connection occurs when material strengths are exceeded in either the adhesive, adherend or at the interface between the former two. Cyclic (traffic) loads lead to crack propagation, ultimately to failure of the entire connection. Crack initiation is most likely to occur at locations with stress concentrations. Insight in stress distributions and stress levels in bonded FRP/steel deck-to-girder connections are therefore crucial for design.

1.3. Aim and objectives

The overall aim of this thesis is to determine whether an adhesively bonded connection between FRP bridge decks and steel girders has appropriate strength performance for renovation of movable bridges.

With this aim, the following objectives and tasks are defined and covered in this thesis:

1. To review the state-of-the-art on stress analysis and strength performance of bonded (FRP/steel) connections.
2. To design a FRP deck and bonded connection suitable for renovation of a movable bridge.
3. To obtain a reliable method to determine the stress state in a bonded FRP/steel connection.
4. To identify governing load cases for movable FRP/steel bridges with bonded deck-to-girder connections.
5. To find critical locations, i.e. stress concentrations, in the bonded deck-to-girder connection.
6. To investigate the effects of different adhesive thickness and elastic modulus on the structural behaviour of bonded FRP/steel deck-to-girder connections.
7. To determine which reference levels of stress need to be used to compare the stresses from the analysis, i.e. strength of the bonded connection.
8. To determine the utilisation ratio of the bonded FRP/steel deck-to-girder connection under governing design loads.

1.4. Methodology

Stress levels in the bonded FRP/steel deck-to-girder connections from structural analysis of a case study bridge are compared with strength values from literature.

1.5. Limitations

The following limitations apply in this work:

- Linear static analysis in Finite Element Analysis (FEA) software packages.
- Stress based method for strength prediction of the bonded connections.

1.6. Outline

This thesis starts with a literature review on the most recent developments regarding bonded (FRP/steel) joints. A case study of an existing movable bridge, used for stress analysis of the bonded FRP/steel deck-to-girder connections, will be introduced in Chapter 3. Subsequently, Chapter 4 reviews the numerical models and methods considered to determine the stress states in the bonded deck-to-girder connections. Chapter 5 presents the structural analysis results of the case study bridge. A comparison is made between stress results from the numerical models in Chapter 6. Chapter 7 deals with the effects of adhesive thickness and elastic modulus on the stress states in the bonded FRP/steel deck-to-girder connections. In Chapter 9, the main conclusions of this work are drawn and suggestions made for future work.

2

State-of-the-art

Many reviews have been made on the state-of-the-art on FRP decks and is therefore not included in this work. The author recommends reading the state-of-the-art reviews on FRP decks by Csillag [5], Gürtler [8] and Schollmayer [14]. Parts of other work have been used to establish this chapter and is referenced to.

2.1. Composite FRP/steel girders

It was shown by Gürtler [8] and Schollmayer [14], that an adhesively bonded connection between FRP bridge decks and steel girders is a feasible and reliable connection method. They proved the existence of a good load-bearing behaviour under static and fatigue loads, where the bonded connection is loaded with uplift forces and moments acting in the bridge deck (Schollmayer, [14]), in addition to the shear in the bonded connection due to composite action, which was investigated by Gürtler [8].

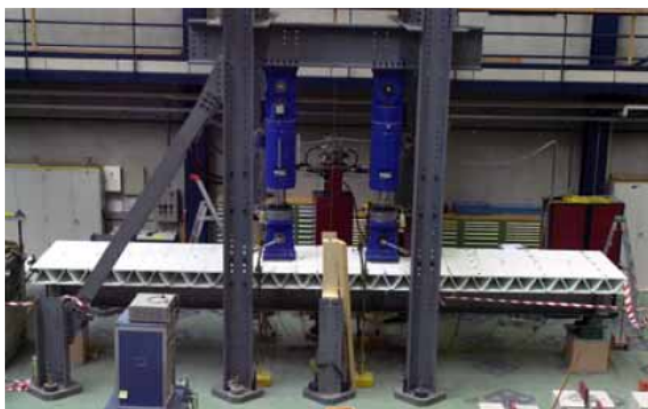


Figure 2.1: Composite FRP/steel girder with adhesively bonded connection [8]

”The bonded connection provided full composite action which increases stiffness and the resistance and reduces deflections of the composite girders considerably, even for high adhesive thicknesses and soft adhesives. Possible deck contribution depends mainly on the in-plane deck stiffness in the longitudinal direction of the bridge axis.” [8]. ”In transverse direction, the bonded connections act as a simple support for the FRP bridge deck, if a certain adhesive thickness is provided, since the rotation mainly results from the adhesive layer.” [14]. ”A ductile failure mode could be achieved for the composite girder loaded in bending due to deck compression failure during yielding of the steel girder”. [8].

There is currently no movable composite FRP/steel bridge known to the author with solely adhesively bonded deck-to-girder connections. The Friedberg bridge in Germany does however have bonded FRP/steel deck-to-girder connections but is not movable.

Another method to connect FRP decks and steel girders is by bolted connections. They can provide excellent shear resistance, ductile behaviour up to failure and have the ability to demount the composite FRP/steel girders. Structural behaviour of bolted connections in composite FRP/steel girders is extensively investigated by Csillag [5] and therefore not further discussed in this work.

2.2. Adhesively bonded FRP/steel connections

2.2.1. Stress analysis

Shear stress distribution in the adhesive layer of bonded joints are among load conditions highly dependent on stiffness of the adherends. Bonded joints with rigid adherends show constant shear stress along the overlap length as they do not deform under loading (Fig. 2.2a). Bonded joints with elastic adherends however, show differential shear strain in the adhesive. Shear stress concentrations occur at the ends of the bonded connections due to relative large deformation of the adherend compared to the mid-section of the overlap length (Fig. 2.2b). Dissimilar adherend thickness and elastic modulus, i.e. stiffness, results in different peak shear stress levels. Not only shear stresses are present in bonded lap-shear joints. Also tensile or peeling stresses occur due to load eccentricity, which results in bending of the adherends and affect the bond strength.

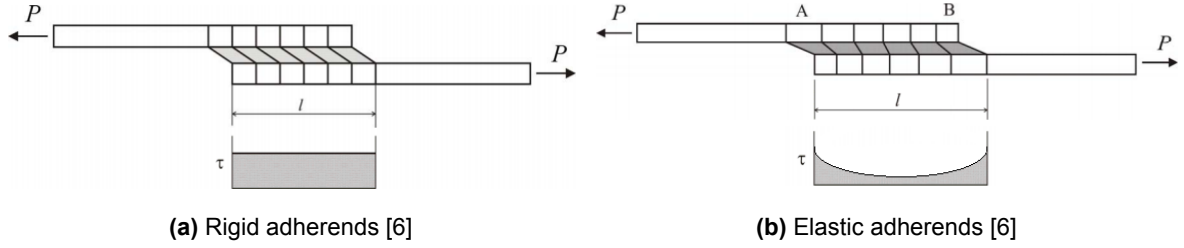


Figure 2.2: Adhesive shear stress distribution in single-lap joint

Researchers have developed analytical and numerical models to determine the stress distributions in the adhesive layer of bonded joints for many decades. Stress predictions in adhesively bonded single-lap joints from Volkersen (1938) and Goland and Reissner (1944) can be considered as the classic and first successful analyses. Volkersen (1938) used an one-dimensional bar model in which the adherends can only deform in longitudinal direction and uniformly through thickness. Effects of adherend bending is neglected, therefore load eccentricity effects are not considered. The adhesive shear stress distribution (τ) according to the model of Volkersen (1839) is given by

$$\tau = \frac{P}{bl} \frac{w}{2} \frac{\cosh wX}{\sinh w/2} + \left(\frac{\psi - 1}{\psi + 1} \right) \frac{w}{2} \frac{\sinh wX}{\cosh w/2} \quad (2.1)$$

where P is the applied load, b the joint width, and l the overlap,

$$w^2 = (1 + \psi) \phi$$

$$\psi = t_t/t_b$$

$$\phi = \frac{G_a l^2}{E t_t t_a}$$

$$X = \frac{x}{l}, -\frac{1}{2} \leq X \leq \frac{1}{2}$$

where t_t the top adherend thickness, t_b the bottom adherend thickness, E the adherend modulus, G_a the adhesive shear modulus, and t_a the adhesive thickness. The origin of the longitudinal co-ordinate x is the middle of the overlap [7].

Goland and Reissner (1944) were the first to developed a theory that included the effect of the discontinuity in the load path. They considered a beam model for predicting deflections in the joint and, subsequently, shear and peel stresses in the bond layer. The analysis is limited to joints bonded between identical adherends and thicknesses, because the derivation of the edge bending moment assumes both adherends to have identical material and thicknesses [6].

Silva et al. [6] made a summary of both linear and nonlinear two-dimensional analytical models available in literature, seen in Table 2.3. It can be concluded that most analytical solutions for adhesively bonded joints are two-dimensional and limited to simple geometries. For three-dimensional, complex

geometries, including composite materials, under multi-axial loading conditions numerical methods like FEA are recommended.

	Material linearity		Adherends				Adhesive stresses			Solution			
	Adhesive		Adherend		Isotropic	Composite	Similar	Dissimilar	σ_x	σ_y	τ_{xy}	Closed-form	Numerical
	Linear	Nonlinear	Linear	Nonlinear									
Volkersen [1]	X		X		X		X	X		X	X		
Goland and Reissner [2]	X		X		X		X		X	X	X		
Wah [21]	X		X		X	X	X			X	X		X
Hart-Smith [13,50]	X	X	X		X		X		X	X	X		
Pirvics [22]	X		X		X		X	X	X	X	X		X
Grimes and Greimann [58]	X	X	X	X	X	X	X	X	X	X	X		X
Renton and Vinson [23-24]	X		X		X	X	X	X	X	X	X		
Srinivas [25]	X		X		X	X	X	X	X	X	X		
Allman [18]	X		X		X	X	X		X	X	X		
Ojalvo and Eidinoff [16]	X		X		X		X	X	X	X	X		
Delale et al. [32]	X	X	X		X	X	X	X	X	X	X		
Bigwood and Crocombe [12]	X		X		X		X	X	X	X	X		X
Bigwood and Crocombe [51]	X	X	X		X		X	X	X	X	X		
Cheng et al. [26]	X		X		X		X	X	X	X	X		X
Crocombe and Bigwood [59]	X	X	X	X	X		X	X	X	X	X		X
Adams and Mallick [31]	X	X	X		X	X	X	X	X	X	X		
Tong [54]	X	X	X		X		X	X	X	X	X		
Yang and Pang [27]	X		X		X	X	X	X	X	X	X		X
Frostig et al. [48]	X		X		X	X	X	X	X	X	X		X
Sawa et al. [28]	X		X		X		X	X	X	X	X		X
Mortensen and Thomsen [33]	X	X	X		X	X	X	X	X	X	X		
Adams et al. [61]	X	X	X	X	X		X					X	
Wang et al. [60]	X	X	X	X	X		X	X	X	X	X		X
Smeltzer and Klang [56]	X	X	X	X	X	X	X	X	X	X	X		X

Figure 2.3: Summary of both linear and nonlinear two-dimensional analytical models available in the literature [6]

2.2.2. Strength performance

Strength of bonded FRP/steel joints is governed by one or combination of failure modes: (1) cohesive failure, meaning failure within the adhesive layer, (2) adhesive failure, meaning failure at the FRP/adhesive or steel/adhesive interfaces, and (3) substrate failure, meaning failure of the FRP or steel adherend. Substrate failure in bonded FRP/steel joints will most likely be delamination of the FRP material, which is characterised by interlaminar shear strength of the FRP material. The failure modes, shown in Figure 2.4, are depended on material strengths, geometry and surface pretreatment of the bonded joint. In addition, environmental ageing can affect the constituents of the bonded joints differently, which can alter the failure mode of the bonded joints [9]. Heshmati [9] has accurately predicted the static lap shear strength of bonded connections using Cohesive zone modelling. This numerical method circumvents stress singularities and is based on cohesive laws. It requires predefined failure paths in the numerical model to account for different failure modes. Cohesive laws can be determined from fracture toughness tests for mode 1 (e.g. DCB) and mode 2 (e.g. ENF).

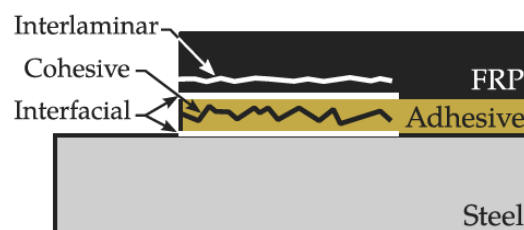


Figure 2.4: Possible failure modes in bonded FRP/steel joints [9]

Table 2.1: Experimental strength results of bonded FRP/steel joints. *Tensile-shear loading device.

PhD thesis	Test setup	Shear strength	Tensile strength	Adhesive thickness
Gürtler (2004), [8]	T-beam	2 MPa	-	6 mm
Schollmayer (2009), [14]	Composite girder	-	0.8 MPa	8 mm
Heshmati (2017), [9]	DLJ	5.6 MPa	-	6 mm
Jiang (2013), [10]	TSD*	9.6 MPa	1.5 MPa	6 mm

Table 2.1 shows experimental static strength results of bonded FRP/steel joints from different PhD studies relevant for civil engineering structures, i.e. adhesive thicknesses in the range of 5 to 20 mm. Strength values are calculated by dividing ultimate loads at failure by the bonded surface area, thus averaged. Note that each study considered different experimental setups, i.e. materials, geometry, surface pretreatment and loading conditions. These strength values can therefore not be compared and are indicatively. See corresponding theses for more details.

2.2.3. Thickness effect

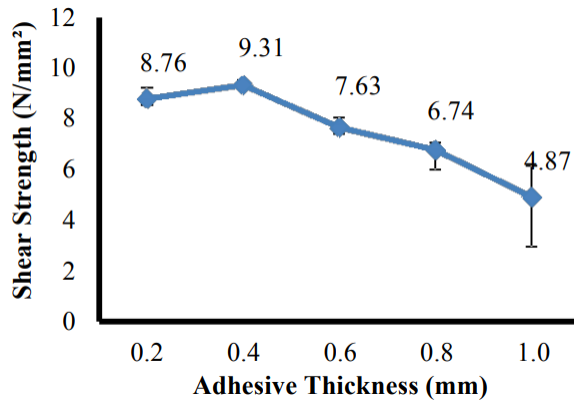


Figure 2.5: Relationship between lap shear strength and adhesive thickness [13]

Multiple studies are performed on the adhesive thickness effect on the strength of a bonded joint considering analytical and numerical models, and experimental results. However, the relationship between the strength and adhesive thickness is still not well understood. Diharjo et al. [13] performed single-lap joint (SLJ) tests using epoxy adhesive and aluminium adherends for different adhesive thicknesses up to 1 mm. Highest lap shear strength was found for 0.4 mm. There was an almost linear decreasing trend seen for adhesive thicknesses between 0.6 and 1 mm (Fig. 2.5). This thickness effect is explained by the fact that increasing adhesive thickness means increasing volume of adhesive material and therefore also the amount of material defects like voids and microcracks, which are locations for crack initiation.

2.2.4. Fatigue strength

Gürtler [8] and Schollmayer [14] concluded from their fatigue tests that there was no visible damage in the bonded deck-to-girder connection, nor stiffness and/or strength decrease in the composite GFRP/steel girders after 10 million cycles. These stress ranges were determined according to fatigue loads from Eurocode 1 and their reference bridges. Unfortunately, only one or two fatigue tests were performed at roughly 10% of the ultimate load at failure.

No information is currently known to the author on the fatigue performance of bonded FRP/steel joints. There is however experimental data on the fatigue performance of bonded FRP/FRP double-lap shear joints (DLJ) from Keller [11], Zhang [16], Khabbaz [11] and Vassiloupolos [15]. Geometry of the DLJ specimen from the PhD thesis of Khabbaz is presented in Figure 2.6.

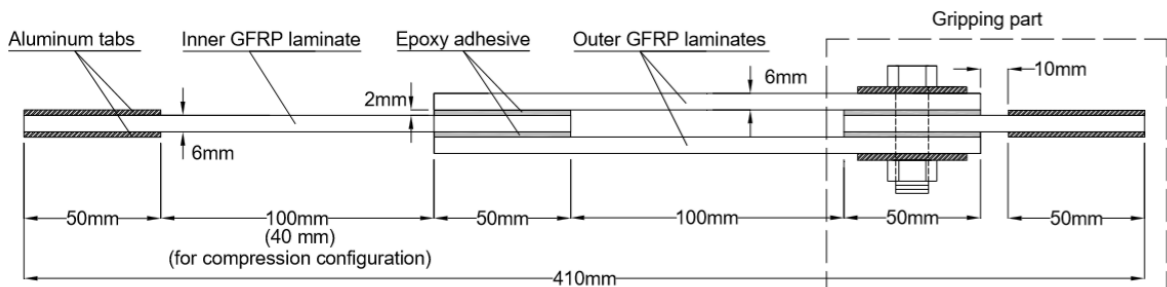
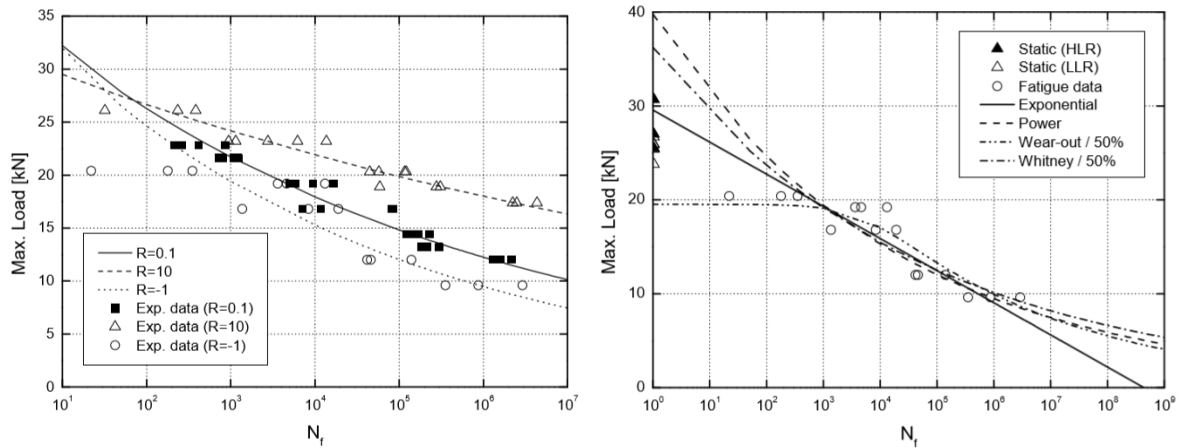


Figure 2.6: DLJ geometry, PhD Khabbaz [12]

Experimental results on fatigue strength of adhesively bonded GFRP double-lap joints showed the high dependency on loading parameters such as the mean load level, loading sequence and load transition [12]. Dependency on the mean load level is seen in Figure 2.7a. Lower fatigue strength is obtained for $R=-1$, marked with circles. This corresponds to a reversed loading type. R-ratio is defined by $R = F_{min}/F_{max}$.



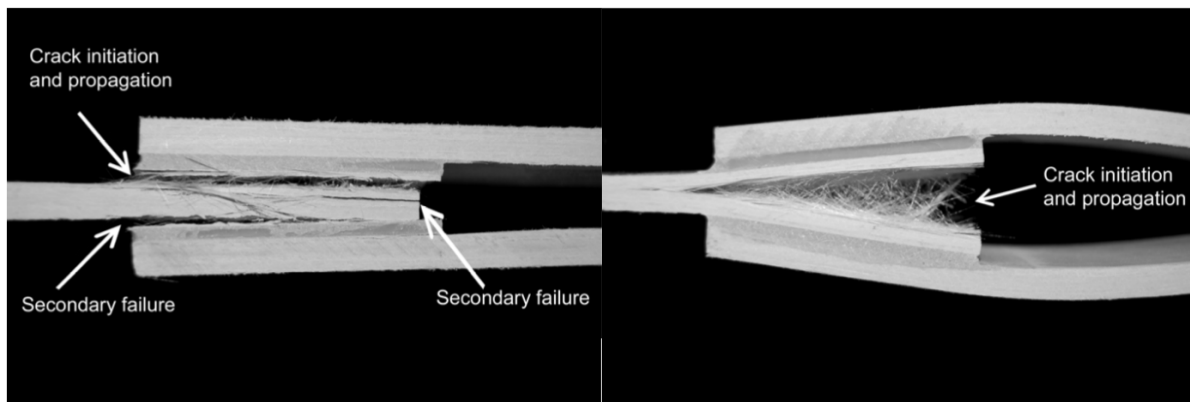
(a) Comparison of load-life data at different R-ratios [12] (b) Comparison of derived S-N curves with experimental data for R=-1 (excluding static data) [12].

Figure 2.7: Fatigue strength bonded GFRP double-lap joint [12]

The fatigue failure modes were found to be similar to the quasi-static failure modes [12]. Evident difference in failure mode under tension and compression loading is seen in Figure 2.8.

Keller [11] and Khabbaz [12] found a slope of 1:10 for the S-N curve related to the fatigue strength of the GFRP DLJ considering the power law model in log-log scale load-life diagram.

Additionally, static strength (28 kN), marked in Figure 2.7b with triangles, is lower than the fatigue strength at $N=1$ (40 kN), dashed line (power). This is caused by the difference in failure mechanism under static and fatigue loading.



(a) DLJ failure mode under tension loading

(b) DLJ failure mode under compression loading

Figure 2.8: DLJ failure modes [12]

2.2.5. Environmental effects

”Mechanical properties of adhesive and FRP materials are affected by moisture content and temperature levels. This could lead to altering failure modes of bonded FRP/steel joints,” [9]. Heshmati [9] and Jiang [10] found up to 40 % strength and 20 % stiffness decrease of bonded FRP/steel joints under hygrothermal ageing. Jiang [10] stated that for tensile/shear loading conditions, the environmental degradation is not that obvious, which is due to the post curing mechanism, improving the bonding quality between the FRP and adhesive. Please note that these environmental conditions were severe, i.e. fully immersed at 40 degree Celsius for a long period of time (months). See their theses for more details.

2.2.6. Surface pretreatment

Jiang [10] concluded that surface pretreatment cannot improve the stiffness of an adhesively bonded FRP/steel joint. However, the shear strength, for the surface pretreatment methods using sandpaper and sand blasting increased more than twice compared to specimens pretreated only using acetone. Tensile strengths increased only by 9.5 % for using sandpaper and sand blasting.

2.3. Summary

- Adhesively bonded connections between FRP decks and steel girders is found to be a feasible and reliable method to build composite FRP/steel girders.
- Analytical solutions for 2D stress states in adhesively bonded joints are limited to simple geometries. Numerical methods are recommended for complex geometries, material properties and loading conditions
- Fatigue strengths of bonded GFRP DLJ's show high dependency on loading parameters such as mean load level. Its S-N curve slope is approximately 1:10 for R=-1.
- Mechanical properties of adhesives and GFRP adherents of bonded connections are affected by moisture content and temperature levels. Strength and stiffness of bonded FRP/steel joints can decrease up to 40 and 20 % respectively.
- Quality of surface pretreatment for bonded FRP/steel connections mainly affect its strength. Sandblasting is considered as preferable surface pretreatment method.

3

Case study

This chapter introduces an actual renovation project of a movable bridge that is considered as case study in this thesis. It is assumed to be a representative movable bridge for future renovation projects in which its current deck will be replaced by a GFRP deck and connected by a bonded connection to the steel structure. Focus in this chapter will be on the bridge deck design and design loads considered in this case study.

3.1. Background

The Kwekersbrug is an existing bascule bridge located at a local road in the municipality of Amersfoort, The Netherlands. Its built in 1956 and spanning over the river the Eem. According to the statement of the municipality, traffic loading mainly consist of line busses with a frequency of 40 per hour and local cars. Traffic signs that prohibit heavy traffic passing the bridge are absent, therefore the heavy traffic loading models from the Eurocode should be considered.

Its originally timber deck has been replaced for a steel deck in 1971 and again in 2017. Former steel deck from 1971 showed unacceptable fatigue damage at welds in the deck and needed replacement. The steel structure of the bridge deck supporting the deck was however in good condition and could be re-used in future service life. Again a orthotropic steel deck is installed in 2017. Application of a GFRP deck would have been a excellent alternative compared to a steel orthotropic deck mainly due to the high strength-to-weight ratio, fatigue and corrosion resistance.



Figure 3.1: Kwekersbrug, Amersfoort [2]

3.2. Structural design

Main structural components of the bridge deck are four main girders, five cross beams, 14 secondary girders, two counterweights and its deck supported by concrete abutments. Figure 3.2a shows the longitudinal section of the bridge in one of the original drawings from 1956. Counterweights are seen at the left, front of the bridge deck on the right. The bridge deck spans roughly 9m over the river. Also the five cross beams with centre-to-centre distance of 2.15 m can be seen in the figure.

Dimensions of the main bridge deck for road traffic are 9.7 m width by 9.3 m length. A walkway for pedestrians is located next to the outer main girders (Fig. 3.2b). Only the main bridge deck for heavy traffic is considered in the structural analysis. Furthermore, the cross beams are welded to the webs of the main girders. Cross beams between the middle main girder have a different profile compared to the outer main girders. Centre-to-centre distance of the main girders are 3 and 3.35 m. Secondary girders,

INP220 profiles, are welded on top of the cross beams spanning in traffic direction. Top flanges of both main and secondary girders are in the same plane. The deck is connected to all those top flanges. Dimensions of the bridge deck considered for structural analysis is shown in Figure 3.3.

Table 3.1 contains the dimensions of the steel profiles in the bridge leaf. Where h is the height, t_w the web thickness, b_f the flange width and t_f the flange thickness. All profiles are symmetrical I-sections.

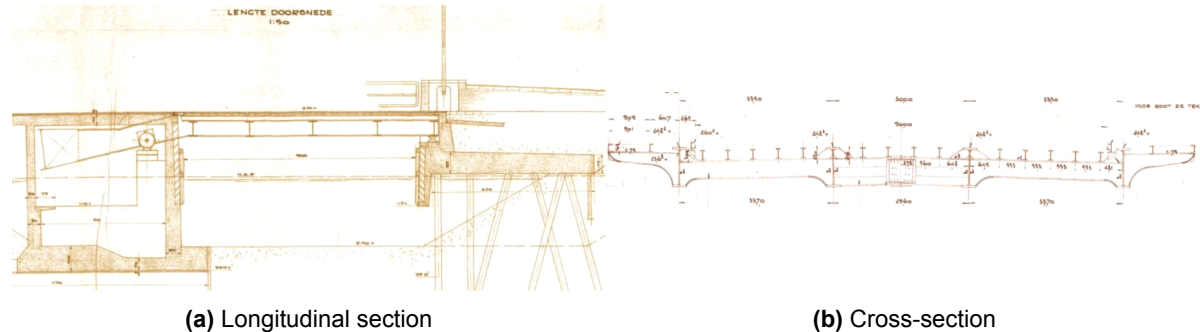


Figure 3.2: Technical drawings of the Kwekersbrug [ref?]

Table 3.1: Steel profiles

	h [mm]	t_w [mm]	b_f [mm]	t_f [mm]
Main girder	850	19	300	36
Cross beams	420, 585	10	150	15
Secondary girder	220	8.1	98	12.2

3.3. Renovation project

The following project requirements and boundary conditions are set for the renovation of the Kwekersbrug:

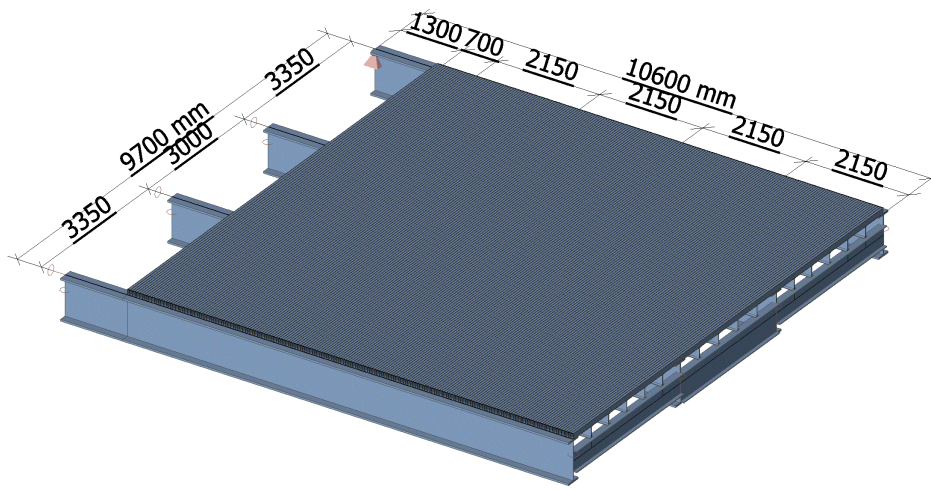
- Its original timber deck will be replaced by an FRP deck. Other structural components are in adequate condition for future service life.
- FRP deck is adhesively bonded onto the top flanges of the steel girders.
- Composite action between the FRP deck and girders is not required.
- Construction height of the deck needs to be equal tot the former bridge deck.
- Reference period of 30 years is considered for renovation.

3.4. Design proposal

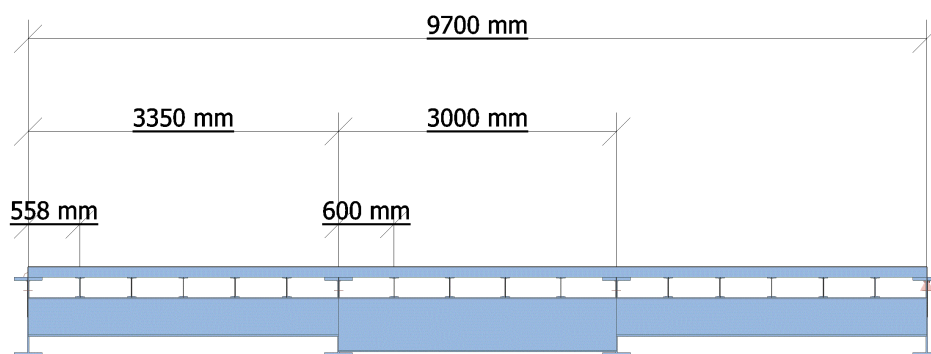
Starting point for the design of the FRP deck and adhesively bonded deck-to-girder connection is that composite action between the deck and girders is not required. Stiffness of the FRP deck, adhesive thickness and elastic modulus can be designed to lower the stresses in the bonded connection as much as possible, but still provide sufficient strength and stiffness. For preliminary design of FRP structures it is recommended to satisfy the 1.2% tensile and 1.6% shear strain limit. The deck design proposal presented in this section does satisfied these requirements.

3.4.1. Deck type

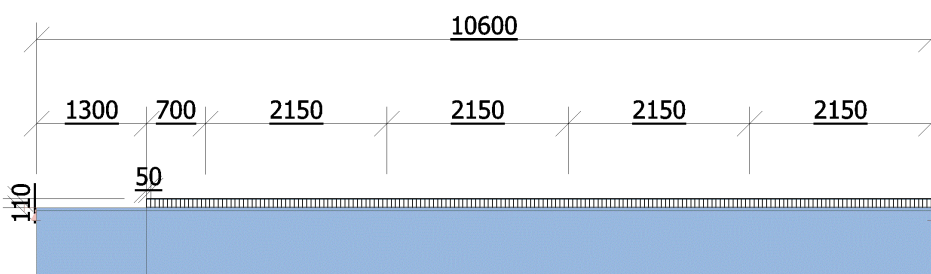
A vacuum infused panel with integrated webs made out of GFRP laminates is considered in for the design. Different types of loads on the deck require freedom in laminate design. CFRP laminates



(a) Isometric view (top)



(b) Front view



(c) Side view

Figure 3.3: Dimensions main bridge deck

are not cost effective in a FRP deck with dimensions of 9 m by 9 m, therefore GFRP laminates are considered in the deck design as they also provide sufficient stiffness.

3.4.2. Geometry

Total height of the GFRP deck and bonded connection is equal to the former deck to match the road profile. The height of the GFRP deck is 110 mm and has a wearing layer of 8 mm on top. Nominal thickness of the adhesive layer is 10 mm. The GFRP deck design is based on designs of vacuum infused GFRP panel used in reference projects. It consists of a 12 mm thick top and bottom facing, 5 mm thick vertical webs and foam cores (Fig. 3.4). Centre-to-centre distance between the webs is 50 mm. **The GFRP deck's bending and shear resistance is verified based on axial and shear strain limits of 1.2 % and 1.6 % respectively, which are recommended for preliminary design of GFRP structures. The strain limits are satisfied for the high local axle load from load model 2 positioned at mid-span between the secondary girders and centrally on it.**

3.4.3. Stiffness properties

The fibre volume in GFRP vacuum infused panels with polyester resin is commonly 50 percent. Properties of FRP laminates can be highly orthotropic, meaning different in other directions of the material, depending on the ply layup. Direction 1 is set to be in transverse direction of the bridge deck. Direction 2 is set to be in the traffic direction of the bridge. Thus, also in the direction of the main and secondary girders.

Anisotropic (stiffness) properties are considered for the top and bottom

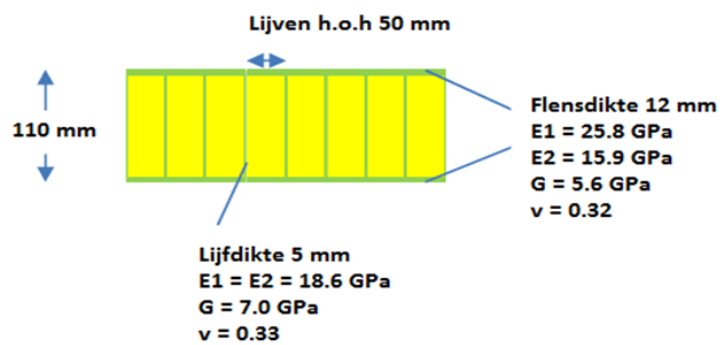


Figure 3.4: GFRP deck design

facings, as seen in Figure 3.4. The stiffest direction, E1, is in the load bearing direction of the deck, i.e. between the girders in transverse direction of the bridge deck. Lower stiffness is allowable, and even desirable, in the longitudinal direction. Composite action is not required, therefore less contribution of the deck leads to lower stresses in the deck-to-girder connection. Quasi-isotropic (stiffness) properties are considered for the vertical webs. Laminate lay-up is more uniform and therefore similar stiffness in both directions. It will also provides higher shear stiffness compared to anisotropic laminates, which is desirable for webs mainly loaded in shear. PUR foam is considered in the cores between the webs. Those are mainly useful during production of the vacuum infused panels. Elastic modulus of the foam cores is approximately 0.03GPa. It does however provide stability support for the webs. Similar symmetrical ply lay-ups, $[0^\circ 45^\circ -45^\circ 90^\circ]_s$, are considered for the GFRP facings and webs. In order to obtain the desired orthotropic stiffness the relative ply thicknesses are different. For quasi-isotropic webs (25%, 25%, 25%, 25%) and anisotropic facings (55%, 15%, 15%, 15%) respectively. Indicative stiffness values are seen in Table 3.2, in which the equivalent stiffness of the laminates are calculated according to the classical laminate theory.

Table 3.2: GFRP laminate, foam and adhesive properties

	t [mm]	E_1 [GPa]	E_2 [GPa]	G_{12} [GPa]	ν_{12}	$\alpha_1 [\cdot 10^{-6} K^{-1}]$	$\alpha_2 [\cdot 10^{-6} K^{-1}]$
UD ply	-	37.2	11.4	3.4	0.29	10.5	50.8
Facings	12	25.8	15.9	5.6	0.32	15.0	30.3
Webs	5	18.6	18.6	7.0	0.33	21.2	21.2
Foam	-	0.03	0.03	0.01	0.5	-	-
Adhesive	10	0.6	0.6	0.2	0.3	70	70

3.4.4. Thermal properties

Composite structures, i.e. consisting of different materials, can be sensitive to thermal loading. Restraint structural components and differences in expansion cause internal stresses. Steel, glass fibres, resin, foam and adhesives have their own thermal properties. Most important thermal properties are (1) coefficient of thermal expansion, α , and (2) thermal conductivity, λ . Coefficient of thermal expansion (CTE) is the amount of material change in dimension per temperature change. It is the magnitude of strain due to thermal expansion per degree Kelvin or Celsius in units of K^{-1} . The thermal conductivity is the rate of heat transfer through a material. The polymeric materials like polyester and acrylic have larger CTE's compared to glass fibres and steel. This is why unidirectional plies and also anisotropic laminates have larger CTE in transverse direction compared to the fibre direction. Conservative CTE's are considered and given in Table 3.2. Equivalent CTE's of the laminates are calculated with classical laminate theory. Thermal conductivity of steel is significantly larger compared to the GFRP laminates, foam and adhesive. This means that the heat transfer through steel is much faster and the GFRP deck acts as an insulator when exposed to (sun) radiation. Difference in thermal conductivity does affect the vertical temperature gradient over bridge deck height which is defined in the Eurocode.

3.4.5. Adhesive properties

An acrylic based adhesive is selected for this renovation project, mainly due to its high strength and low elastic modulus. Besides, its large elongation at failure, i.e. ductile behaviour, is favourable in connection when it comes to failure mechanisms of the structure. Also its high viscosity and long pot life make it easy to apply and suitable in bridges with large bonded surfaces and gaps. Table 3.3 shows the lower limits of available material properties provided by the manufacturer of the adhesive. Coefficient of thermal expansion of the adhesive is assumed to be $70 \cdot 10^{-6} K^{-1}$.

Table 3.3: Material properties of methacrylic SG230 HV, SciGrip [4]

Tensile strength	21 MPa
Tensile modulus	0.6 GPa
Shear strength	15 MPa
Maximum tensile elongation	100%

3.5. Considered loads

A selection of important permanent and variable loads for composite bridge decks are considered for structural analysis according to the Eurocode and national annexes.

3.5.1. Permanent loads

Permanent loads consist of self-weight of the steel structure, counterweights, GFRP deck and wearing layer. Density of steel is assumed to be $7850 kg/m^3$. Density of the laminates of the GFRP deck are assumed to be $1855 kg/m^3$ considering a fibre volume of 50% in the unidirectional plies. The 8mm thick wearing layer has a weight of $0.2 kN/m^2$. Self-weight of the adhesive is neglected due to the low volume and density. Gravitation acceleration of $9.81 m/s^2$ is considered.

Requirement according to the Dutch norms (NEN6785) for movable bridges is a minimum resulting support reaction at the front of the bridge deck, preventing opening of the bridge deck by wind. Counterweights are therefore slightly 'pushed', which is accounted for in the model.

10.000 cycles of opening and closing per year is considered for this case study. Reference period is 30 years.

3.5.2. Traffic load model 1

Traffic load model 1 and 2 from the Eurocode are considered as static traffic loads, see EN 1991-2 for more details. Load model 1 consists of a set of tandems and an uniformly distributed load on the corresponding notional lanes. The uniformly distributed load in the first notional is $9 kN/m^2$ and the axle loads of the corresponding tandem set are 300kN. Second lane respectively $2.5 kN/m^2$ and

200kN. Dimensions of the tandem sets are shown in Figure 3.5a. Traffic load model 1 is recommended to be used to analyse global effects.

According to NEN 6876, Dutch norm for assessment of existing structures in case of reconstruction, allows for notional lane layout which corresponds to the actual/current use of traffic lanes. That is two in this case. Remaining width of the bridge deck is used for bicycles. As mentioned earlier, on each side of the bridge deck a walkways for pedestrians is located. These are supported by steel cantilever beams welded on the outer main girders. Since they are separated by curbs of height larger than 200mm no heavy traffic can be located there. This is also reason not to consider them for the analysis of the deck-to-girder connections. Since adding them has negligible effect on the stress state in the deck-to-girder connections.

3.5.3. Load model 2

Traffic load 2 consists of a single axle load of 400kN, which can be positioned anywhere on the notional lanes. Most unfavourable location must be considered. It is recommended to be used to analyse local effects. Dimensions of the axle load is shown in Figure 3.5c

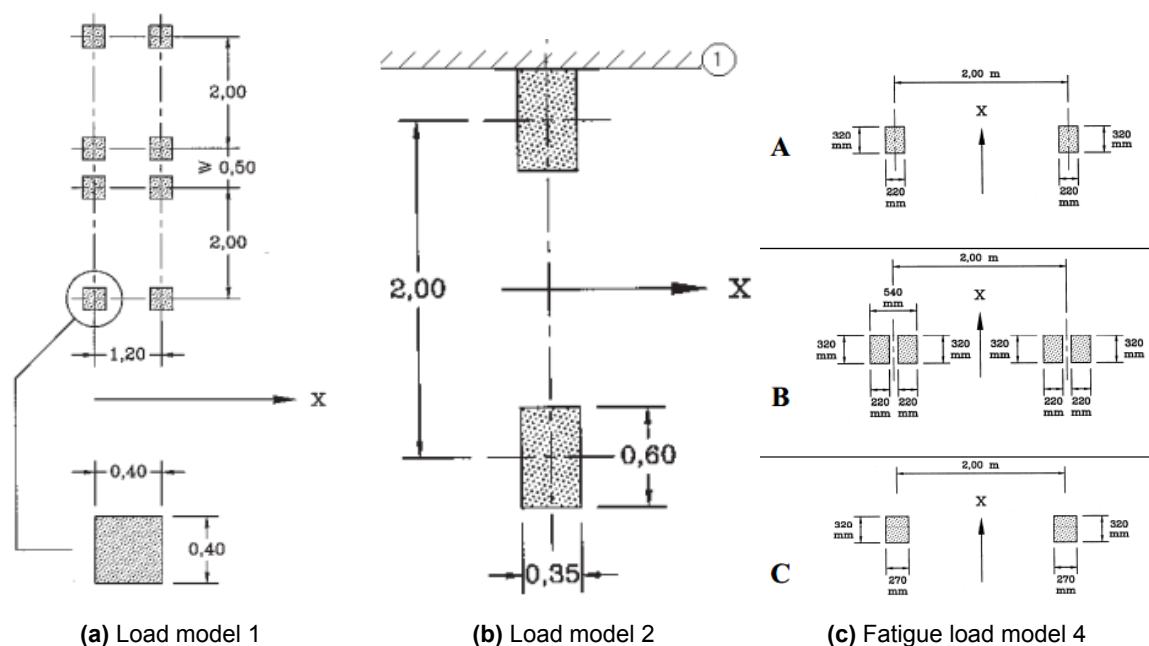









Figure 3.5: Axle loads from traffic load models, EN 1991-2

3.5.4. Fatigue load model 4b

Fatigue load model 4b (FLM4b) is a set of seven lorries with different geometry and axle load, which are intended to simulate the effects equivalent to those of typical heavy traffic on European roads. Each standard lorry is defined by the number of axles and the axle spacing, the equivalent load of each axle and the wheel contact areas. Fatigue load model 4b should be used instead of 4a if not only the stress range but if the nominal stress level is important in the considered fatigue detail. It is assumed to be important for an adhesively bonded GFRP/steel connection.

Traffic types are accounted for by defining different composition of lorries as percentage of the heavy traffic volume. Local traffic type is considered for this case study as the bridge is located on a local road. For the application of fatigue load model 4b on road bridges, a definition of the total annual number of lorries crossing the road bridge (Nobs) has also been defined by the Eurocode or specified for specific projects. FLM4b is mainly intended to be used in the stress-time-history analysis in association with a cycle counting procedure to assemble stress cycle ranges when assessing the fatigue life of the structure. In other words, FLM4b is recommended to be used with the cumulative damage assessment concept.

Tabel NB.8 — Verzameling van gelijkwaardige vrachtwagens voor belastingsmodel 4b

Type voertuig	Type voertuig		Verkeerstype			Wiel-type
	Afbeelding van de vrachtwagen	Afstand tussen de assen m	Gelijkwaardige aslast kN	Lange afstand (%) ^a	Middellange afstand (%) ^a	
	4,5	70 130	20,0	50,0	80,0	A B
	1,50 2,40 1,30	70 120 120 120	7,0	4,0	4,0	A C B B
	3,20 5,20 1,30 1,30	70 130 100 100 90	37,0	20,0	5,0	A B C C C
	3,40 6,00 1,80	70 140 90 90	20,0	12,0	4,0	A B C C
	4,80 3,60 4,40 1,30	70 150 80 80 70	10,0	10,0	5,0	A B C C C
	3,20 1,30 4,40 1,80 1,80	80 160 100 100 100	4,5	3,0	1,5	A B C C C
	3,20 1,40 4,40 1,30 1,30 1,30	70 180 170 80 80 90	1,5	1,0	0,5	A B B C C C

^a Percentage vrachtwagens.

Figure 3.6: Fatigue load model 4b

3.5.5. Thermal loads

Thermal loads according to EN 1991-1-5 are considered on the composite bridge deck. Bridge decks are grouped in (1) steel decks, (2) composite steel-concrete decks and (3) concrete decks. Unfortunately, there are no norms available for composite FRP/steel bridge decks. As the thermal conductivity and dimensions of a concrete deck is similar to a FRP deck, thermal loads are considered from group (2) steel-concrete bridge decks.

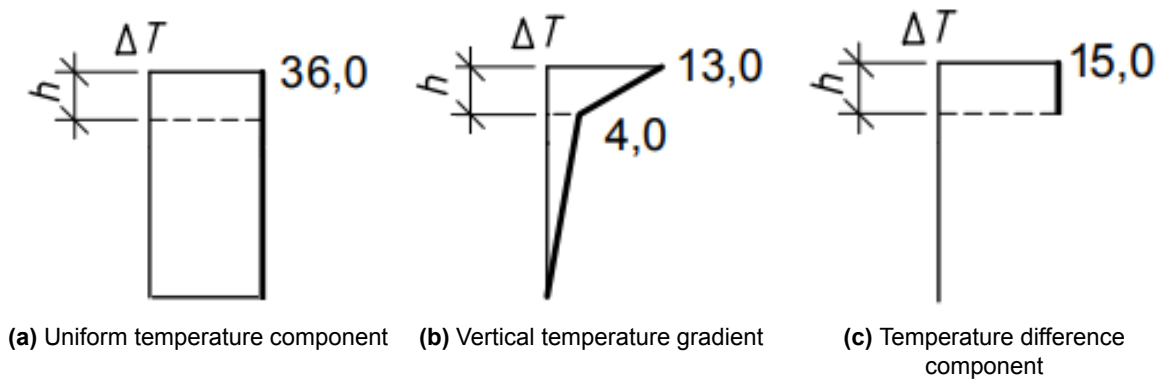


Figure 3.7: Thermal expansion load cases on the GFRP/steel bridge deck

Three thermal load cases are distinguished: (1) uniform temperature component, (2) vertical temperature gradient, and (3) temperature difference component. Both expansion and contraction should be considered for each load case. Simultaneity of the former two load cases is accounted for with an a combination factor according to the Eurocode. Figure 3.7 shows the three thermal expansion load cases. Height of the deck is indicated with h . Reference temperature at time execution is 10 degrees Celsius. Only thermal expansion is considered for structural analysis as it governing over thermal contraction in this case. Difference in CTE between the steel and GFRP times the 36 degrees for the uniform temperature component is gives larger relative expansion compared to the CTE of GFRP times 15 degrees. The last thermal expansion load case, temperature difference component, is therefore not considered in structural analysis. No information is available on thermal cycles on bridge decks due to daily and seasonal variation. They are however deemed to be important for GFRP/steel bridge design.

3.6. Summary

A quick overview of this chapter is given below:

- The Kwekersbrug, an existing bascule bridge, is considered as representative movable bridge suitable for replacing current deck for a GFRP deck using adhesively bonded deck-to-girder connections.
- Its bridge deck has a length of 9.3m and width of 9.7m. Main structural components of the bridge deck are four steel main girders, cross beams, secondary girders and deck.
- Vacuum infused GFRP sandwich deck panels are considered in bridge deck design for retrofitting. It consists of top and bottom skins, vertical webs and foam cores. The GFRP deck is bonded to the entire length and width of the top flanges of the main and secondary girders.
- A methyl methacrylic based adhesive layer of 10mm thick is considered in the bonded connection design. Further mechanical properties: elastic modulus of 0.6 GPa, tensile strength 21 MPa, shear strength 15 MPa and coefficient of thermal expansion of 70ppm per degree Celsius.
- Top and bottom skins of the GFRP sandwich deck are 12 mm thick and have anisotropic stiffness properties. The 5 mm thick vertical GFRP deck webs have quasi-isotropic stiffness properties. PUR foam cores in the deck have very low stiffness (0.03 GPa) and weight, therefore excluded in numerical models.
- Thermal expansion coefficient of the deck skins are 30ppm. per degree Celsius in longitudinal direction and 15ppm. per degree Celsius in transverse direction of the bridge deck. Conservative thermal properties of glass fibres and resin are considered.
- Permanent loads, traffic loading, thermal loading and loads during operation are considered for analysis of the bonded deck-to-girder connection according to the Eurocode. Assumptions are made for thermal loading on the GFRP/steel bridge deck, since currently no norms are available for GFRP/steel bridge decks.

Numerical models and methods

Numerical models and methods used for structural analysis of the case study bridge deck are presented in this chapter.

4.1. Global model

One numerical model is made for global analysis of the bridge deck in the finite element analysis (FEA) software package SCIA Engineer 17.1. This FEA software package is intended for engineering purposes. The global model consists of the entire bridge deck, including main structural components: steel main and secondary girders, cross beams and GFRP bridge deck, see Figure 4.1. Dimensions and material properties are equal to the ones presented in Chapter 3. Counterweights are modelled as external bending moments acting at the main girder ends.

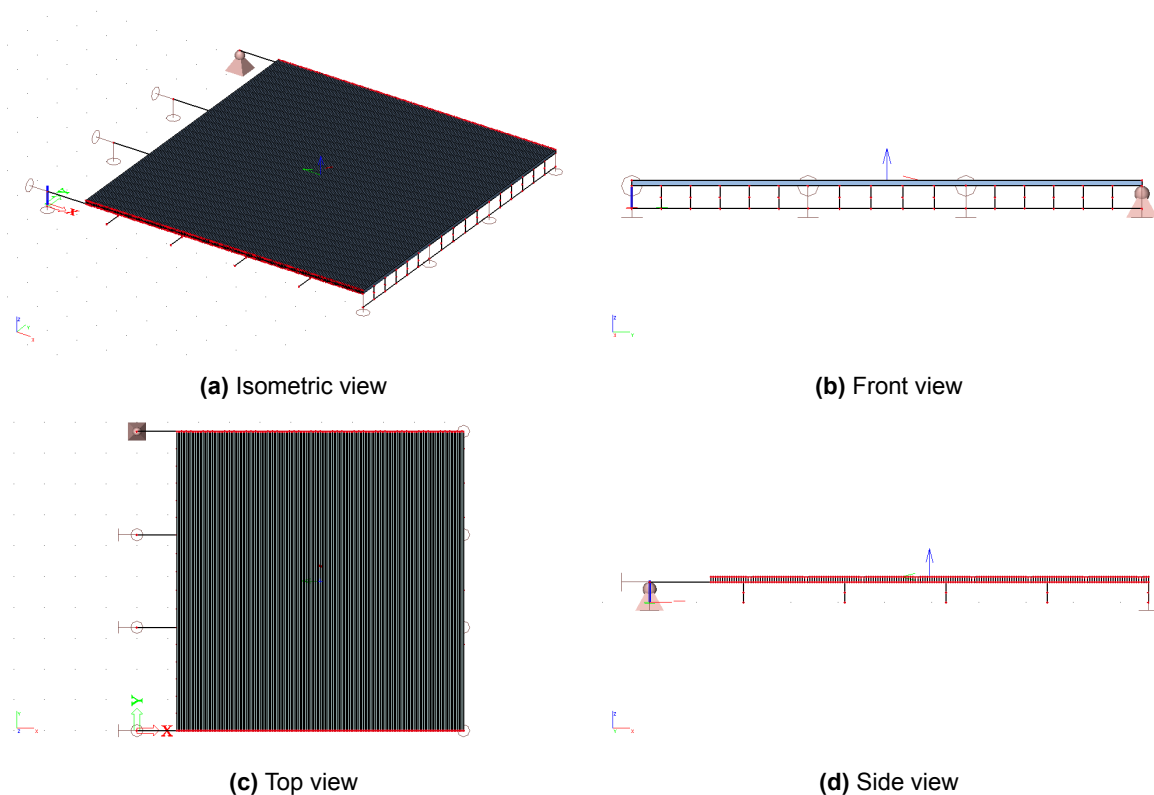


Figure 4.1: Global model

4.1.1. Boundary conditions

The trunnion bearings in the main girders are modelled as pinned supports at the ends of the four main girders. Translation in transverse direction is however unrestrained for three out of four supports (Fig. 4.2a). Front of the main girders are supported only vertically. The bridge deck is structurally indeterminate due to the four supports in transverse direction.

4.1.2. Element types

The steel structure is modelled in 1D beam elements, while the GFRP deck is modelled in 2D shell elements. The facings and webs of the GFRP deck are modelled separately with orthotropic stiffness properties in order to take the different laminate layups into account.

4.1.3. Orthotropic stiffness GFRP

The orthotropic stiffness properties are calculated using classical laminate theory. Elastic stiffness properties of the entire laminates are computed in the software tool, eLamX. This tool from the Dresden University is based on the classical laminate theory. Output from the tool, ABD-matrix, is used as input in SCIA Engineer for the GFRP deck and validated by hand and similar software tools. Since the laminates are symmetric and balanced the B part of the matrix has zero value entries. Also the A_{16} and A_{26} are zero. D_{16} and D_{26} have non-zero values since the laminates are not full isotropic, meaning torsion and bending coupling for the laminates.

4.1.4. Deck-to-girder connections

The deck-to-girder connections are modelled as a 'rib', i.e. 1D beam elements (steel girders) are fixed to 2D shell element (bottom facing) and acts as a composite beam. It represents an infinite stiff bonded connection with zero thickness. Eccentricities between the girders and cross beams are modelled by master-slave connections and 'dummy' elements. These are infinitely stiff connections between two nodes without cross-sectional dimensions and weight.

4.1.5. Stress state bonded deck-to-girder connection

FEA software package SCIA Engineer does not compute interface stresses for the 'rib' connection. Stress states in the deck-to-girder connections are therefore manually calculated post-process. Since the girders are modelled using beam elements only the longitudinal shear flow and distributed line load can be calculated. Stresses are obtained if these are divided by the width of the flange. The longitudinal shear stress can be calculated in either two ways:

1. Determine the in-plane membrane shear forces, n_{xy} force per unit length, in the bottom facing of the GFRP deck connected to the girders. The jump in shear force over the connected 'rib' corresponds to the longitudinal shear flow in the deck-to-girder connection. Longitudinal shear stress can be calculated dividing the shear flow by the width of the bonded connection, or in this case the full flange width:

$$\tau_{xz} = \frac{\Delta n_{xy}}{b} \quad (4.1)$$

2. The derivative of the normal force in the girder corresponds to the longitudinal shear flow in the deck-to-girder connection based on equilibrium in the cross-section. Longitudinal shear stress is again calculated dividing the shear flow over the bonded width:

$$\tau_{xz} = \frac{dN}{dx \cdot b} \quad (4.2)$$

Similar approach for determining the normal stress in the connection:

1. Determine the out-of-plane shell shear forces, v_y force per unit length, in the bottom facing of the GFRP deck connected to the girders. The jump in shear force over the connected 'rib' corresponds to the distributed line load in the deck-to-girder connection. Normal stress can be calculated dividing the line load by the width of the bonded connection:

$$\sigma_z = \frac{\Delta v_y}{b} \quad (4.3)$$

2. Derivative of vertical shear force in the cross section is equal to the normal stress in the connection:

$$\sigma_z = \frac{dV_z}{dx \cdot b} \quad (4.4)$$

Both methods result in the same stress. Extracting internal forces from beam elements is however more convenient than internal forces from shell elements in SCIA. Stress states in the bonded deck-to-girder connections from the global model are calculated using the second method.

4.1.6. Limitations

Bear in mind the following limitations of the global model:

1. The adhesive layer itself is not modelled. The bonded deck-to-girder connections are modelled by fixed connections. Thus, no slip occurs in the composite beams. In addition, stress state through thickness of the adhesive layer is not obtainable.
2. Due the use of 1D beam elements for the girders, stress states in transverse direction are not obtainable and uniform over width of the bonded connection. In addition, bending of the deck in transverse direction is not fully accurate as it supported by a line instead of a top flange with width.
3. A relative coarse mesh (50 mm) is used, due to computational limits, corresponding with the centre-to-centre distance of the webs of the deck. Local effects in longitudinal direction are therefore not seen.
4. It is not possible to assign orthotropic coefficients of thermal expansion to materials in SCIA Engineer. The governing CTE of the GFRP facings, which is in longitudinal direction, is considered as both longitudinal and transverse direction of the laminate.

4.2. Local model

An additional model is made to analyse the stress state in the connection between the deck and secondary girder in more detail under traffic and thermal loads. Finite element analysis software package Abaqus 6.14 is used for the local models. Purpose of the software is more research/educational oriented.

4.2.1. Dimensions

The local model consists of one and half secondary girder, adhesive layers and FRP deck. Adjacent secondary girder is modelled to include vertical load distribution. The entire length (9.3 m) is considered. Width of the deck is 1.5 times the c.t.c distance of the secondary girders, 900 mm. The adhesive layer thickness is 10 mm. Width of the adhesive layer is equal to the width of the top flange of the secondary girder, i.e. 98 mm. Deck and girder can be considered as an continuous composite beam with a cantilever end (Fig. 4.2). Dimensions and material properties are equal to the ones described in Chapter 3.

4.2.2. Boundary conditions

Symmetry boundary condition is considered on the left side of the local model (Fig. 4.2b). This is allowed since the loads considered for this model are symmetrical with respect to the symmetry boundary condition on the left side, i.e. level of the web of the girder. Meaning, restrained rotation around the longitudinal axis, restrained rotation around the vertical(trough-thickness) axis, and restrained translation in transverse direction.

The secondary girders are supported by pinned supports at level of the cross beams, marked with the yellow crosses in longitudinal direction (Fig. 4.2d). Width of the cross beams are taken into account by applying the boundary conditions on the corresponding surface.

The right side of the model, the GFRP deck, is also restrained in rotation around the longitudinal and vertical axis. However, translation in transverse direction is unrestrained, allowing thermal expansion as it is in the bridge deck (Fig. 4.2b).

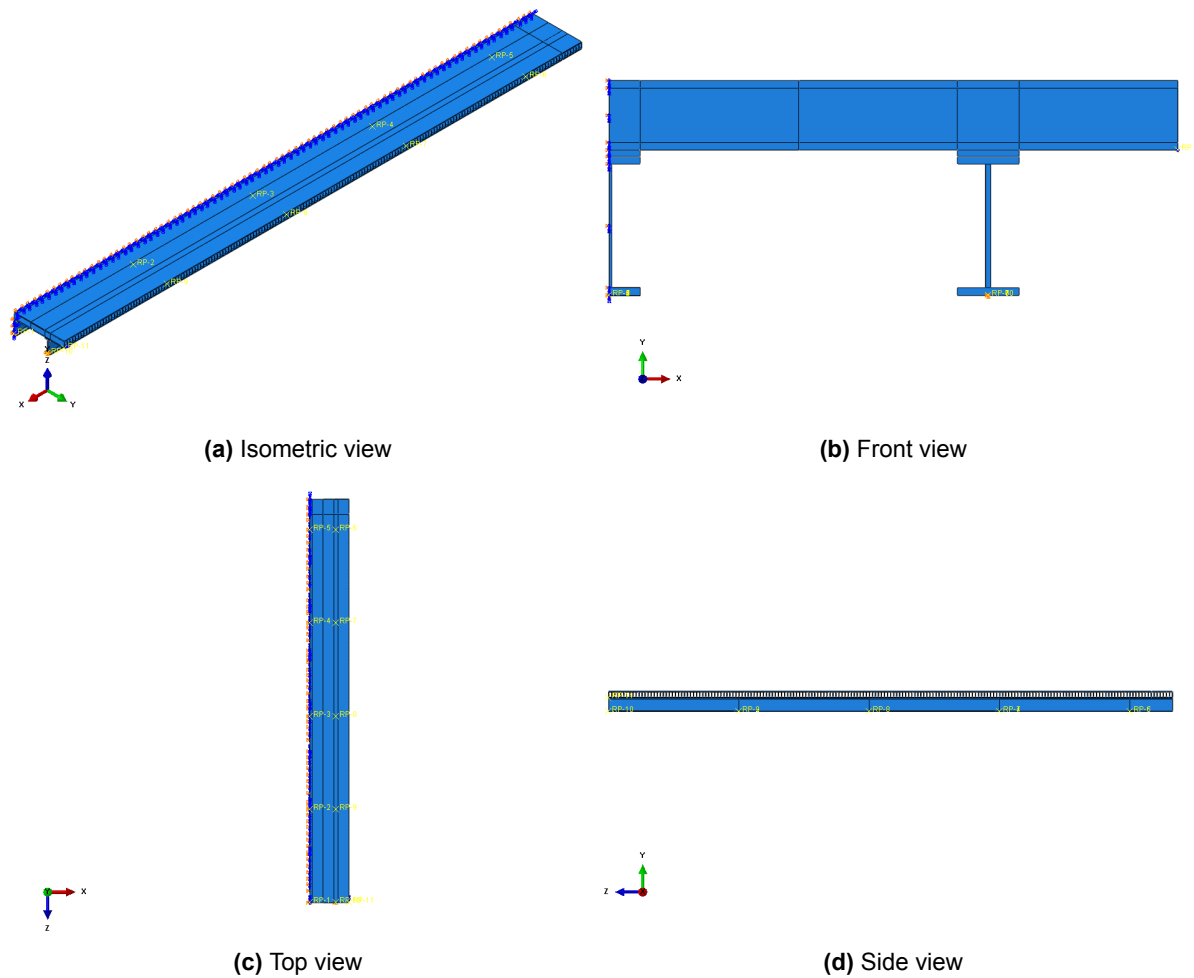


Figure 4.2: Local model

4.2.3. Element types

Two element types are considered in the local model: continuum shell elements (2.5D) for the GFRP laminates and steel girders, and solid elements (3D) for the adhesive layer. The GFRP laminates and steel webs and flanges are considered thin walled and through-thickness stresses and out of plane shear are not of interest, therefore suitable for shell elements. Continuum shell elements differ from conventional shell elements by their three dimensional dimension instead of one plane. They however consists of an equivalent shell that drives deformation of nodes in a solid body. Both elements have equal amount of degrees of freedom. Continuum shell elements can be well connected to solid elements used for the adhesive layer. Tied connections are used to connect the facings, webs, adhesive layer and steel girders. Nodes of tied elements have coupled degrees of freedom of the nodes, which in fact means a fixed connection. Since the through-thickness stress and out of plane shear is relevant in the adhesive layer, solid elements are used.

An 8-node linear brick (C3D8R) with reduced integration and hourglass control is considered for the adhesive layer. Four elements through thickness of the adhesive layer are meshed to have non-constant shear stress through thickness. Aspect ratio of the adhesive elements are kept as close to unity, maximum 10. The aspect ratio of an element is defined as the largest edge divided by the shortest edge of the element. Too high aspect ratio causes overly stiff elements, therefore inaccurate results.

An 8-node quadrilateral in-plane general-purpose continuum shell (SC8R) with reduced integration with hourglass control and finite membrane strains is used for the GFRP laminates and steel girder. Only one element through thickness is used for the continuum shell elements. The entire layup of the GFRP laminate is set in one element.

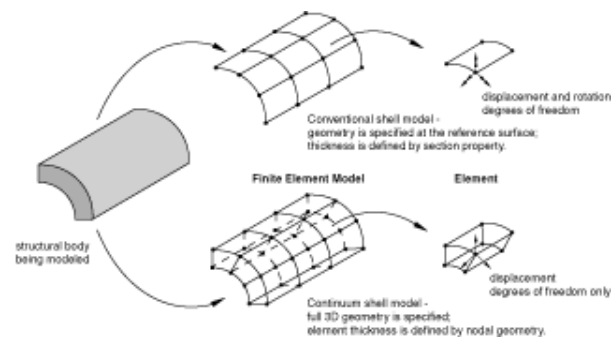


Figure 4.3: Continuum shell element, [1]

4.2.4. Modelling GFRP laminates

Abaqus 6.14 has an in-built composite lay-up tool, based on classical laminate theory, to implement orthotropic stiffness and thermal properties of the GFRP laminates. Input required for the model are material properties of the unidirectional plies and layup. These are equal to the ones used for the global model.

4.2.5. Modelling adhesive layer

The adhesive layer is modelled by solid elements. Four elements through thickness of the adhesive layer are considered to obtain a non-uniform (shear) stress distribution through-thickness. Aspect ratio of the adhesive elements is in all cases 10 or lower to prevent overly stiff elements.

4.2.6. Stress state bonded deck-to-girder connection

Direct nodal stress results from the solid adhesive elements are given by Abaqus. Longitudinal shear, transverse shear and normal stress through-thickness are considered.

Multi-axial stress states in the adhesive layer require a combination stress to include axial and shear components. It is convenient to have one reference stress to compare. Similar to steel structures for which the Von Mises stress is compared to the yielding stress of steel.

Maximum Principal stress is considered as combination stress for the stress state in the adhesive layer (Eq. 4.5). Different from Von Mises, tensile and compressive states are distinguished. Tensile strengths of adhesives are generally lower compared to compressive strengths. Similar to the interlaminar strength of GFRP laminates. Max. Principal stress is therefore considered suitable as combination stress. However, in the case of high compressive and shear stress it could be possible that Max. Principal stress is non-conservative compared to shear only.

$$\sigma_{1,2} = \frac{\sigma_x + \sigma_y}{2} \pm \sqrt{\left(\frac{\sigma_x - \sigma_y}{2}\right)^2 + \tau_{xy}^2} \quad (4.5)$$

4.3. Validation methods

The methods used to determine the stress levels in the deck-to-girder connections are validated by comparing the longitudinal shear stresses from the numerical models with an analytical solution, based on classical beam theory, for the longitudinal shear stress in a composite cross-section (Eq. 4.6). Full effective width of deck plate is considered in the analytical solution.

$$\tau_{xz} = \frac{\sum ES_x V_z}{\sum EI_y b} \quad (4.6)$$

The same composite girder is considered as the one in shown in Figure 4.2. Only difference it that the deck is removed. It is replaced by a GFRP laminate with the same properties as the bottom facing of the GFRP deck considered in the case study. Width of the GFRP laminate is equal to the flange width (Fig. 4.4b This is done to minimise the influence of the Vierendeel effect in the GFRP deck and the shear lag effect. Goal is to compare the methods to determine the stress levels only. Both models and

analytical solution consider an uniformly distributed load of 9 kN/m^2 , corresponding to the uniformly distributed load from traffic load model 1, in order to validate the model.

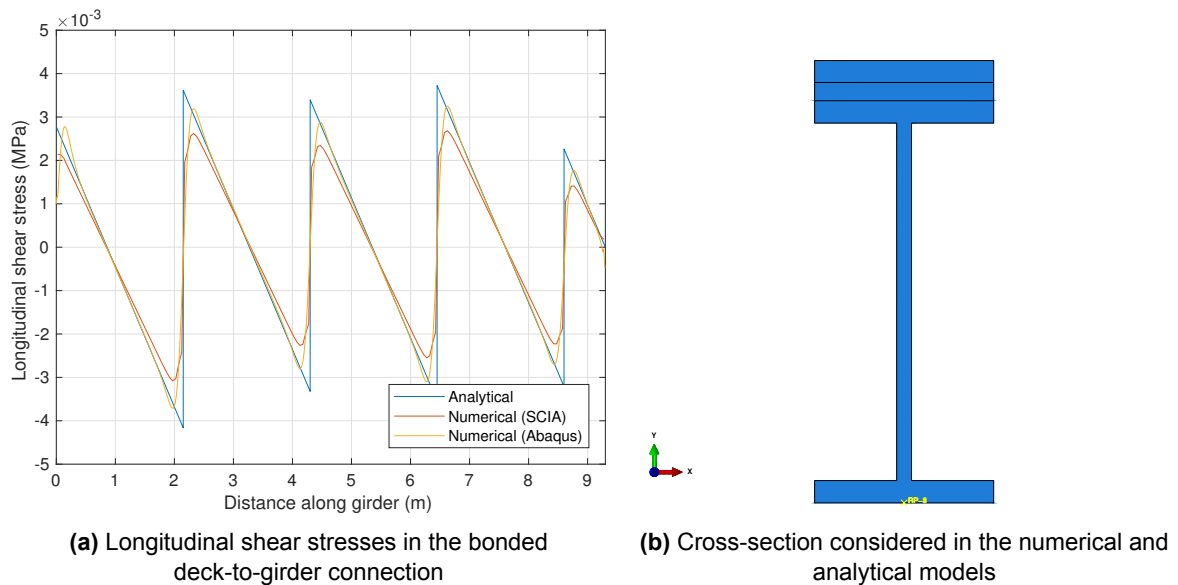


Figure 4.4: Validation of method to determine stress state in bonded deck-to-girder connections

Similar stress distribution is seen in Figure 4.4a for both numerical and analytical models. The analytical solution shows slightly larger stresses at the supports. This is due to the absence of shear lag effect in the analytical solution. Difference in stresses from the numerical models is likely to be caused by the difference in modelling the bonded connection. The model in Abaqus has the elastic adhesive layer with 10mm thickness. The model in SCIA Engineer a fixed connection with zero thickness.

4.4. Summary

A quick overview of this chapter is given below:

- A global and local model are made for structural analysis of the bridge deck from the case study. The global model consists of the main structural components of the entire deck, while the local model only consists of one part. The local model is made to obtain a more detailed stress state in the connection as the global model was not able to do so.
- An analytical solution for the stress in a deck-to-girder connection, based on classical beam theory, is compared to the numerical solutions in order to validate the methods to obtain the stress states.

5

Structural analysis

Results from the structural analysis of the case study bridge deck are presented in this chapter. Considered loads and structural design are described in Chapter 3. Stress states in the bonded deck-to-girder connections for global and local analysis are determined according to the methods and corresponding numerical models described in Chapter 4.

5.1. Composite action

Composite structures consist of two or more different materials. They can act together as one unit if there are connected strongly enough. If this occurs, it's called composite action. This concept is for example deliberately used in composite concrete-steel girders. Goal is to design more slender and reduce deflections due to increased bending moment resistance. The concrete slab acts as compressive part in the composite cross section under sagging bending moments. Requirement is however the presence of shear connectors between the steel girder and concrete slab to prevent slip between both materials. The less slip, the more the concrete slab contributes to bending moment resistance of the composite girder. This can be expressed in the degree of composite action, no slip means full composite action. Contribution of the deck is however very much depending on stiffness of the deck.

Same principle occurs in composite FRP/steel girders in which the shear connectors are represented by an adhesively bonded connection. Normal and shear stresses occur in the bonded connection as result of external loading on the composite girder.

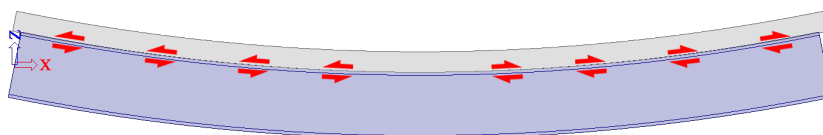


Figure 5.1: Longitudinal shear stresses in bonded connection due to composite action [3]

5.2. Bonded deck-to-girder connections

Stress results in this chapter are presented for two bonded deck-to-girder connections. One for the bonded connection between the (central) main girder and the FRP deck, and one for the bonded connection between the (central) secondary girder and FRP deck, shown in red boxes in Figure 5.2. These two connections proved to be the governing bonded deck-to-girder connections in a preliminary phase, i.e. largest stress levels.

Stress states are plotted along the longitudinal path shown in Figure 5.2. Distance along the girder at 0 m corresponds with the beginning of the girder, i.e. origin of the red arrow. To recall, cross beams are welded between the main girders with a centre-to-centre distance of 2.15 m. Secondary girders are connected on top of the cross beams and the FRP deck is bonded on all top flanges of the main and secondary girders. The last cross beam is located at 8.6 m, the remaining 0.7 m of the secondary girder is therefore a cantilever.

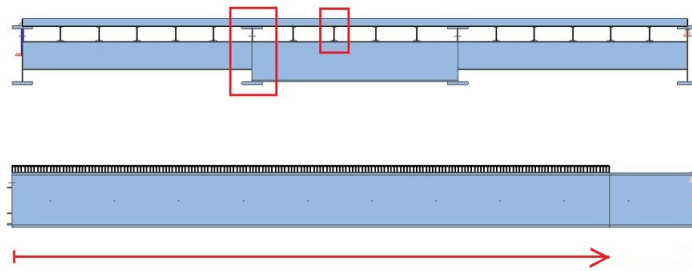


Figure 5.2: Considered deck-to-girder connections, front view (top). Longitudinal path along girders, side view (bottom)

5.3. Permanent loads

Figure 5.4 shows the stress states in the considered deck-to-girder connections under permanent loads in closed and opened position (Fig. 5.3). Permanent loads comprise self-weight of the steel structure, counterweights, GFRP deck and wearing layer. External bending moments are applied at the ends of the main girders to account for the counterweights.

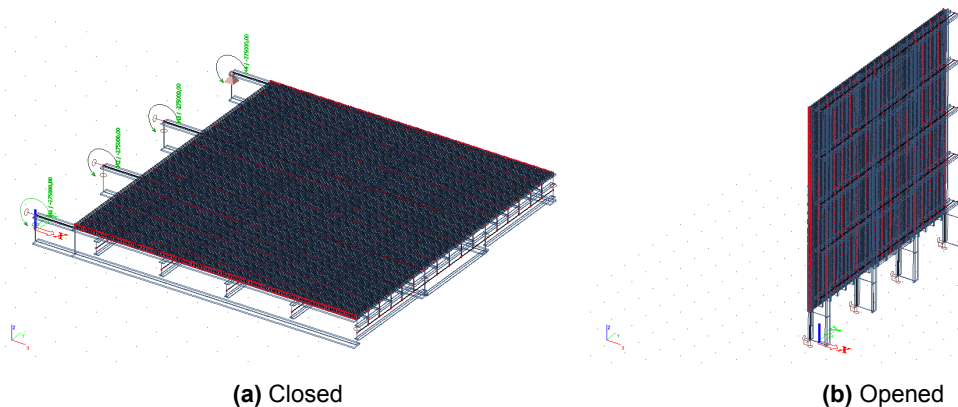


Figure 5.3: Permanent loads on bridge deck in opened and closed position

Longitudinal shear stress concentrations are seen at the end of the bonded connection between the main girder and FRP deck in both opened and closed position (Fig. 5.4). In closed position, the counterweights cause a hogging bending moment in the main girder, resulting in peak longitudinal shear stress of 0.15 MPa at the end of the bonded connection. Varying longitudinal shear stresses are seen in the connection between the deck and secondary girder. It follows the 'jigsaw' shear force diagram expected for a continuous girder loaded by a uniformly distributed load. Stress levels are low, maximum 0.03 MPa.

In opened position, for a bridge deck opening angle of 90 degrees with respect to ground level, also shows a concentration of longitudinal shear stress at the end of the bonded connection between the deck and main girder. Weight of the FRP deck is entirely beared via shear by the deck-to-girder connections. This results in increasing longitudinal shear stresses towards the ends of the bonded connections. Maximum shear stress level of 0.05 MPa occurs between the main girder and deck, seen in Figure 5.4b.

Normal stresses in the deck-to-girder connections are rather low, 0.01 MPa. Not surprising, considering the low weight of the GFRP deck.

5.3.1. Opening/closing

Opening and closing of the bridge deck results in cyclic stresses in the deck-to-girder connections. Three stages can be considered during operation: (1) closed position, (2) opening; just when the front of the bridge deck is not in contact with the supports, and (3) opened; when the bridge deck has an opening angle of 90 degrees with respect to ground level.

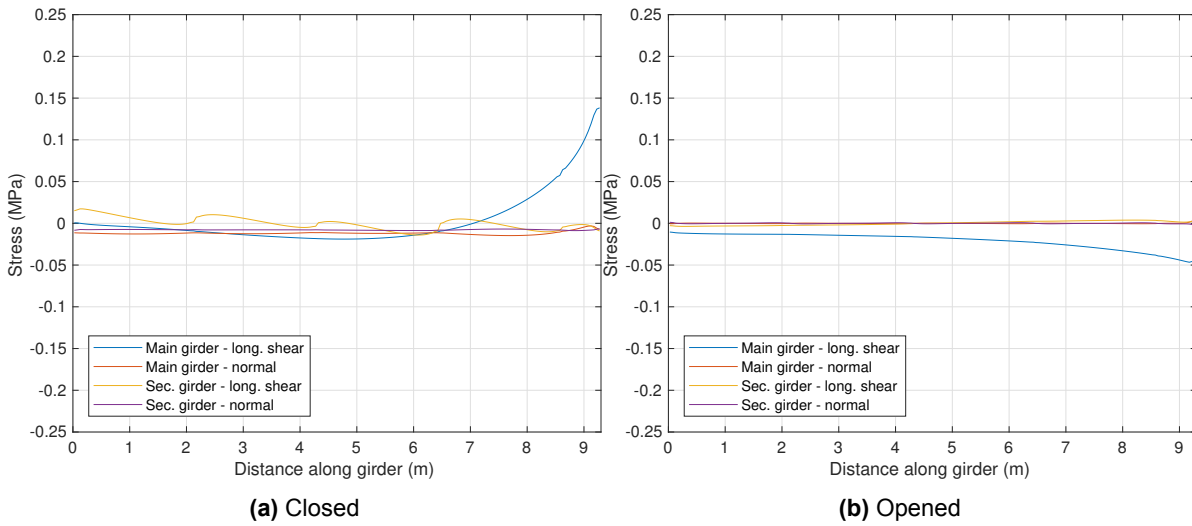


Figure 5.4: Stress states in the deck-to-girder connections under permanent loads

As mentioned in Chapter 3, the counterweights are slightly 'pushed' in closed position to prevent opening by wind. Maximum longitudinal shear stress range is obtained at the end of the bonded connection between the main girder and deck. In stage (2), just when the deck can be considered as a cantilever, the maximum stress level is 0.2 MPa. Stress range for one cycle is therefore 0.25 MPa (Fig. 5.5). Considering a reference period of 30 years and 100.000 opening/closing cycles per year result in (only) 300.000 cycles at 0.25 MPa.

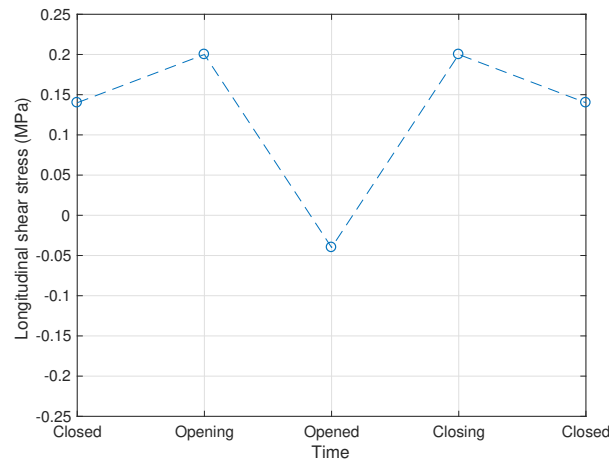


Figure 5.5: Peak longitudinal shear stresses in the bonded deck-to-main girder connection during opening/closing

5.4. Traffic loads

Stress results in the bonded deck-to-girder connections due to traffic loads are presented in this section. Both static and fatigue traffic load models are considered, as mentioned in Chapter 3. Considered static traffic load models are load model 1 (LM1) and 2 (LM2). Load model 1 consists of three tandem systems and a uniformly distributed load. The actual traffic lane layout may be considered for renovation projects according to the Dutch norm NEN 6786. Therefore only two tandem systems are considered in the structural analysis. Load model 2 consists of a single axle load of 400 kN.

Fatigue load model 4b (FLM4b), according to the Dutch national annex NEN-EN 1991-2, is considered for the fatigue analysis. It consists of a set of lorries with different axle loads and configuration as mentioned in Chapter 3. FLM4b should to be used for fatigue details in which not only stress range but also nominal stress level is of importance. This is the case for bonded FRP joints, as shown in Chapter 2.

Stress results presented in this section are divided in global and local analysis, corresponding to the results from the global and local models respectively. Limitations of the global model, discussed in Section 4.1.6, made it necessary to develop an additional model to obtain a more detailed stress state in the adhesively bonded deck-to-girder connections.

5.4.1. Global analysis

Figure 5.6 shows the critical positions, i.e. largest stress levels, of the tandem systems from the traffic load models 1 and 2. This is for both cases at the end of the deck positioned on the cantilever part of the secondary girder. Stress states in the deck-to-girder connections are presented in Figure 5.7. Obviously, compressive stress concentrations are seen in the vicinity of axle loads. Also longitudinal shear stress peaks occur at this location, due to the internal shear forces in the composite FRP/steel girders.

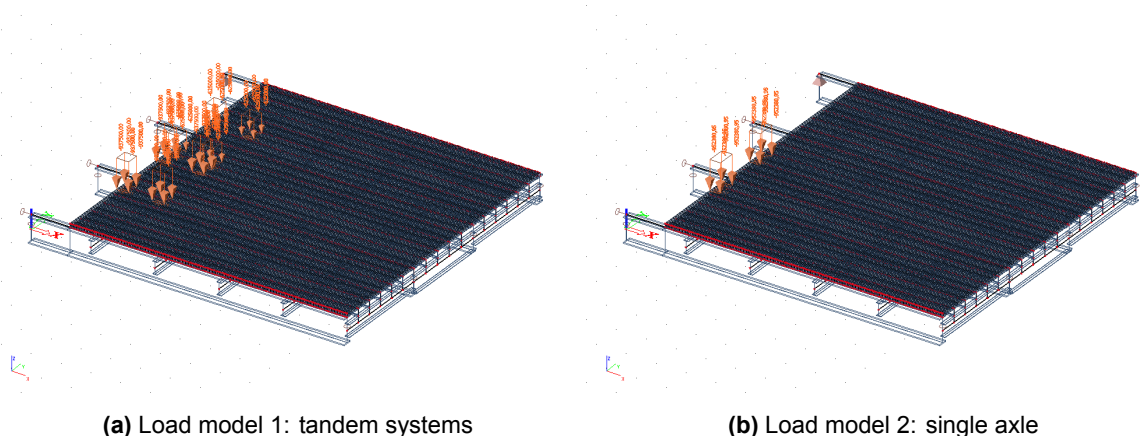


Figure 5.6: Governing positions for the traffic load models on bridge deck

Maximum stresses occur in the bonded connection between the deck and secondary girders compared to main girders (Fig. 5.7). This is mainly due to the large difference in bending stiffness between the main and secondary girders. Lower stresses are obtained in the bonded connection between the deck and secondary girder for LM1 compared to LM2. This is mainly due to the difference in axle loads from LM1 and LM2, 300 kN and 400 kN respectively.

Peak longitudinal shear stress is 1.4 MPa at 8.95 m distance along the girder for load model 2 (Fig. 5.7b). Length of the wheel print is 0.35 m, therefore maximum shear force occurs at this location. Maximum normal stress is 3.7 MPa. A slight decrease in compressive stress is seen towards the end of the girder. Bending of the FRP deck in transverse direction causes peeling stresses at the end of the bonded connection.

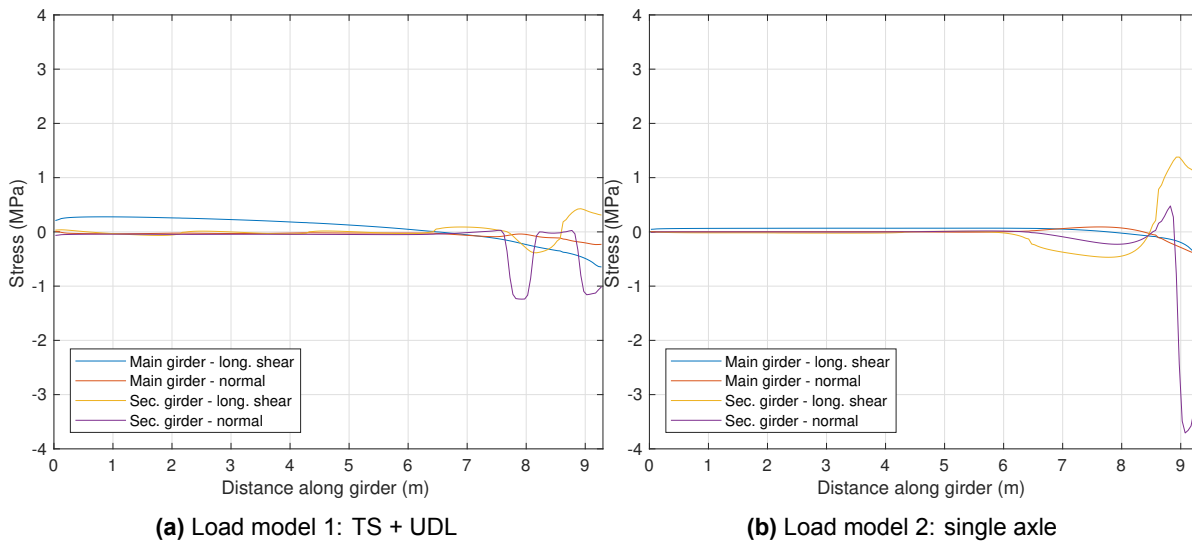


Figure 5.7: Stress states in the deck-to-girder connections under traffic loads

5.4.2. Local analysis

It can be concluded that maximum stress levels are obtained in the bonded connection between the GFRP deck and secondary girder loaded by the single axle load from traffic load model 2, positioned at the end of the deck. As mentioned before, limitations of the global model call for a local model to obtain a more detailed stress state in this critical location. Stress results presented in Figure 5.9 are obtained from the local model described in Chapter 4. It consists of the GFRP deck, adhesive layers and secondary girders.

The model is loaded by the single axle load from LM2, shown in red, positioned at the cantilever end of the deck (Fig. 5.8). Effect of the second wheel of the axle, at 2 m distance, has negligible effect on the stress state in the considered bonded connection. Therefore only one wheel of the axle load is considered. Additionally, the adjacent secondary girder is considered to account for distribution of the axle load in transverse direction. To recall, symmetry boundary condition is used as the axle load is symmetric with respect to the symmetry plane.

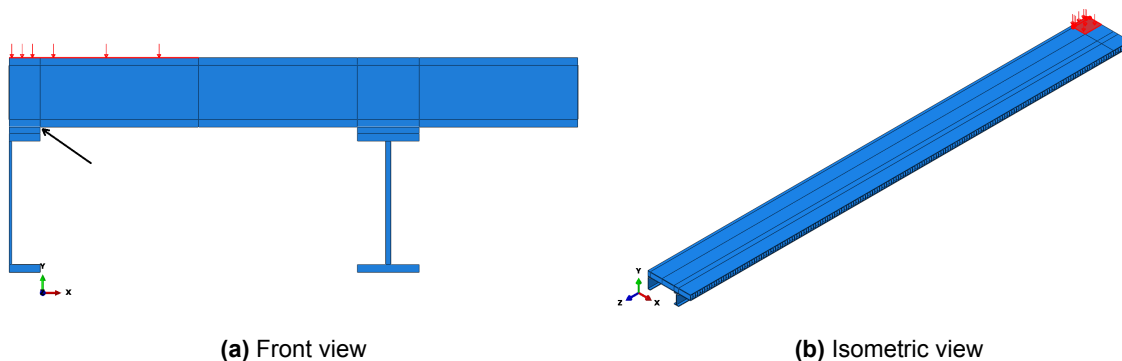


Figure 5.8: Local model loaded by traffic load model 2

Longitudinal direction

Figures A.8a and A.8b show the stress state in the adhesive layer in longitudinal direction. The peak stresses are plotted along the edge of the bonded connection at the GFRP/adhesive interface, shown with the black arrow in Figure 5.8a. Maximum longitudinal shear stress is now 2.2 MPa and maximum compressive stress is 5.2 MPa.

Varying stresses are observed in longitudinal direction (Fig. A.8b). It is not a surprise to see increased compressive stresses in the bonded connection at level of the webs of the GFRP deck, con-

sidering load transfer through the webs to the adhesive layer. Stress variations are however seen along the entire length of the bonded connection, only less pronounced outside the vicinity of the axle load. Distance between the stress peaks is 50 mm, which corresponds to the centre-to-centre distance of the vertical webs of the GFRP deck. **The varying stresses are explained by the local bending moments through thickness of the GFRP deck, i.e. in the vertical webs of the deck. The GFRP deck can be considered as a Vierendeel truss, and deforms like it (Fig. 5.10a). Stress variations due to longitudinal effects are called by the Vierendeel effect from now on.**

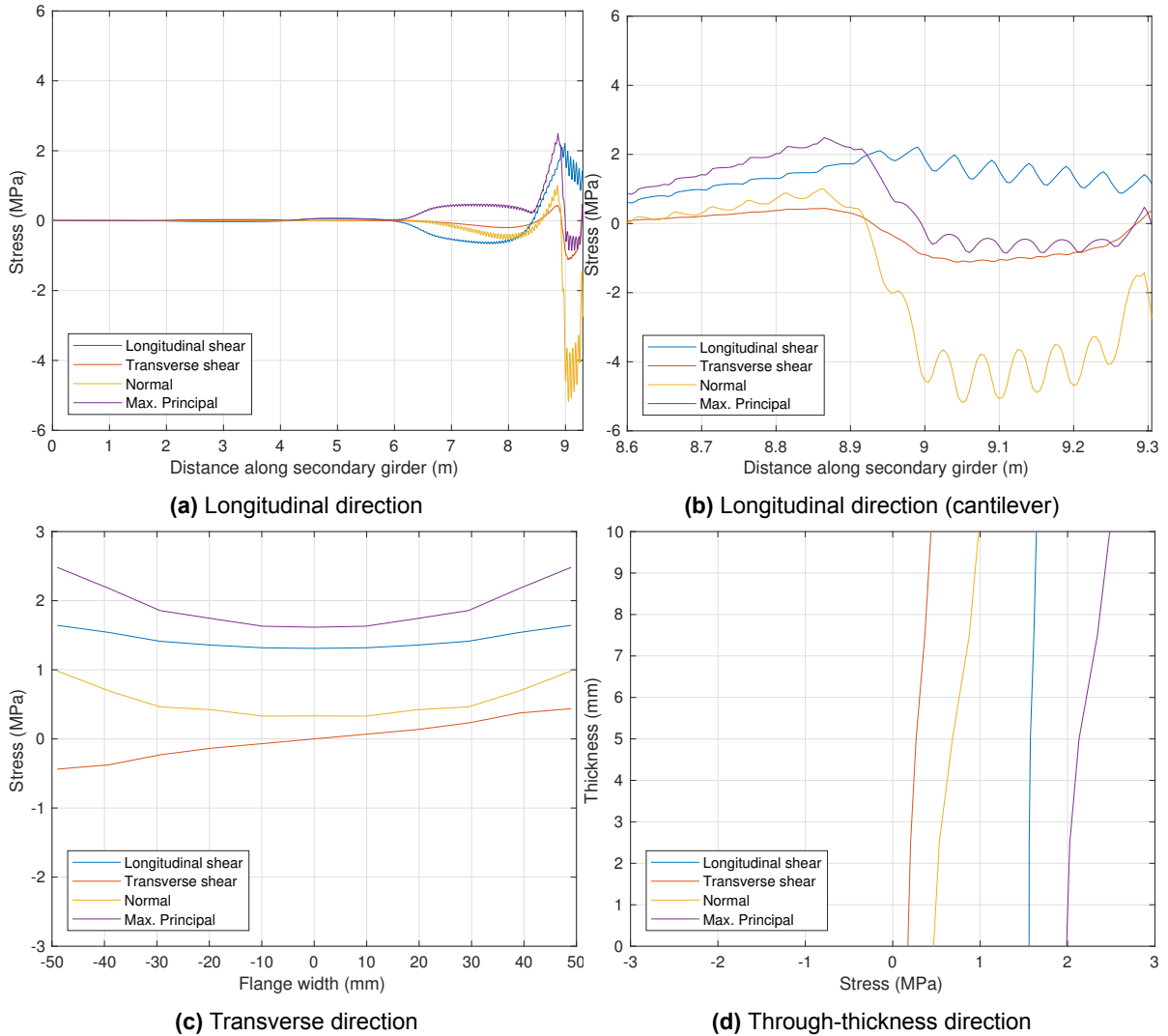


Figure 5.9: Stress state in adhesive layer between deck and secondary girder under traffic load model 2

Tensile stress of 1 MPa is seen in front of the wheel load (Fig. A.8b). This effect also seen for axle loads from trains on the wheel track. A point load on an infinite beam supported by elastic foundation could cause upward deflection outside the vicinity of the wheel load. The analogy can be made for the GFRP deck 'supported' by the elastic adhesive layer loaded by the axle load.

Peak Max. Principal stress of 2.7 MPa occurs at this location with maximum tensile stress. Combination of shear and tensile stresses make this the critical cross-section. A slight increase in Max. Principal stress is seen towards the end of the deck, due to increase of tensile/peeling stresses in the corner of the bonded connection as mentioned before. This location is marked with the red arrow in Figure 5.10b.

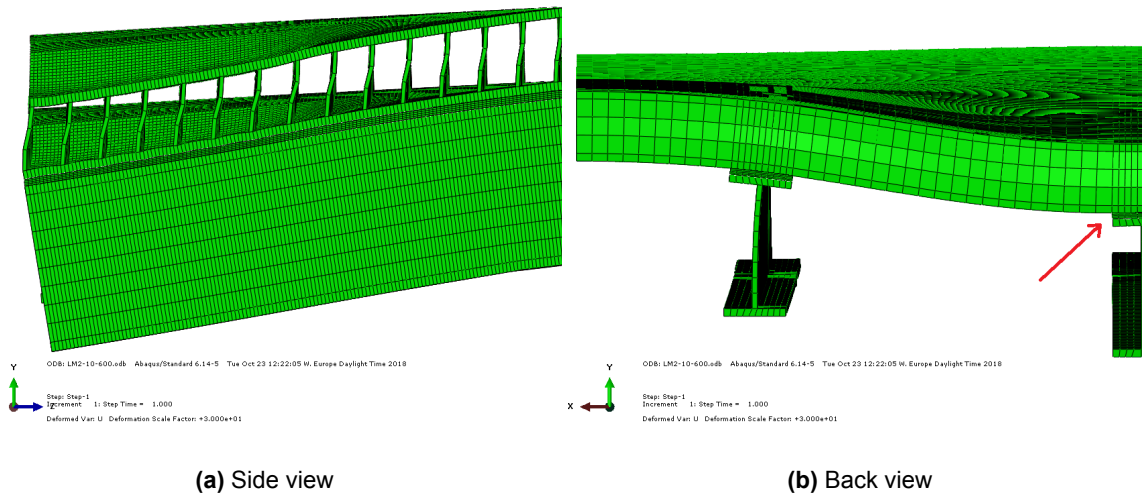


Figure 5.10: Deformation GFRP deck under traffic load model 2 (cantilever end)

Transverse direction

The stress state in transverse direction, i.e. over the width of the flange, is plotted at the location of peak Max. Principal stress, $x=8.865$ m, seen in Figure 5.9c. Stress concentrations occur at the edges of the bonded connection for both shear and normal stresses. This is explained by the larger difference of in stiffness between the FRP deck and steel girder. Stiffness of steel is roughly 10 times larger compared to the GFRP laminates. **As a result of the low (shear) stiffness, local shear lag effect is observed over the width over the flange.** Longitudinal shear stresses show non-uniform distribution in transverse direction, with peak stresses at the edges.

Increasing the in-plane stiffness of the bottom facing would results in a more uniform longitudinal shear stress distribution over the width of the connection. This can be seen in Figure 5.11. Nearly uniform longitudinal shear stress distribution is seen for $G=80$ GPa (similar to the stiffness of steel). Opposite effect is seen for $G=0.8$ GPa, where stress peaks increase.

Through-thickness direction

The stress state through thickness of the adhesive layer is plotted in Figure 5.9d. Thickness at 0 mm corresponds with the steel/adhesive interface, while 10 mm thickness corresponds with the GFRP/adhesive interface. Stresses are plotted along the edge of the same cross section with peak Max. Principal stresses, $x=8.865$ m. Longitudinal shear stresses are very much constant through-thickness. Increase in tensile and transverse shear stresses are however seen towards the GFRP/adhesive interface. This is cause by the local bending of the bottom facing of the GFRP deck.

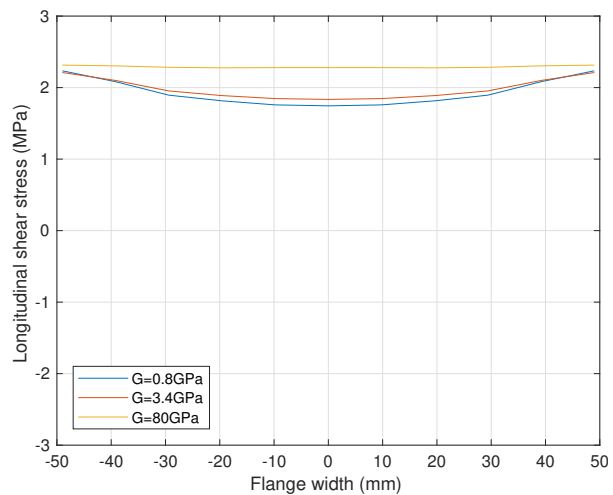


Figure 5.11: Longitudinal shear stress distribution in transverse direction for different in-plane shear stiffness of the GFRP laminates

5.4.3. Fatigue analysis

Fatigue load model 4b (FLM4b), according to national annex from NEN-EN 1991-2, is considered for the fatigue analysis of the bonded connection due to traffic loads (Fig. 5.12). Longitudinal shear stress ranges are determined at the location of the peak stress (9 m) for the seven different lorries. This location is deemed as critical fatigue detail as maximum longitudinal shear stresses are found for both LM1 and LM2. In addition, it is close to the expansion joint which is prone to dynamic effects and therefore fatigue damage.

Influence lines are determined for each wheel type. These are used to construct the stress history diagrams of each lorry (7 total) which have different axle loads, configuration and wheel types. The stress history diagram of the lorry with the largest axle loads, lorry 7, is shown in Figure 5.12a. Maximum longitudinal shear stress range of 0.75 MPa is seen for the second axle (180 kN). As the stress history diagram consist of almost separate stress peaks, it can be concluded that the axle loads can be considered as uncoupled of the lorry. The stress spectra for the considered fatigue detail is shown in Figure 5.12b. It consists all stress ranges including the dynamic amplification factor versus the number of cycles taking into account a reference period of 30 years and local traffic type. Figure 5.12b also includes an S-N curve for the considered bonded GFRP/steel connection detail. This S-N curve represents the required fatigue strength as the total fatigue damage is equal to 1. The slope of the S-N curve, 1:10, is based on available literature on bonded GFRP joints, described in Chapter 2. Required static strength of the fatigue detail should be in the range of 3 MPa. **Please note that these results are obtained from the global model. Calculated longitudinal shear stresses are therefore constant over the width of the bonded connection. In previous section it is seen that the peak stress from the global model is larger. This will be elaborated in next chapters.**

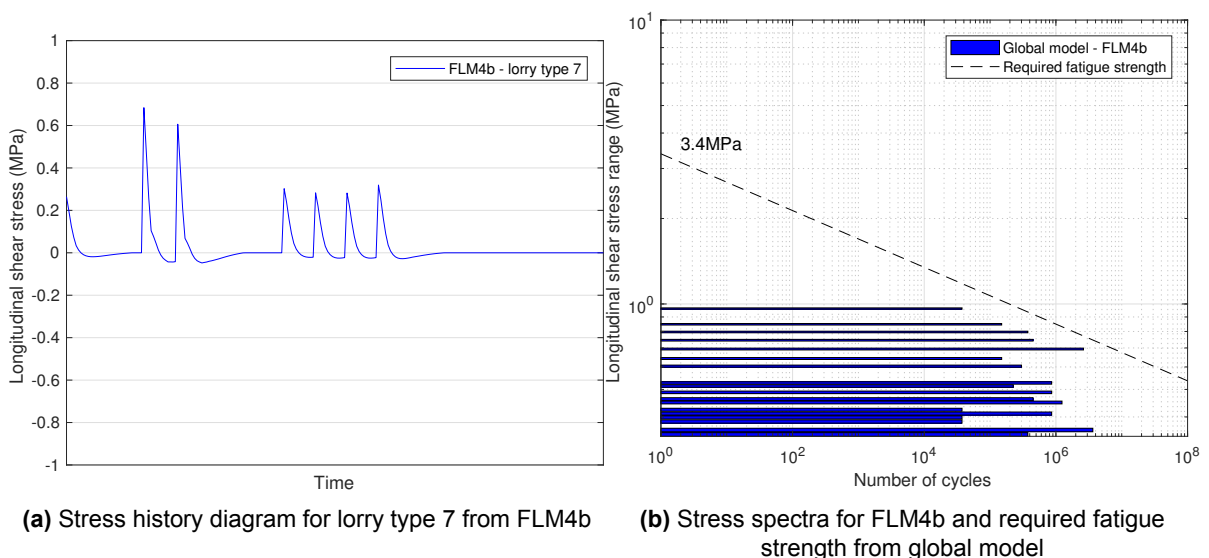


Figure 5.12: Fatigue analysis of critical deck-to-secondary girder connection ($x=8.95\text{m}$) for FLM4b

Additional to the longitudinal shear stress ranges also the normal stress ranges are determined at the same cross section. Corresponding stress history diagram of lorry 7 and spectra is shown in Figure 5.13b. Compressive stress peaks are observed for each passing axle (Fig. 5.13a accompanied with the small tensile peaks in front of the wheel as discussed before. Required fatigue strength is plotted in Figure 5.13b. The slope of the S-N curve is similar to the one for shear loading, 1:10. This is a wild guess and it is most likely that the S-N curve for mode 1 loading, i.e. normal stresses, with a mean load mainly in compression is much less steep due to better performance of bonded joints in compression.

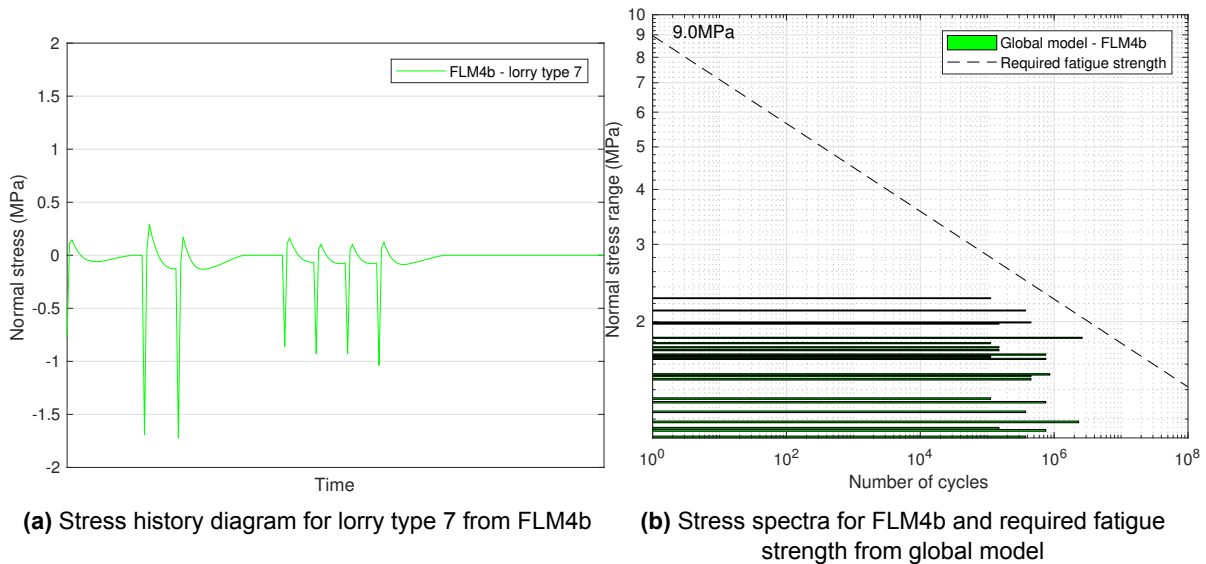


Figure 5.13: Fatigue analysis of critical deck-to-secondary girder connection (x=8.95m) for FLM4b

5.4.4. Effect of main girder

Traffic loads are distributed in transverse direction to adjacent girders and thereby influences the stress state in the adhesively bonded deck-to-girder connection. Stress states in transverse direction are not obtainable from the the global model and the local model (Fig. 4.2) did not included the main girder. This is reason to create a new model that consists of main and secondary girder, cross beams, deck and adhesive layer, and determine the effect of the main girder on the stress state in the critical location, i.e. end of the cantilever part of the secondary girder.

Global bending of the deck is of less importance as we consider the bonded connection between the deck and secondary girder and stress concentrations occur at this location of the wheel load. Stiffness in transverse direction is however important. Therefore, the entire width of the deck is modelled from the second last cross beam to the end, see Figure 5.14. **All main girders are supported by a hinged line support in longitudinal direction.** Global bending of the main girders in longitudinal direction is therefore not possible. Local bending of the deck in transverse and longitudinal direction is investigated. Ten different positions of the single axle from traffic load model 2 are analysed. All of them are positioned at the end of the deck.

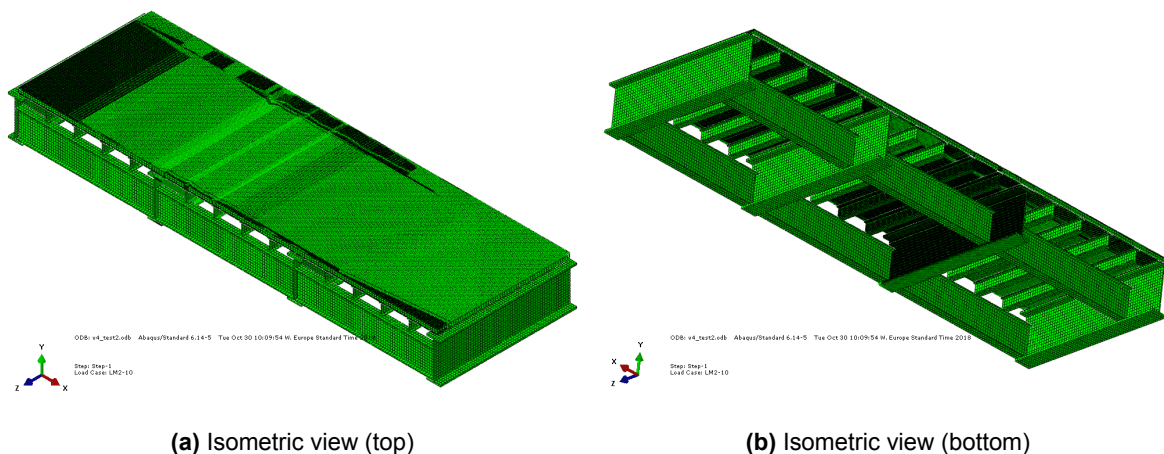


Figure 5.14: Local model to analyse effect of main girder under traffic loads

Max. Principal stress

Governing position of the axle load from traffic load model 2, i.e. largest Max. Principal stresses, is the one that was found by the global model, namely one wheel load is positioned centrally at the secondary girder second from the main girder. The other wheel load of the axle is positioned in the other span between the main girders, see Figure 5.16a. Figure 5.16b shows the deformed model and critical bonded connection. No significant difference is found in stress state between the local model with only deck and secondary girders and the one including main girders. See Figures 5.6b and A.6.

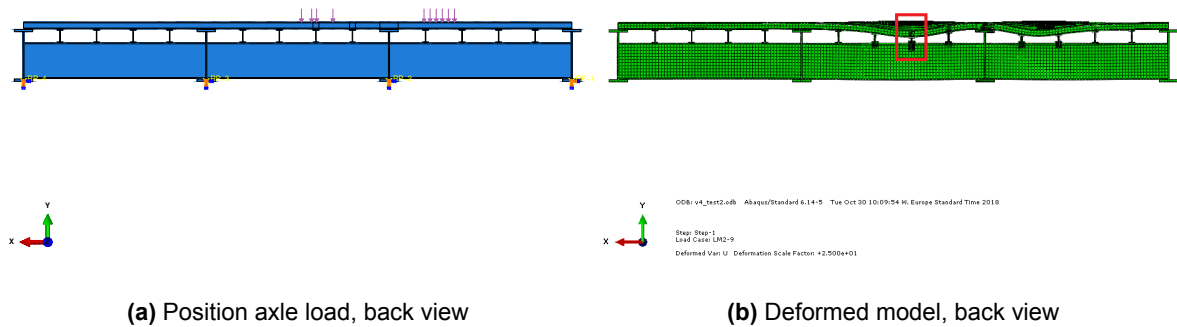


Figure 5.15: Axle position for maximum Max. Principal stress

Peeling stresses

Peeling stresses in the corner of the extreme end of the bonded connection between the secondary girder and deck adjacent to the main girder is maximum when the wheel load of the axle is positioned at mid-span (shown with the red arrow). The maximum peeling stress is 1.2 MPa. It is expected to increase for higher elastic modulus and lower thickness of the adhesive layer.

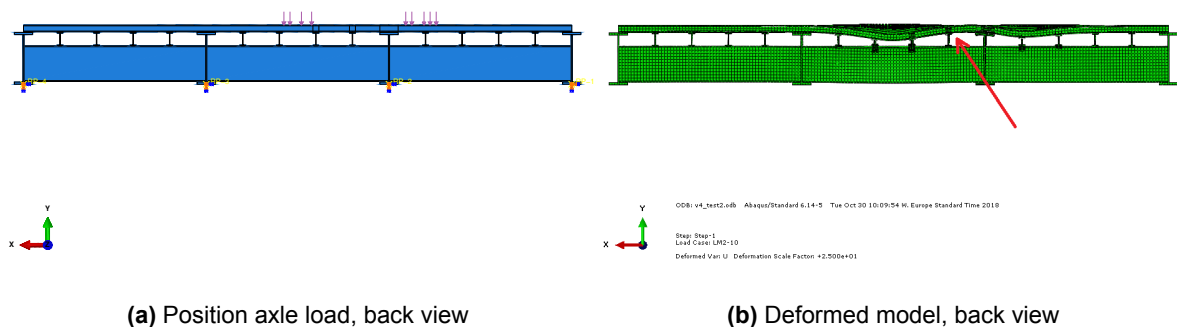


Figure 5.16: Axle position for maximum peel stress

5.5. Thermal loads

Expansion and contraction of the GFRP deck is restraint by the bonded deck-to-girder connections in longitudinal and transverse direction. However, the bridge deck as a whole is free to expand in both directions as bearings at the trunnion allow translation in transverse direction and the supports at the front of the bridge deck only provide vertical support.

The steel structure, GFRP deck and adhesive layer expand under increasing temperatures. Difference in coefficient of thermal expansion (CTE) in combination with the restraining bonded connections between the steel and GFRP induce curvature of the bridge deck. To recall, the conservative CTE of the GFRP deck in longitudinal direction is 2.5 times larger compared to steel. In transverse direction is it 1.3 times larger compared to steel. This thermal curvature causes stresses in the bonded deck-to-girder connections, as they restrain the relative expansion. Distribution of longitudinal shear stresses in the adhesive layer due to thermal expansion will have similar shape of the distribution for an double-lap shear joint, where peaks are located at the extreme ends of the bonded connection.

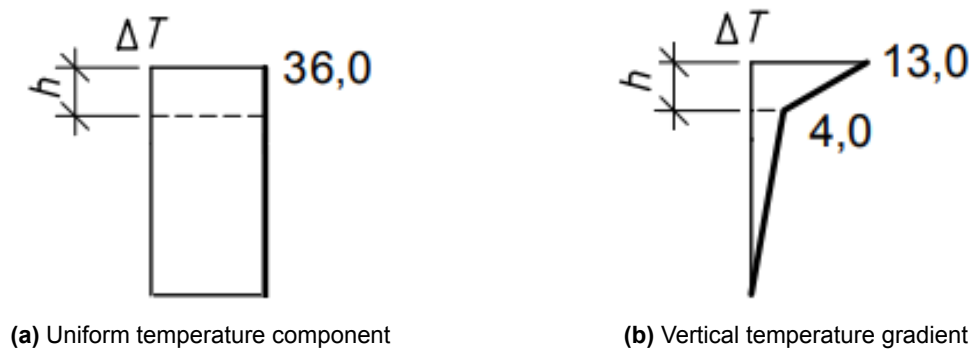


Figure 5.17: Thermal loads on bridge deck

Two temperature load cases are considered for the thermal analysis: uniform temperature component and the vertical temperature gradient on the bridge deck (Fig. 5.17). The height of the GFRP deck is indicated with h . The two thermal load cases should be combined with a combination factor, 0.75, according to the Eurocode (NEN-EN 1991-1-5). They are analysed separately to investigate their individual contribution to the stress states in the bonded deck-to-girder connections. Only thermal expansion is considered as thermal contraction load cases showed lower stress levels in the bonded connections. Magnitudes of the temperature differences are based on thermal loads for composite concrete/steel bridge decks as no norms are available for GFRP/steel bridges. Height and thermal properties of a concrete deck is somewhat similar to the GFRP deck.

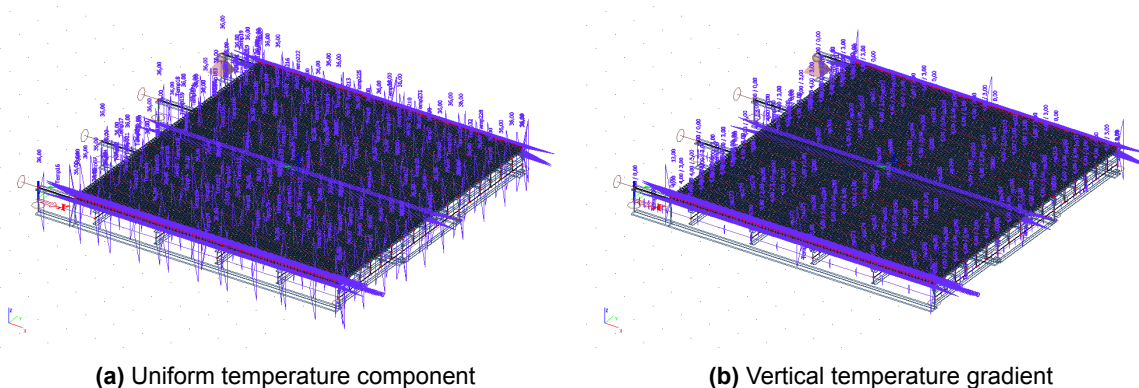


Figure 5.18: Thermal loads on bridge deck

5.5.1. Global analysis

The considered thermal load cases on the bridge deck are shown in purple in Figure 5.18. The uniform temperature component of 36 degrees Celsius is applied on all structural components: steel girders, cross beams and GFRP deck. The vertical temperature gradient is 13 degrees at the top of the deck, 4 degrees at the bottom of the deck, and 0 at the bottom of the main girders.

Stress states in the bonded deck-to-girder connections are plotted in Figure 5.19. The same bonded deck-to-girder connections are considered as the ones for the traffic loads on the global model (Fig. 5.2). Stress concentrations are seen at the ends of the connections. Longitudinal shear stresses increase exponentially towards the ends of the connections. Analogy can be made by the rod pull out problem in which the GFRP deck is represented by the (elastic) rod, the adhesive by the elastic foundation and the thermal expansion by the axial loading on the rod's free end. Tensile longitudinal strains increase exponentially in the rod towards the free end. The exponential elongation of the FRP deck caused the same profile of longitudinal shear stresses in the bonded deck-to-girder connection.

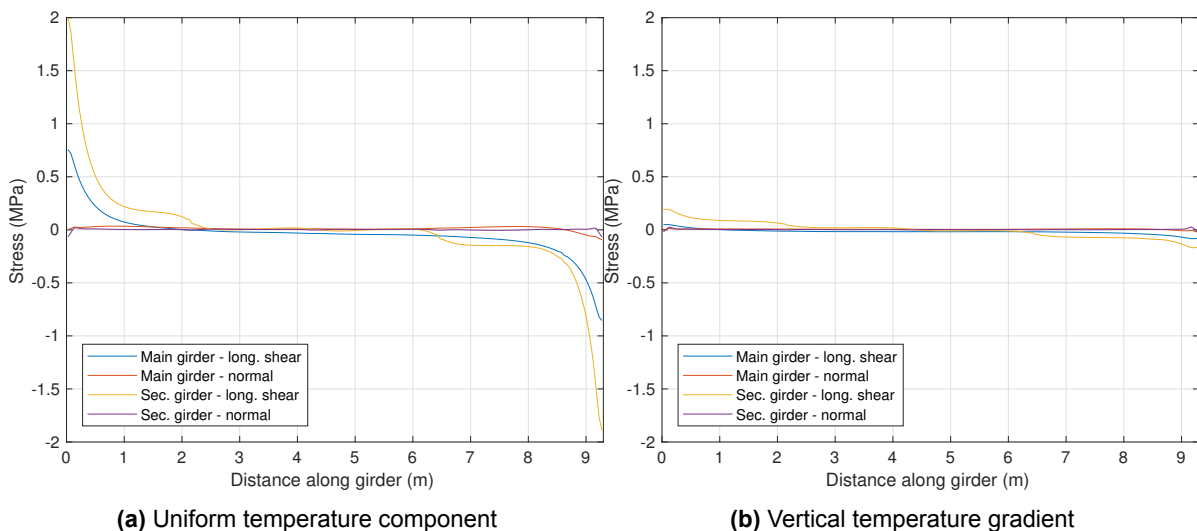


Figure 5.19: Stresses in the deck-to-girder connections under thermal loading

The uniform temperature component causes maximum longitudinal shear stresses in the connection between the deck and secondary girder, up to 2 MPa. (Longitudinal shear) stresses are significantly lower for the vertical temperature gradient (0.2 MPa). This is mainly caused by the temperature difference at level of the bonded connection (4 vs. 36 degrees Celsius). Longitudinal shear stresses are significantly larger compared to the normal stresses for both thermal load cases. Obviously, there is no vertical loading. Peeling stresses are however expected at the ends of the bonded connections due to local bending of the FRP deck.

Lower longitudinal shear stresses are seen for the bonded connections with the main girders (0.9 MPa) compared to the secondary girder (2 MPa). Difference is mainly caused by the difference in flange width (98 vs. 300 mm) and the structural indeterminacy of the bridge deck. The middle main girder is 'pulled' downwards as the bridge deck wants to curve upwards due to thermal expansion. Longitudinal shear stresses in the bonded connection between the deck and main girder are therefore reduced at the ends. This is explained in more detail in Section 5.5.4.

5.5.2. Local analysis

As mentioned earlier, stress distributions in the bonded connection in transverse and through-thickness direction cannot be obtained from the global model as the girders are modelled as beam elements that are fixed to the shell elements. In addition, the orthotropic coefficients of thermal expansion of the GFRP material are limited to only isotropic CTE in SCIA Engineer FEA software used for the global model.

The same local model (Fig. 4.2) is considered for the thermal analysis presented in this section. Orthotropic coefficient of thermal expansion are assigned to the unidirectional GFRP plies, thus more accurate results. Only the uniform temperature component of 36 degrees Celsius (Fig. 5.17a) is con-

sidered on the local mode because maximum longitudinal shear stress levels occurred for this thermal load case as seen in previous section. Figure 5.20 shows the stress state in the adhesive layer under the considered thermal loads.

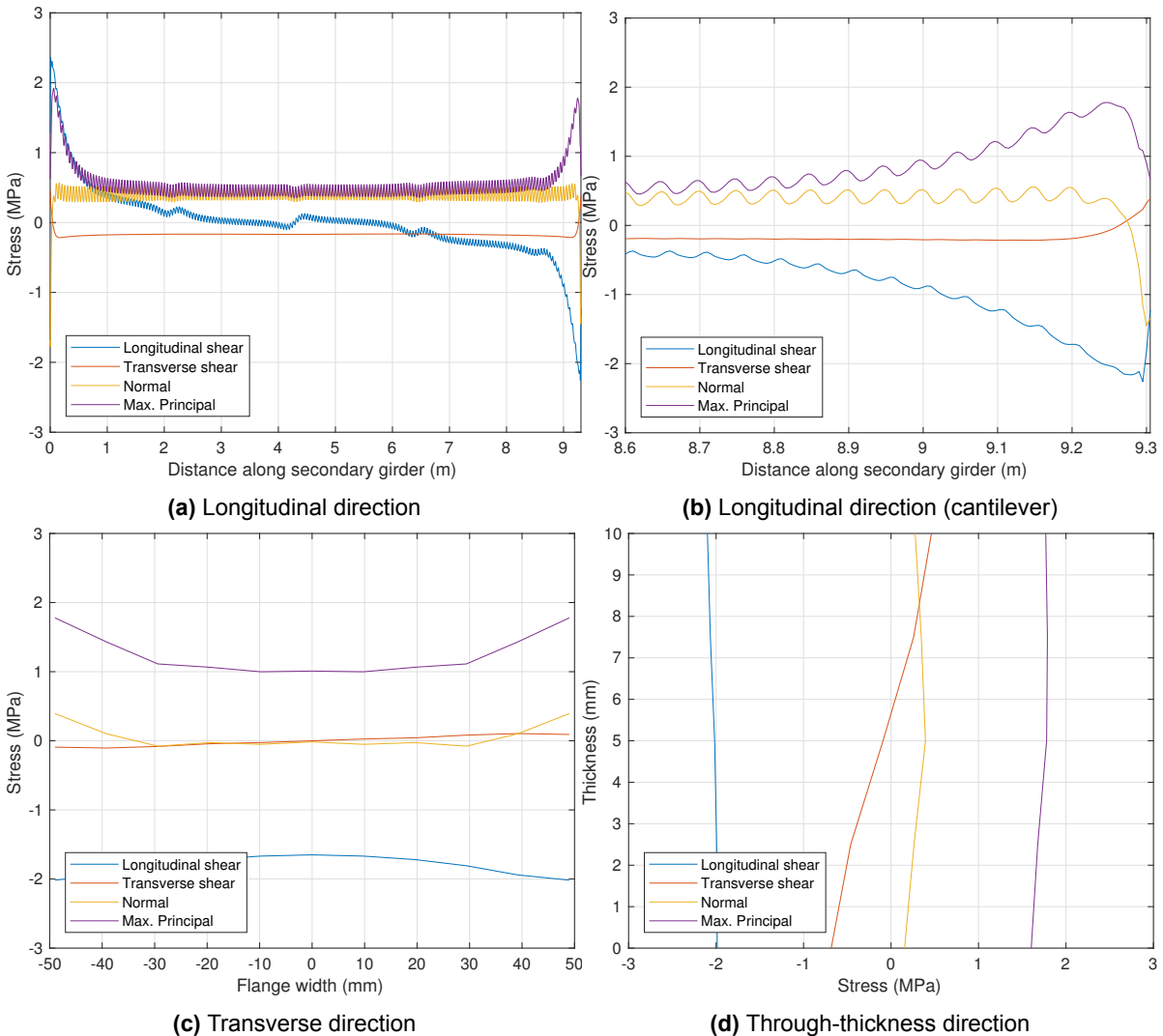


Figure 5.20: Stress state in adhesive layer under thermal loads

Longitudinal direction

Figure 5.20a and 5.20b show the stress state in the bonded connection between the deck and secondary girder along mid-thickness of the adhesive layer, because Max. Principal stress shows maximum at this thickness. Stress concentrations are located at the ends of the connection. Peak Max. Principal stress is 1.9MPa, where peak longitudinal shear stress is 2.4 MPa. Max. Principal stress is not governing over the longitudinal shear stress as the ends of the bonded connection is in compression and reduce the Max. Principal stress. This compression also causes the transverse shear stress to increase.

Little variations in longitudinal shear and normal stresses can be seen near the (cross beam) supports (2.15, 4.3, 6.45 and 8.6m). The vertical supports cause 'jumps' in shear force in the composite beam, affecting the longitudinal shear and normal stress distributions.

Local bending moments in the webs of the deck, due to the aforementioned Vierendeel effect, cause stress variations in longitudinal shear and normal stress along the entire length of the bonded deck-to-girder connection. Similar effect as for traffic loads. Figure 5.21b shows the deformed (Vierendeel) deck and girder at the end of the cantilever under thermal loading.

Transverse direction

Stresses in transverse direction are plotted in Figure 5.20c at the cross section where Max. Principal stress is maximum in the cantilever part, $x=9.245\text{m}$. It is interesting to see the tensile stresses at the edges of the bonded connection. These tensile are also seen along the entire length of the girder (Fig. 5.20a). **The tensile stresses are caused by the thermal expansion of the adhesive layer itself, which has relative high CTE ($7 \cdot 10^{-5}K^{-1}$). It is restrained between the stiff top flange and FRP bottom facing and tries to expand horizontally. This effect results in tensile stresses at mid-thickness at the edge of the adhesive layer, but also affects the stress state at the end of the bonded connection.**

Transverse shear stress peaks are located at the edge of the bonded connection. Although, the difference in CTE between steel and GFRP in transverse direction is small, the GFRP expands more in transverse direction compared to the steel flange. This results in increasing transverse shear stress towards the edge as the slip in transverse direction is maximum at this location. Again, longitudinal shear stresses show peaks at the edges of the bonded connection. This is caused by the aforementioned local shear lag effect due to larger difference in stiffness between FRP deck and steel girder.

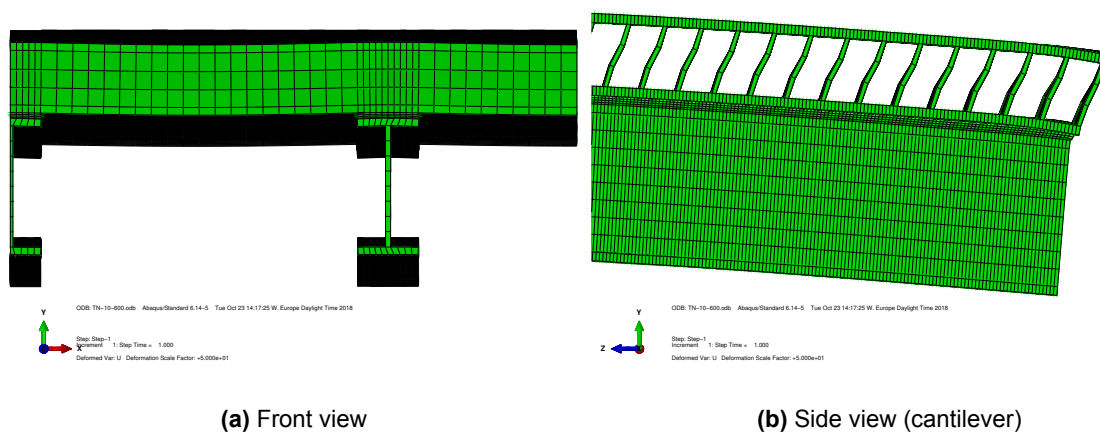


Figure 5.21: Deformation local model under thermal loads

Through-thickness direction

Stress state through-thickness is plotted along the edge of the bonded connection from the steel/adhesive interface to GFRP/adhesive interface in Figure 5.20d. Longitudinal shear stress distribution is somewhat constant over height as expected. Tensile stress peak is seen at mid-thickness as discussed in previous section. Transverse shear stress distribution through-thickness confirms the restrained expansion of the adhesive layer in horizontal direction. Nearly zero transverse shear stress is seen at mid-thickness, analogy with simply supported beam with uniformly distributed load.

5.5.3. Thermal cycles

There are currently no norms or recommendations known to the author on dynamic thermal loads, i.e. thermal cycles, for composite bridge decks. This is however of importance for FRP/steel bridges considering the large difference in coefficients of thermal expansion. And seen from stress levels up to 2.4 MPa in the bonded deck-to-girder connections obtained from the static thermal analysis (Fig. 5.20).

Daily and yearly thermal cycles are assumed based on the stress results from the local model under the uniform temperature component. Yearly thermal cycles of 36°C are considered, corresponding to a stress range of 2.4 MPa. For the daily temperature cycles, 50 % of the yearly cycles are assumed, corresponding to 18°C and 1.2 MPa longitudinal shear stress range. For a reference period of 30 years there are 30 and 10,950 cycles for yearly and daily thermal cycles, respectively.

5.5.4. Effect of main girder

Longitudinal shear stresses are lower in the bonded connection between the deck and main girder compared to the secondary girder in the global model (Fig. 5.19a). However, it is probable that stress peaks at the edges could be larger compared to the stress peaks in the bonded connection with the secondary girder, because of the main girder is much stiffer and has larger flange width.

Another local model is made which does include the main girder (and cross beams), seen in Figure 5.22. Similar boundary conditions are used at the longitudinal sections as the ones used in the local model; symmetry boundary condition at the left side, which allows deflection, but restraints rotation around the longitudinal direction. Same boundary condition at the right side, only then translation in transverse direction is allowed. The secondary girders are fixed on the cross beams. Ends of the main girder are supported by a pinned support. Front of the main girder is only vertically supported, allowing for translation in longitudinal direction. Again, only the uniform temperature component is considered as thermal load on this model.

The state of stress in the adhesive layer between the deck and main girder under thermal loading is shown in Figure A.7. Stresses are plotted along the edge of the main girder at mid-thickness. Stress concentrations are also seen at the end of the bonded connection. Longitudinal shear stress peak is 2.9 MPa, much larger compared to the stress (0.75 MPa) found in the global model.

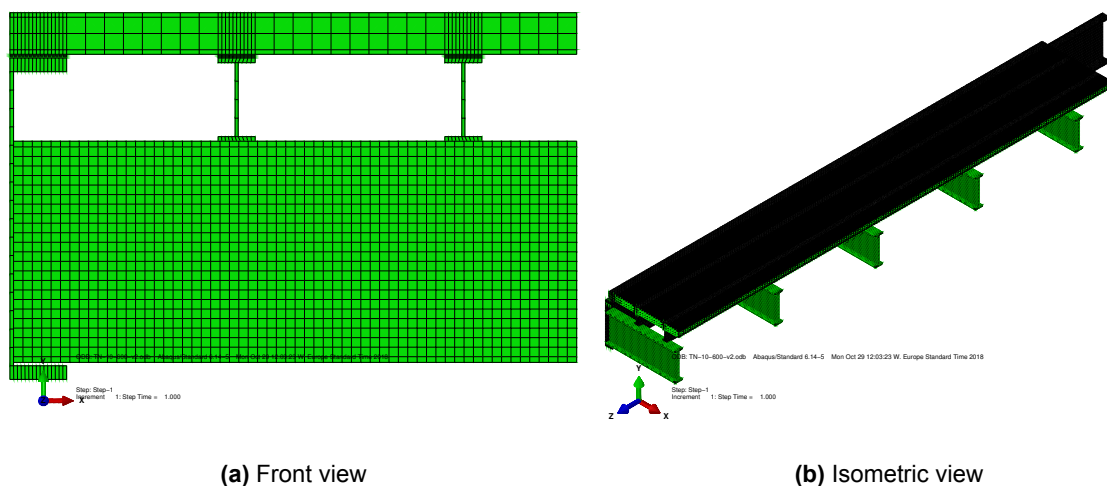


Figure 5.22: Model consisting of main girder, secondary girders, cross beams, adhesives, deck used for thermal loading

Next to the effect in transverse direction, i.e. local shear lag, which is now more pronounced (Fig. A.7c). Also the longitudinal shear stress averaged over width is lower because of the Vierendeel effect but also due to the incorrect modelling of the local model. The local model is statically determinate, while the global modal is statically indeterminate due to the four supports in transverse direction. Vertical supports at the ends of the main girders at the centre of the bridge deck are 'pulled' downwards as they are restrained in translation vertically. Resulting shear force in the deck and main girders have an opposite effect on the end slip. Longitudinal shear stresses are therefore reduced and lower for the global model. The local model is not been adapted due to time limitations.

Stress states in the adjacent and second bonded connection between the deck and secondary girder is not significantly affected by the presence of the main girder. Similar stress state is seen in Figure A.8 for the adjacent secondary girder. This is expected as the stress state is dominated by the longitudinal shear stresses, which are not affected by the main girder.

5.5.5. Deformation

Expansion of the deck in longitudinal direction is 6 mm under uniform temperature component. Upward deformation of the FRP deck is 3 mm in the local model.

5.6. Conclusions

The following conclusions can be drawn from this chapter:

- Maximum stresses occur in the bonded connection between the FRP deck and secondary girder at the cantilever end under thermal and traffic loads. Single axle load (400 kN) shows a longitudinal shear stress peak of 2.2 MPa, while the uniform temperature component shows (36 °C) a peak of 2.4 MPa.
- Stresses vary in longitudinal direction due to local bending moments in the webs of the FRP deck, caused by the Vierendeel effect.
- Longitudinal shear stresses in transverse direction show peaks at the edges of the bonded connection due to local shear lag effect. This is caused by the larger difference in stiffness of the deck and girder.
- Effect of the main girder on the stress state in the critical bonded connection between the FRP deck and secondary girder is negligible.

Comparison of results

Stress results from the global and local models are compared in this chapter. Only the longitudinal shear and normal (through-thickness) stresses are considered because the global model is limited to these two. Goal of this chapter is to determine whether the global/engineering model and corresponding method, with lower computational efforts, is an appropriate method to obtain stress states in a bonded FRP/steel deck-to-girder connection. The stress states are plotted in longitudinal direction for the single axle traffic load (400 kN) and uniform temperature component (36 °C). Stress results from the local model include both the peak stresses and stresses averaged over width. In this way, the Vierendeel effect (in longitudinal direction) and local shear lag effect (in transverse direction) can be distinguished.

6.1. Deck-to-secondary girder

Figures 6.1 and 6.2 show the stress states in the bonded connection between the deck and secondary girder from the global and local model under the governing traffic and thermal loads. Stress results from the global and local models differ significantly, especially at locations of stress concentrations. Obviously, difference in stress results is expected as the stresses from the global model are uniform over width of the bonded connection. Meanwhile, non-uniform distributions are obtained from the local model in Chapter 5 due to the local shear lag effect. This is clearly seen for normal stresses under thermal loading (Fig. 6.2a). Tensile stresses occur along the entire edge of the bonded connection due to thermal expansion of the adhesive layer itself.

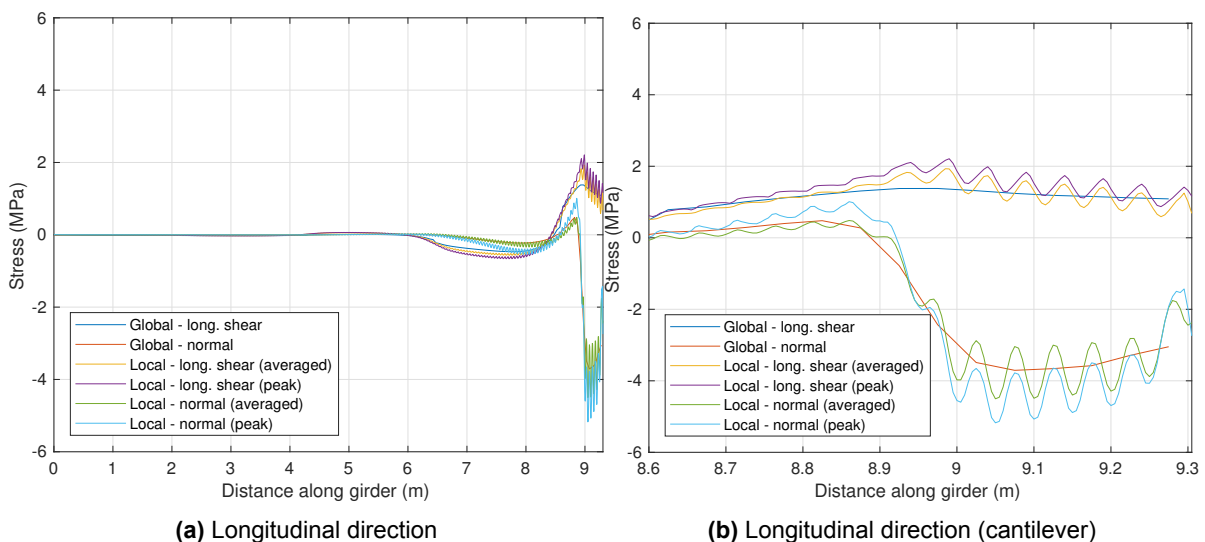


Figure 6.1: Stress state in the bonded deck-to-secondary girder connection under traffic loading

Besides, deviation in longitudinal shear stress is seen in between the cross beams. This is caused by the difference in modelling the supports at level of the cross beams. Roller supports are considered in the local model, therefore not restrained in longitudinal direction. In reality, the secondary girder and cross beam are connected by a weld, thus restrained, which is accounted for in the global model by pinned connections.

Design of bonded connections is governed by stress concentrations, therefore a local problem. Stress states at the critical location, the cantilever end of the secondary girder, are plotted in Figures 6.1b and 6.2b. First to notice, stress results from the global model stop at 25 mm from the ends of the bonded connection. This is due to the considered central difference method to determine the stresses from the internal forces obtained from the global model. Secondly, stress results from the global model show no variations in longitudinal direction compared to the local model. The Vierendeel effect is not visible in results from the global model as the element size is 50 mm, which corresponds to the centre-to-centre distance of the vertical webs of the deck. Local effects in longitudinal direction are therefore not observable, see Figures 6.1b and 6.2b. This effect is very noticeable at the extreme ends of the bonded connection, in which the local effects of the last cell of the FRP deck play a role. A rapid increase in compressive stresses are seen at the last cell of the FRP deck (Fig. 6.2b) due to the Vierendeel effect under thermal expansion (Fig. 5.21b).

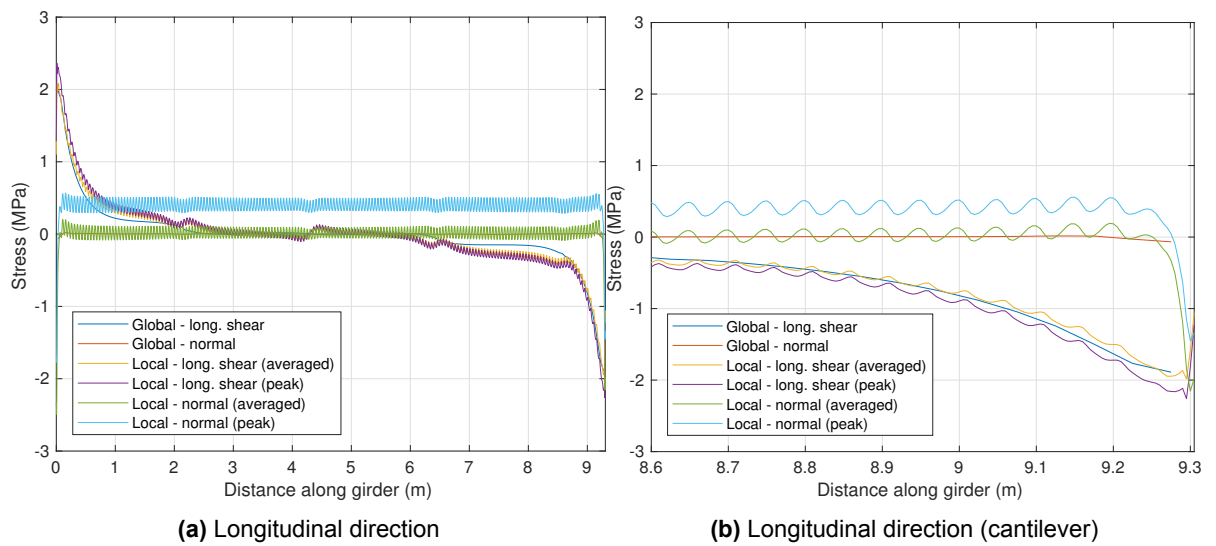


Figure 6.2: Stress state in the bonded deck-to-secondary girder connection under thermal loading

Stress concentration factors (SCF) are determined to relate the peak stress results from the global model to the local model (Eq. 6.1). SCF_{long} is calculated by dividing the averaged (over width) stress levels from the local model by the stress levels from the global model, corresponding with the stress effects in longitudinal direction. Which is in this case due the Vierendeel effect of the FRP deck. SCF_{trans} is calculated by dividing the local peak stresses from the local model by the averaged local stresses from the local model, corresponding to the effects in transverse direction. Which is in this case the local shear lag effect over the width of the flange. Multiplying those two factor results in the total stress concentration factor (SCF_{total}), corresponding to the difference between peak stress levels from the local and global model.

$$SCF_{total} = SCF_{long} \cdot SCF_{trans} \quad (6.1)$$

where

$$SCF_{long} = \frac{\sigma_{local,average}}{\sigma_{global}}, \quad SCF_{trans} = \frac{\sigma_{local,peak}}{\sigma_{local,average}}$$

SCF's presented in Table 6.1 are obtained from the peak stress results from the local model with 10 mm thickness and 0.6 GPa elastic modulus of the adhesive and the global model. The SCF's are somewhat similar for shear stress. Large difference is however seen in SCF_{long} for normal stress

Table 6.1: Stress concentration factors relating stress results from global and local model ($t=10$ mm, $E=0.6$ GPa)

	<i>Traffic</i>		<i>Thermal</i>		
	SCF	Shear	Normal	Shear	Normal
SCF_{long}		1.4	1.2	1.1	30.7
SCF_{trans}		1.1	1.0	1.1	1.2
SCF_{total}		1.6	1.2	1.2	35.3

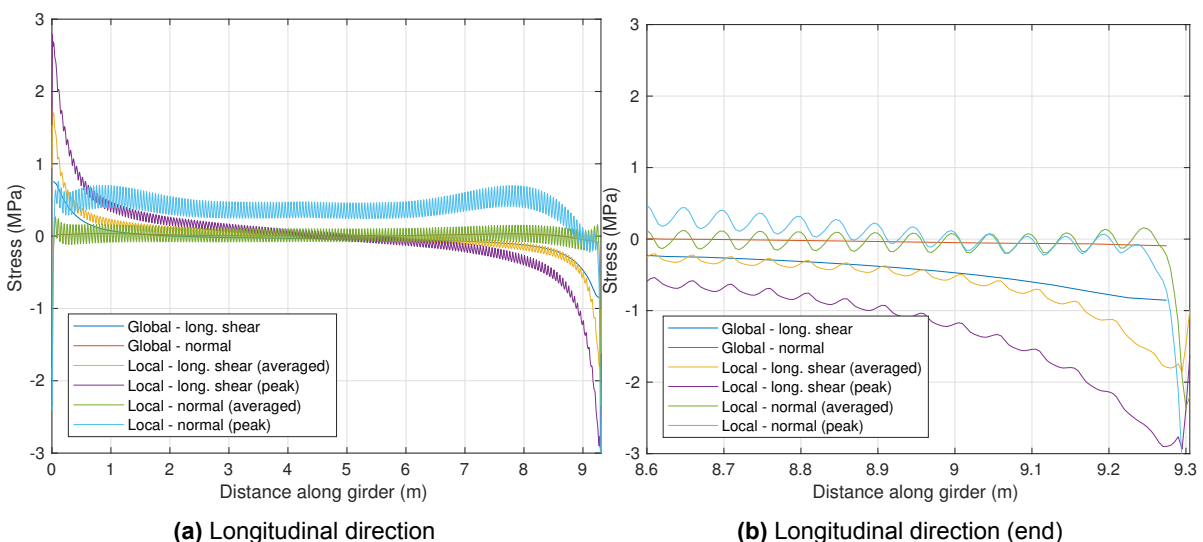
under thermal loading. Vierendeel effect in the last cell of the FRP deck significantly affects the normal stresses under thermal loading. The considered global model is not able to obtain those peak stresses. Compressive stresses found for thermal expansion will be tensile/peeling stresses under thermal contraction, which could be reducing the strength of the bonded connection considerable. It is therefore recommended to improve the global/engineering model to obtain more accurate stress results, especially at the ends of the bonded connection. One could think of decreasing the element size or additionally determine an analytical solution for the Vierendeel effect in the last cell of the FRP deck. Besides, post processing the internal forces to obtain stresses in the bonded connection is rather time consuming. It is suggested to model the adhesive layer with 2D shell elements between the FRP deck (2D elements) and steel girder (1D elements) to directly obtain the stress state from the global model.

Please note that these stress concentration factors depend on many parameters such as geometry, material properties, loading conditions and modelling techniques. Care should be taken when considering these SCF's for engineering purposes.

6.2. Deck-to-main girder

Figure 6.3 shows the stress state in the bonded connection between the deck and main girder from the additional local model considered for thermal analysis (Fig. 5.22). It is loaded by the same uniform temperature component (36°C).

Longitudinal shear stresses from the global model noticeably diverge from the local model towards the ends of the bonded connection (Fig. 6.3b). This effect is caused by incorrect modelling of the local model, as explained in section 5.5.4. A simply supported composite beam is considered as local model consisting of the deck, girders and cross beams, therefore statically determinate. It is loaded by an uniform temperature component that does not result in support reactions.

**Figure 6.3:** Stress state in the bonded deck-to-main girder connection under thermal loading

In reality, the bridge deck is structural indeterminate due to the trunnion bearings at the ends of the four main girders. This is correctly modelled in the global model. Vertical support reactions become

non-zero due to upward curvature of the bridge deck in transverse direction under thermal expansion. Main girders in the centre of the bridge deck are 'pulled' down, additional shear forces are induced in the main girders. These shear forces have an opposite effect on the end slip of the deck and main girder compared to the thermal expansion of the GFRP deck relative to the steel girder. Result is reduced longitudinal shear stresses near the end of the connection for the global model, which is seen in Figure 6.3b. It should be noted that the CTE of the GFRP deck in transverse direction in the global model is twice as large as calculated, leading to non-conservative longitudinal shear stresses.

Apart from the difference in stress results between the global and local model, mentioned above, the local shear lag effect in transverse direction is more pronounced. The SCF_{trans} is 1.6 for the bonded connection with the main girder, which is larger compared to the 1.1 found for the deck-to-secondary girder connection (Table 6.1). It can be concluded that the stiffness of the girder which is bonded to the deck has significantly effect on the stress distribution in transverse direction, SCF_{trans} .

6.3. Conclusions

The following conclusions can be drawn from this chapter:

- Stress results from the global and local models differ significantly (up to 60 % for shear stress), especially at locations of stress concentrations. Effects on local stress distributions in longitudinal and transverse direction are not obtainable in the considered global model.
- Stress concentration factors are determined to relate the stress results from the local and global model; $SCF_{total} = SCF_{long} \cdot SCF_{trans}$. Distinction is made between the longitudinal and transverse effects, in this case Vierendeel and local shear lag effect. Total SCF for longitudinal shear stress is 1.6 for $t=10$ mm and $E=0.6$ GPa under traffic loading.
- Stress concentration factors depend on many parameters (modelling technique, material properties, loading condition, etc.). Care should be taken when these SCF's are considered for engineering purposes.

7

Parametric study

Adhesive selection and geometry are important design choices for the bonded deck-to-girder connections. Elastic modulus and thickness of the adhesive are the main parameters affecting the stiffness of the bonded connection, therefore the local stress state in the adhesive layer and global behaviour, i.e. composite action. A parametric study is performed in this chapter varying adhesive thickness and elastic modulus in the local model loaded by the governing traffic and thermal loads. Goal is to determine and discuss the effects of these two parameters. Additionally, stress concentration factors due to longitudinal and transverse effects are determined as function of the two parameters investigated. Only longitudinal shear stress is considered since it is the predominant component in the Max. Principal stress states determined in Chapter 5 for both load cases. Besides, a fair comparison between combined stresses cannot be made. Many figures are made for this chapter. Figures relating to the results from the thermal loading are therefore put in the appendix.

7.1. Shear stiffness

Relation between the shear stress, elastic modulus and thickness of an isotropic adhesive element loaded in shear is given in Equation 7.4. This equation is derived from the kinematic (Eq. 7.1), constitutive (Eq. 7.2) and material (Eq. 7.3) relations. It can be concluded that the shear stress is proportional to the elastic modulus and inversely proportional to the adhesive thickness. Same relations hold for the bonded deck-to-girder connection, where G corresponds to its shear stiffness, t to adhesive thickness, τ to average lap shear stress and Δx to the relative horizontal displacement between the bottom facing and top flange.

$$\gamma = \frac{\Delta x}{t} \quad (7.1)$$

$$\tau = G\gamma \quad (7.2)$$

$$G = \frac{E}{2(1+\nu)} \quad (7.3)$$

$$\tau = \frac{E}{2(1+\nu)} \frac{\Delta x}{t} \quad (7.4)$$

7.2. Effect of adhesive thickness

Figures 7.1 and A.1 show the longitudinal shear stress distributions in the adhesive layer for four different adhesive thicknesses. As mentioned before, these stress results are from the local model (Fig. 4.2) under the single axle load (400 kN) and uniform temperature component (36 °C). Adhesive thicknesses from 5 to 20 mm are assumed to be representative for (movable) bridges with bonded deck-to-girder connections. In addition, 1 mm thickness is considered as geometrical imperfections and tolerance problems can be expected in real structures. The longitudinal shear stress distributions in the bonded connections between deck and secondary girder are determined for 1, 5, 10 and 20 mm adhesive thickness. Stresses in longitudinal direction, seen in Figures 7.1a and A.1a, are plotted along the edge of the secondary girder. Stresses in transverse direction, seen in Figures 7.1b and A.1b, are plotted at cross section with maximum longitudinal shear stress, i.e. $x=8.99$ m and $x=9.295$ m resp. for traffic and thermal loading. Note that the adhesive elastic modulus of 0.6 GPa and other material properties remained the same.

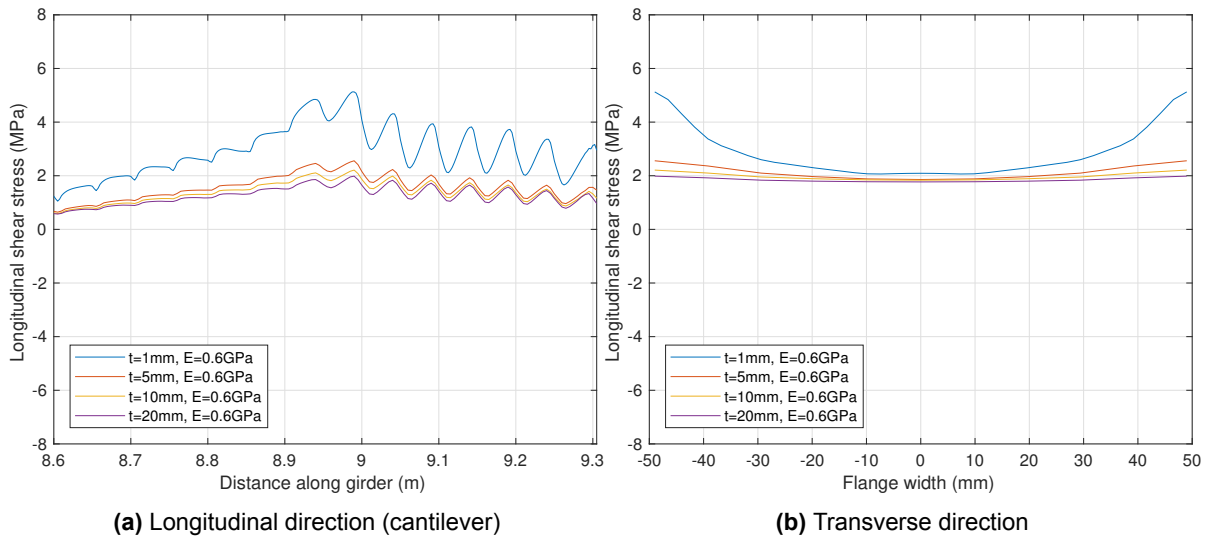


Figure 7.1: Peak longitudinal shear stresses in adhesive layer for different adhesive thickness under traffic loading

Peak stress levels decrease from 5.1 to 2.0 MPa varying the adhesive thickness from 1 to 20 mm under traffic loading. For thermal loading, peak stress level decreased from -6.8 to -1.5 MPa. Large decrease in peak stress level is seen between 1 and 5 mm thickness. Stress peaks due to Vierendeel (longitudinal) and local shear lag (transverse) effect, as explained in Chapter 5, is more pronounced for lower adhesive thickness (Fig. 7.1 and A.1).

7.3. Effect of adhesive elastic modulus

Common type of structural adhesives used in bonded connections are epoxy, acrylic and polyurethane based. Epoxy adhesives generally have high strength and stiffness properties and show brittle behaviour. Polyurethanes are somewhat opposite to epoxies; ductile behaviour, low strength and stiffness properties. Acrylics are characterised by relative high strength, low stiffness and relative high ductility. Best of both worlds one could say for application in bonded deck-to-girder connections in which composite action is not required. Three elastic moduli are considered for the parametric study and ought to be representative for structural adhesives to be used for bonded deck-to-girder connections: 0.6, 3.5 and 7.1 GPa. Figures 7.2 and A.2 show the longitudinal shear stress distributions in the adhesive layer for the aforementioned elastic moduli. Note that the adhesive thickness remained 10 mm for all cases.

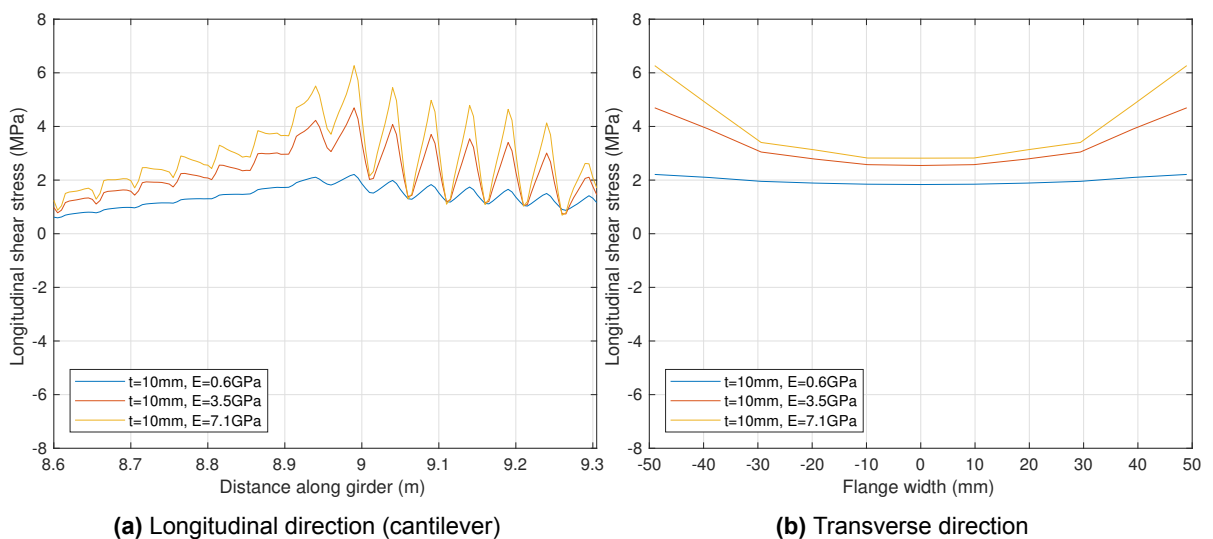


Figure 7.2: Peak longitudinal shear stresses in adhesive layer for different E-modulus under traffic loading

Peak stress levels increase from 2.2 to 6.3 MPa for increasing adhesive elastic modulus from 0.6 to 7.1 GPa under traffic loads, while for thermal loads an increase from -2.3 to -6.2 MPa is obtained. Again, next to increase of total peak stresses, stress peaks due to longitudinal and transverse effects become more pronounced as seen in Figures 7.1 and A.1.

7.4. Extreme cases

Two extreme cases, based on results from previous sections, are considered to determine the longitudinal shear stress distributions with the combined effect of adhesive thickness and elastic modulus resulting in the expected lowest and largest stress peak levels. The two extreme cases consists of (1) $t=1\text{ mm}$ and $E=7.1\text{ GPa}$, and (2) $t=20\text{ mm}$ and $E=0.6\text{ GPa}$. Figures 7.3 and 7.4 show the stress distributions in longitudinal and transverse direction under respectively traffic and thermal loading.

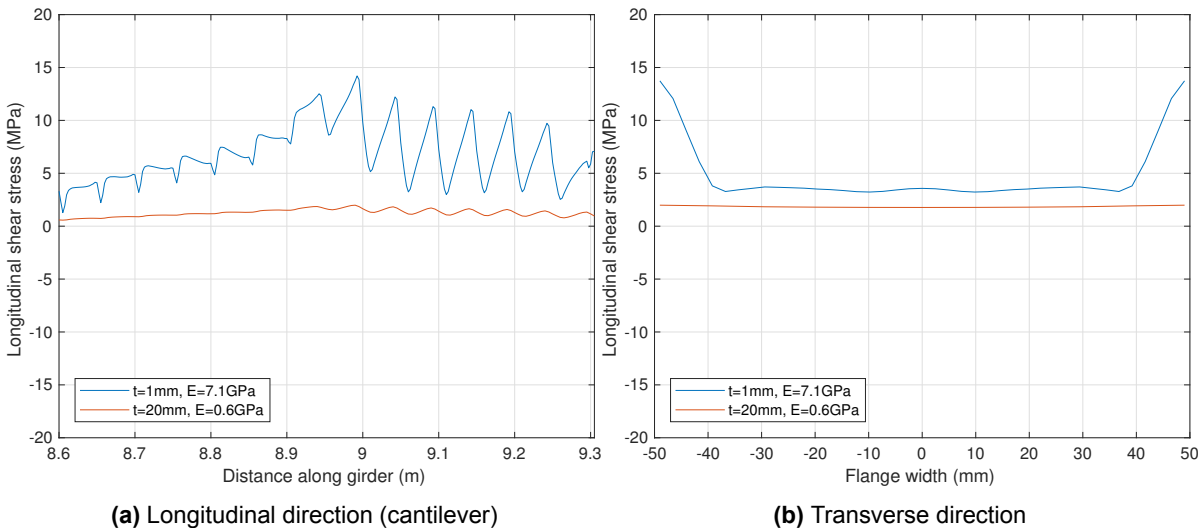


Figure 7.3: Peak longitudinal shear stresses in adhesive layer for two extreme cases under traffic loading

As expected, significant increase is peak stress levels seen between the extreme cases. Stress peak levels increase from 2 to 14 MPa under traffic loading. An increase of -1.5 to -17 MPa is seen for thermal loading. The local shear lag and Vierendeel effect is this time very noticeable (Fig. 7.3 and 7.4).

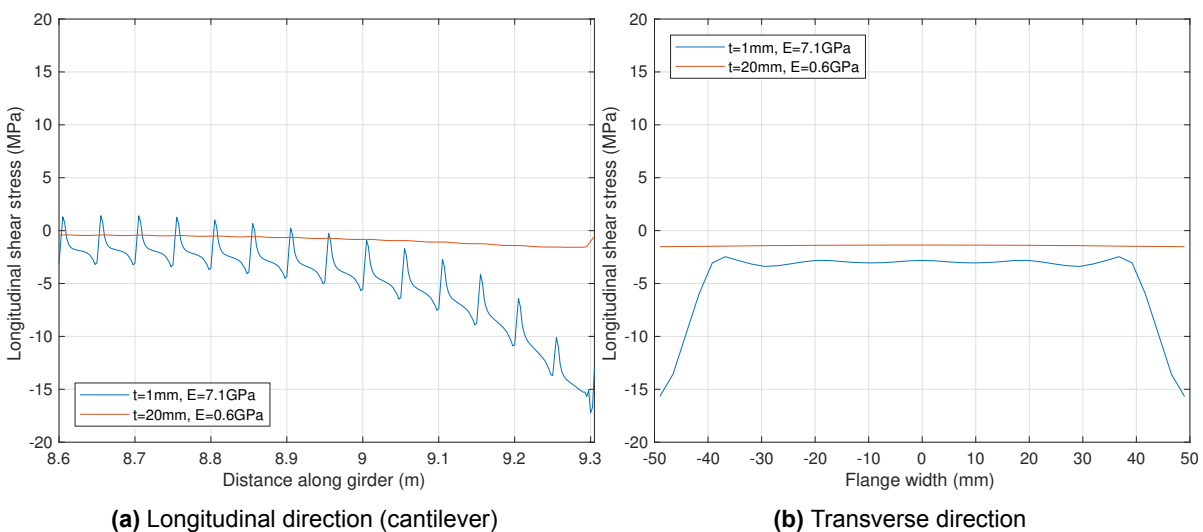


Figure 7.4: Peak longitudinal shear stresses in adhesive layer for two extreme cases under thermal loading

7.5. Parametric relations

It can be concluded that longitudinal shear stress levels increase for decreasing adhesive thickness, especially at locations with stress concentrations. This applies to both traffic and thermal loads.

The increase in stress levels can be explained by the increased shear stiffness of the bonded connection and the adhesive layer itself. Peak stresses due to the Vierendeel (longitudinal) and local shear lag (transverse) effect increase as the adhesive layer becomes more stiff. There is less distribution of stresses for a more stiff adhesive layer, therefore increased stress peaks.

Stresses averaged over width of the flange increases as well. This is caused by the increased degree of composite action between the FRP deck and steel girder. As the shear stiffness of the bonded deck-to-girder increases, the contribution of the FRP deck increase and therefore larger shear stresses in the bonded connection.

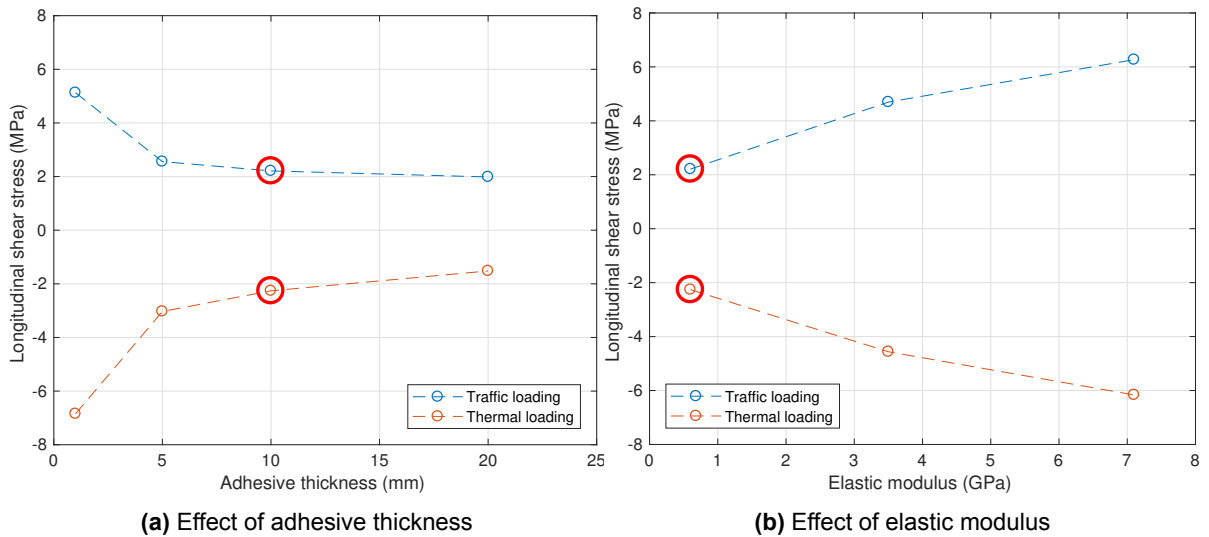


Figure 7.5: Effect of adhesive thickness and elastic modulus on peak longitudinal shear stress levels

Figure 7.5 shows the relationship between the peak longitudinal shear stresses, adhesive thickness and elastic modulus under traffic and thermal loading. As discussed in Chapter 5, longitudinal shear stress peaks occur at 8.990 m and 9.295 m for the single axle and uniform temperature component loads, respectively. The adhesive thickness and elastic modulus considered in the case study design are marked in red. Note that the stress levels under the considered traffic and thermal loads are coincidentally similar. Different axle load or temperature difference would obviously result in other stress levels.

Similar trends are seen for the effects of adhesive thickness and elastic modulus on the longitudinal shear peak stress levels for both traffic and thermal loading (Fig. 7.5). Decrease in longitudinal shear stress, due to the loss of stiffness, is more pronounced in the range of 1 to 5 mm adhesive thickness than between 5 to 20 mm, see Figure 7.5a. Increase in longitudinal shear stress peak levels (roughly 300%) in the range of 0.6 to 7.1 GPa is somewhat constant (Fig. 7.5b). Note that only short-term loads are considered. Long-term effects such as creep and (environmental) ageing have to be investigated separately.

Please note that these stress results are obtained for constant adhesive thickness. In reality, geometrical imperfections of the bonded surface result in varying adhesive layer thickness in longitudinal and transverse direction. Strength and stiffness of the bonded deck-to-girder connection will be affected due to this, leading to different stress distributions and possible reduced strength performance.

7.6. Stress concentration factors

Stress concentration factors due the longitudinal and transverse effects, are determined for different adhesive thickness and elastic modulus. Similar method to determine the SCF's is considered as in Section 6.1. Only SCF's for longitudinal shear stresses are considered since the SCF for normal stress under thermal loading showed a excessive difference with the SCF for normal stress under traffic loading and should be investigated in future work, see Table 6.1. Effects from local bending of the last web of the FRP deck and the expansion of the adhesive layer at the extreme end of the bonded connection has apparently significant effect on the local stress distribution, which is not obtained in the results from the global model.

(Peak) longitudinal shear stress distributions from the global and local model for different adhesive thickness and elastic modulus under traffic and thermal loading are presented in Figure 7.6, A.4, A.3 and A.5. The stress levels are obtained at the FRP/adhesive interface as experimental results showed dominant laminate failure (Sec. 8.2). To recall, SCF_{long} is calculated by dividing the local (average) stresses by the stresses from the global model, corresponding to the effects in longitudinal direction. Meanwhile SCF_{trans} is calculated by dividing the local (peak) stress by the local (average) stress, corresponding to the effects in transverse direction. Multiplying aforementioned SCF's results in the total SCF relating the peak stress levels from the global and local model.

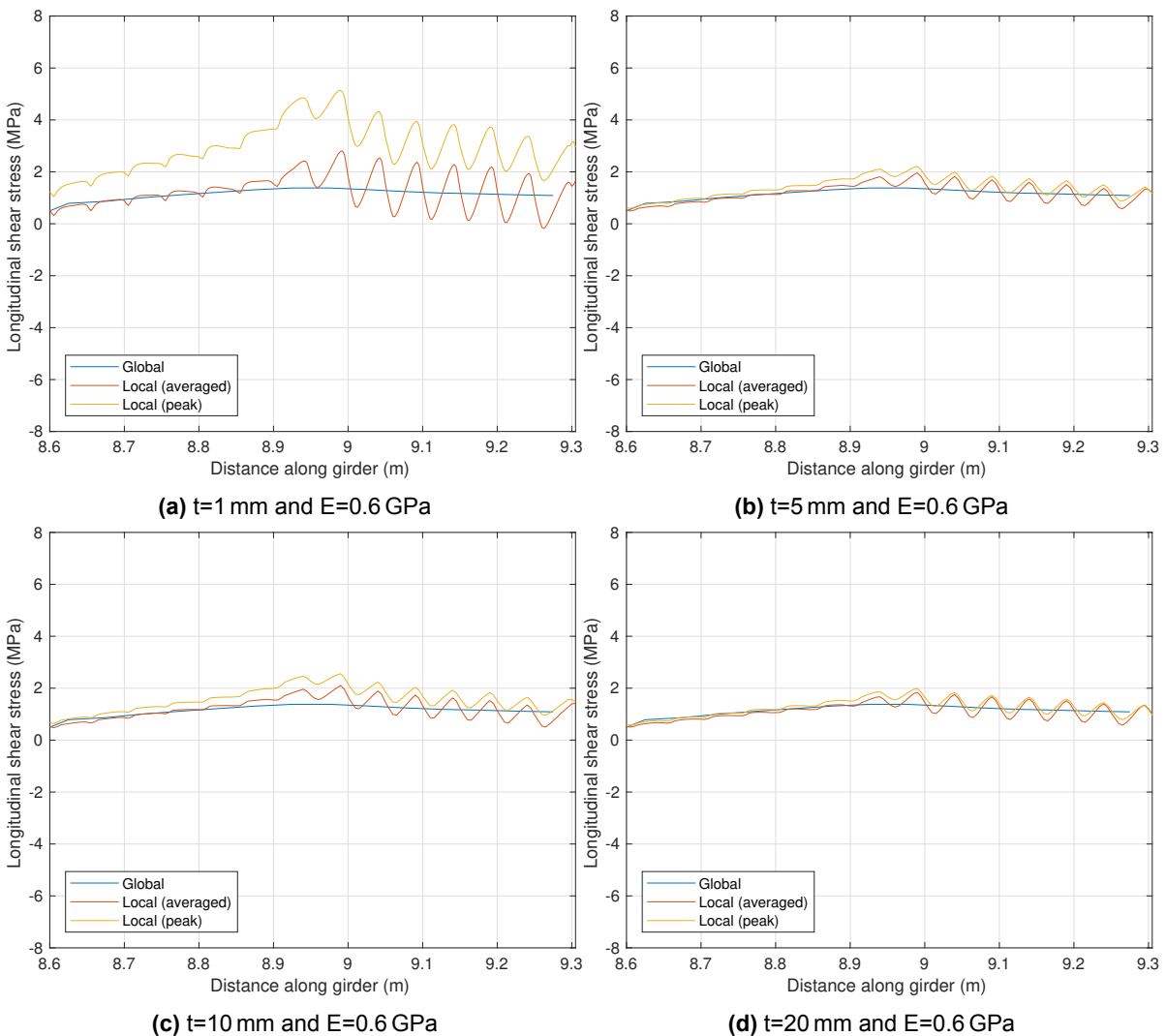


Figure 7.6: Longitudinal shear stresses in longitudinal direction for different adhesive thickness under traffic loading

Table 7.1: SCF's for longitudinal shear stress under traffic and thermal loading

	Traffic						Thermal					
t (mm)	1	5	10	20	10	10	1	5	10	20	10	10
E (GPa)	0.6	0.6	0.6	0.6	3.5	7.1	0.6	0.6	0.6	0.6	3.5	7.1
SCF_{long}	2.0	1.5	1.4	1.3	2.3	2.7	2.1	1.3	1.1	0.8	1.6	1.8
SCF_{trans}	1.8	1.2	1.1	1.1	1.5	1.7	1.8	1.2	1.1	1.1	1.5	1.6
SCF_{total}	3.7	1.9	1.6	1.4	3.4	4.5	3.9	1.6	1.2	0.9	2.2	3.0

Table 7.1 shows the stress concentration factors determined from the aforementioned figures. Maximum total SCF of 4.5 is obtained for traffic loading with $t=10$ mm and $E=7.1$ GPa. Minimum total SCF is obtained for thermal loading at $t=20$ mm and $E=0.6$ GPa, namely 0.9. The latter SCF seems odd as it is below 1.0. Stress peak level obtained from the local model is therefore lower compared to the peak stress level from the global model, seen in Figure A.4d. It can be seen in Table 7.1 that the SCF_{long} is 0.8, therefore the global stress levels are even below average stress levels from the local model. It could be expected that the longitudinal shear stresses become non-uniform through thickness for the large 20 mm adhesive thickness. Longitudinal shear stress distribution in the adhesive layer at the extreme end is seen in Figure 7.7. Stresses do indeed vary much through-thickness and are lower at the FRP/adhesive interface compared to the steel/adhesive interface. Local effects from the Vierendeel at the last web and thermal expansion of the adhesive layer itself have significant effect.

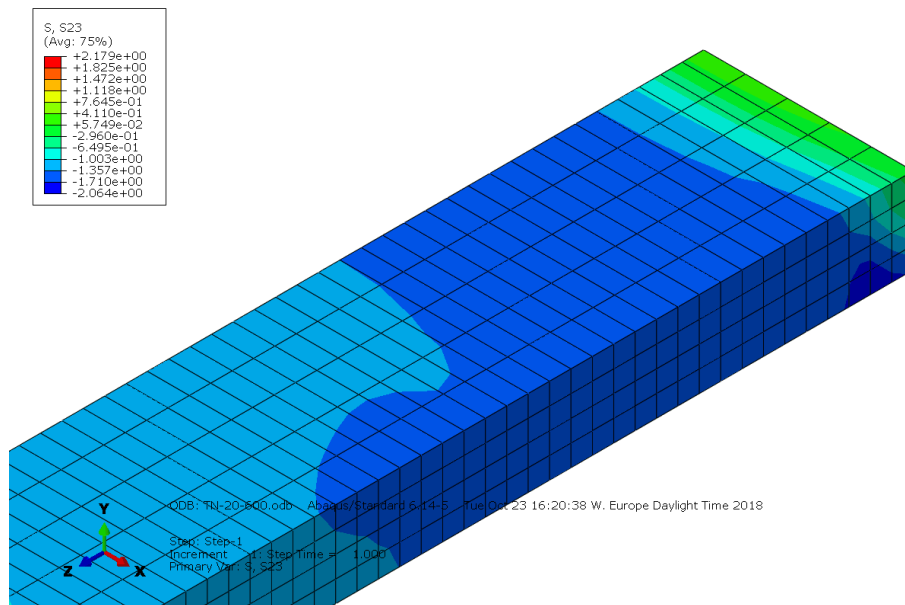


Figure 7.7: Longitudinal shear stress distribution in adhesive layer at extreme end of bonded connection under thermal loading from Abaqus, $t=20$ mm and $E=0.6$ GPa

Figure 7.8 shows the individual SCF's due to effects in longitudinal and transverse direction for different adhesive thickness and elastic modulus for both traffic and thermal loading. SCF's due to effects in longitudinal direction, SCF_{long} , show the largest variation for the considered ranges of adhesive thickness and elastic modulus, namely from 0.8 to 2.1 for different adhesive thickness under thermal loading (Fig. 7.8a), and 1.4 to 2.7 for different elastic modulus under traffic loading (Fig. 7.8c).

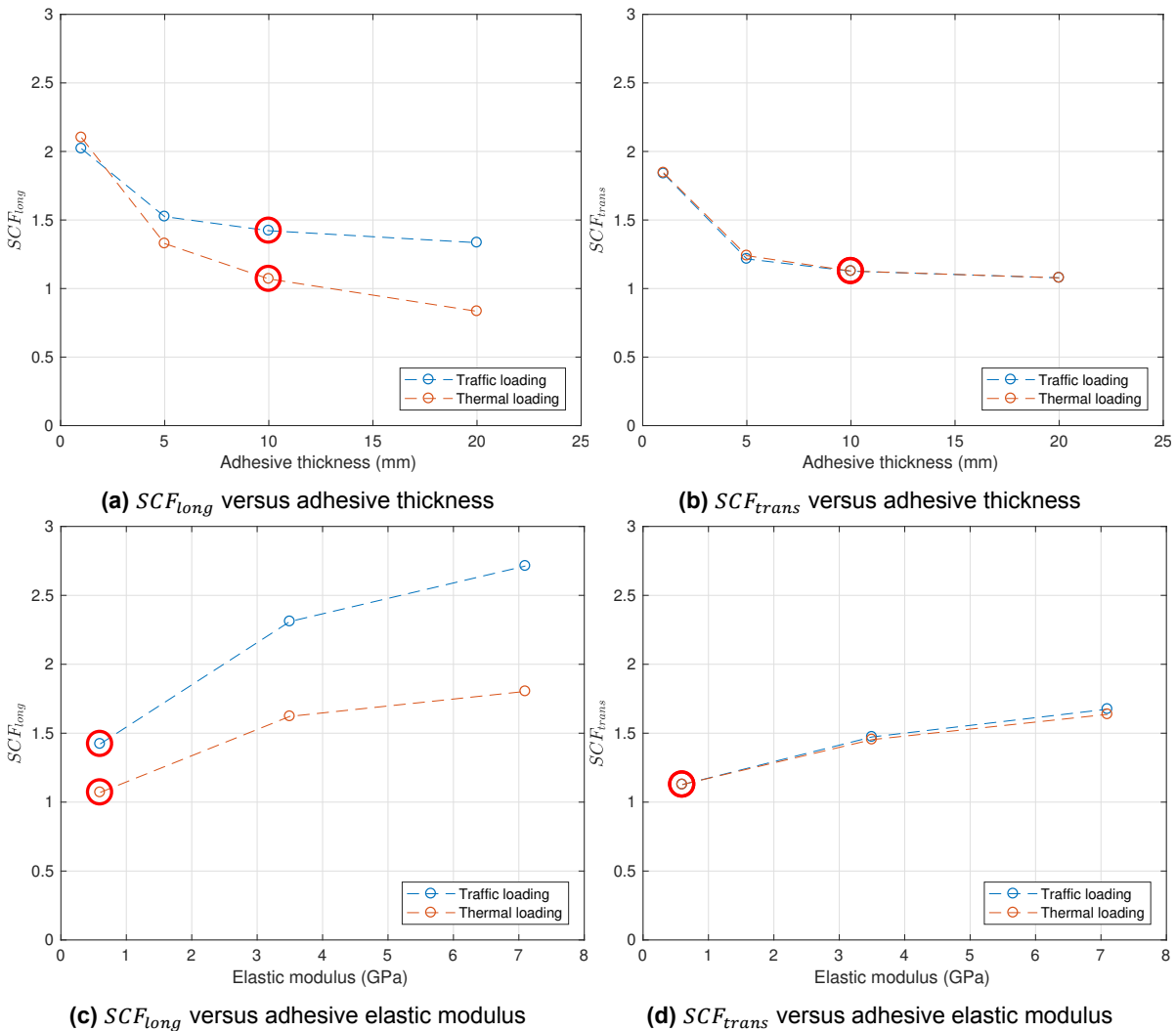


Figure 7.8: Longitudinal shear stress concentration factors for different adhesive thickness and elastic modulus

The SCF_{long} shows diverging trends between traffic and thermal loading for increasing adhesive thickness and elastic modulus. It can be concluded that the SCF due to longitudinal effect, in this case Vierendeel effect, is depending on the loading condition. Meanwhile, the SCF_{trans} shows similar trends for traffic and thermal loading (Fig. 7.8b and 7.8d). It can be concluded that the SCF due to transverse effects, in this case local shear lag, is load independent. Possible explanation for the load dependency could be the additional effect of the thermal expansion of the adhesive layer itself. The stress states become more affected for higher elastic modulus and larger thickness by this effect. Finally, both SCF's show high dependency on adhesive thickness and elastic modulus. SCF_{long} decreases for higher adhesive thickness and lower elastic modulus because the stress variations due to the local bending in the webs of the deck (Vierendeel effect) become lower. A more flexible bonded joint allows redistribution of stresses and lower peaks. Same principle holds for the SCF_{trans} in which the local shear effect becomes less pronounced. Asymptote peak stress levels are expected from the local model for infinite stiffness of the bonded joint, therefore also for the SCF's.

Next step for future work could be to determine stress levels from local model averaged in longitudinal direction and compare those with global results.

7.7. Composite action

Three cases are considered to determine the effect on the composite action between the FRP deck and steel girder under traffic loading, namely $t=5$ mm and $E=7.1$ GPa, $t=10$ mm and $E=3.5$ GPa, and $t=20$ mm and $E=0.6$ GPa. The longitudinal strain distribution over the height of the FRP deck, adhesive layer and steel girder at level of the web of the girder is plotted in Figure 7.9 to observe possible slip between the deck and girder, i.e. reduced composite action. The cross section just after the last cross beam, $x=8.775$ m, is considered because maximum hogging bending moment occurs in this cross section as it is the begin of the cantilever part (Fig. 5.10a). Longitudinal strain levels are obtained at four locations: (1) bottom of the steel girder (0 mm), (2) at the interface of the top flange and adhesive layer (220 mm), (3) at the interface of the GFRP bottom facing and adhesive layer (225, 230 or 240 mm), and (4) at the GFRP top facing (335, 340 or 350 mm). Strains are linearly interpolated between these locations.

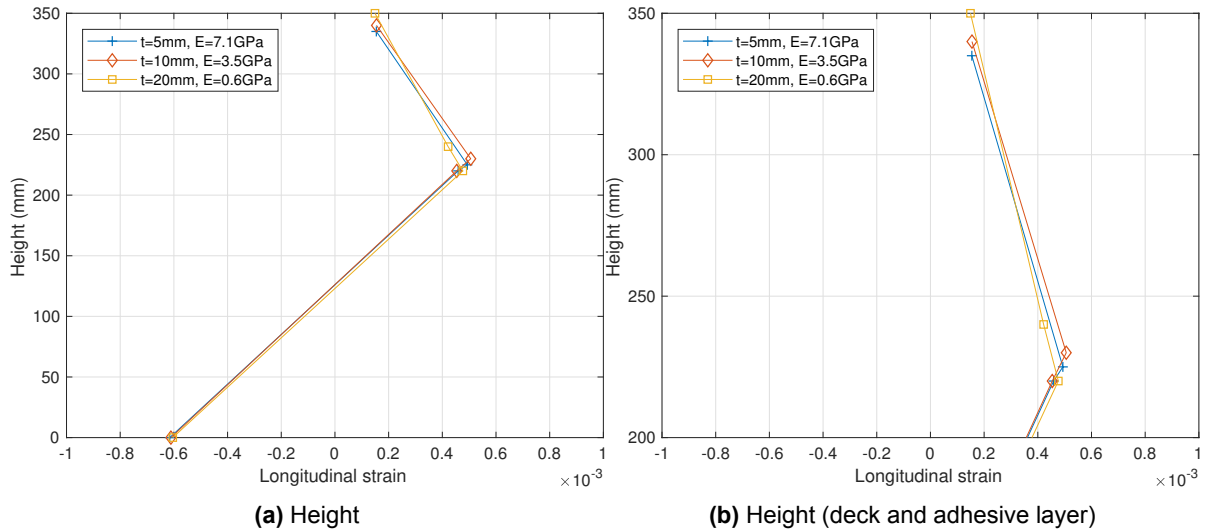


Figure 7.9: Longitudinal strain over height under traffic loading ($x=8.775$ m, $y=0$ mm)

Compressive strains are seen at the bottom of the girder. Tensile strains at the top flange, adhesive and FRP deck. Not surprising considering the hogging bending moment in the cross section. Strain distributions over the height of the girder (0 to 220 mm) are almost equal for all three cases. Also the strains at the top facing are similar.

Difference is however seen at location of the adhesive layer (Fig. 7.9b). Slip, i.e. relative displacement between deck and girder, is seen for the case with $t=20$ mm and $E=0.6$ GPa. The slip is however negligible, only 0.02 mm. No slip is seen for the other two cases.

It can therefore be concluded that the bonded FRP/steel deck-to-girder connection has sufficient shear stiffness to provide full composite action, even for large thickness and low elastic modulus of the adhesive. In addition, deflections at the cantilever end of the secondary girder under the traffic load are similar all three cases, see Table 7.2.

Table 7.2: Deflection cantilever end secondary girder under traffic loading

Adhesive thickness	Elastic modulus	Deflection
5 mm	7.1 GPa	3.89 mm
10 mm	3.5 GPa	3.86 mm
20 mm	0.6 GPa	3.88 mm

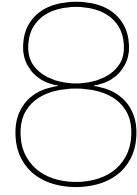
Although the bonded connection provides full composite action, effects on global behaviour, i.e. reduced deflections are negligible. This is due to the low in-plane shear stiffness of the FRP facings and low out-of-plane shear stiffness of the entire FRP deck. The latter effect is seen in Figure 7.9b.

Longitudinal strains at the top facing are lower compared to the bottom facing (Fig. 5.10a). Besides, the neutral axis is seen at almost half the girder height, therefore low contribution of the FRP deck to the bending moment resistance of the composite girder (Fig. 7.9). **Please note that composite action was not required for the case study bridge, therefore deliberately low stiffness is considered for the FRP deck in longitudinal direction, reducing stresses in the bonded connection.**

7.8. Conclusions

Following conclusions can be drawn from this chapter:

- Total increase of peak stress levels due to longitudinal and transverse effects is dependent on thickness and elastic modulus of the adhesive. Stress peaks increased with 610 % and 1,047 % between the extreme cases under traffic and thermal loading, respectively. This is caused by the increased stiffness of the bonded deck-to-girder connection.
- Larger increase in peak stress is seen in between the range of 1 to 5 mm adhesive thickness (136 %) compared to 5 to 20 mm (83 %) under thermal loading.
- Peak stresses increase almost linearly in the adhesive elastic modulus range of 0.6 to 7.1 GPa (147 %) for both traffic and thermal loading.
- Maximum total SCF of 4.5 is obtained for $t=10$ mm and $E=7.1$ GPa under traffic loading. Minimum total SCF is obtained for $t=20$ mm and $E=0.6$ GPa under thermal loading.
- SCF's due to effects in longitudinal direction show larger variation (0.8 to 2.0) compared to the SCF due to effects in transverse direction (1.1 to 1.8) between the considered ranges of adhesive thickness and elastic modulus. Both dependent on adhesive thickness and elastic modulus. SCF_{trans} is independent of the loading condition, while SCF_{long} is dependent on loading condition.
- Bonded deck-to-girder connections have sufficient shear stiffness to provide full composite action, even for large thickness and low elastic modulus of the adhesive.
- Contribution of the FRP deck to the bending resistance of the composite girder is rather low due to relative low stiffness of the FRP deck compared to steel girder.



Strength performance

8.1. Required strength

The required (static) strength of the considered bonded GFRP/steel deck-to-girder connection is determined based on the stress results from the structural analysis in Chapter 5 and literature on fatigue strength from Chapter 2.

Peak longitudinal shear stress level of 2.2 MPa is obtained in the bonded connection between the FRP deck and steel secondary girder under the single axle load (400 kN) from the local model (Fig. 5.6b). In addition, the stress concentration factors obtained from the comparison of stress results from the global and local model (Table 6.1) are used to tweak the fatigue shear stress ranges obtained from the global model under FLM4b (Fig. 5.12). The stress concentration factor for longitudinal shear stresses is 1.6 considering the local model with adhesive thickness 10 mm and 0.6 GPa elastic modulus. The tweaked fatigue stresses are presented in Figure 2.7. The vertical position of the slope is set such that the total fatigue damage is equal to 1. The fatigue damage is calculated according to Palmgren-Miner rule assuming a constant slope of 1:10, obtained from the work of Keller [11] and Khabbaz [12].

Static strength is generally lower compared to the dynamic strength, i.e. fatigue strength at $N=1$, due to the difference in failure mechanism/mode. This is also in the experimental results from Khabbaz [12]. Static strength values seen in Figure 2.7b are lower compared to the extrapolated S-N curve (dashed line) according to the power model, namely 40 kN versus 28 kN static strength (marked in black triangles). This is roughly 70% of the static strength. **If similar ratio between static and dynamic strength is considered applied on the required fatigue lap shear strength shown in Figure 5.12b, the required static lap shear strength of the bonded GFRP/steel deck-to-girder connection is in the range of 4 to 5 MPa.**

The assumed stress ranges due to the thermal cycles from Section 5.5.3 had negligible effect on the required lap shear strength, namely 5.41 MPa compared to 5.40 MPa without thermal cycles. Required fatigue normal strength, i.e. tension or compression, is not determined because there is no data known to the author on the possible S-N curve for fatigue performance of bonded GFRP joints in mode 1 loading.

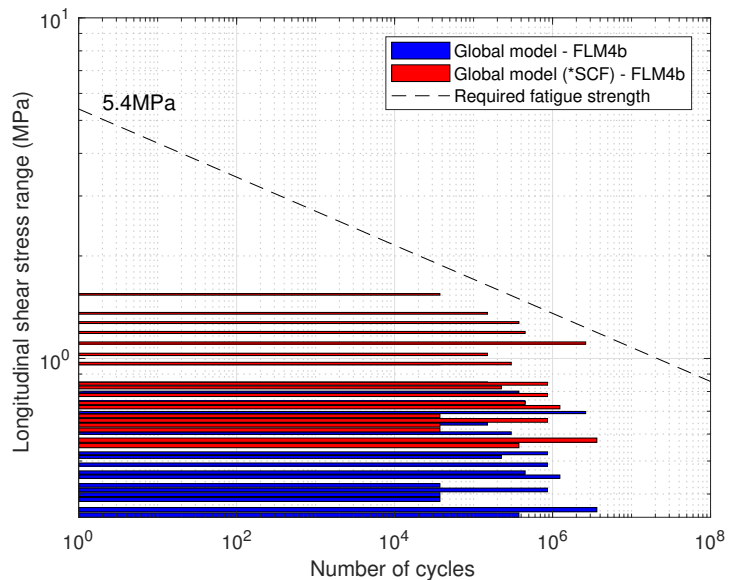


Figure 8.1: Fatigue shear stress ranges from global model under FLM4b and required lap shear fatigue strength

8.2. Strength prediction

Subsequently, key question would be if the static strength of the bonded GFRP/steel connection satisfies the requirement of 4-5 MPa. Only little information is available on the strength of bonded FRP/steel joints. Therefore a strength prediction is made based experimental results from literature and data on the adhesive manufacturer.

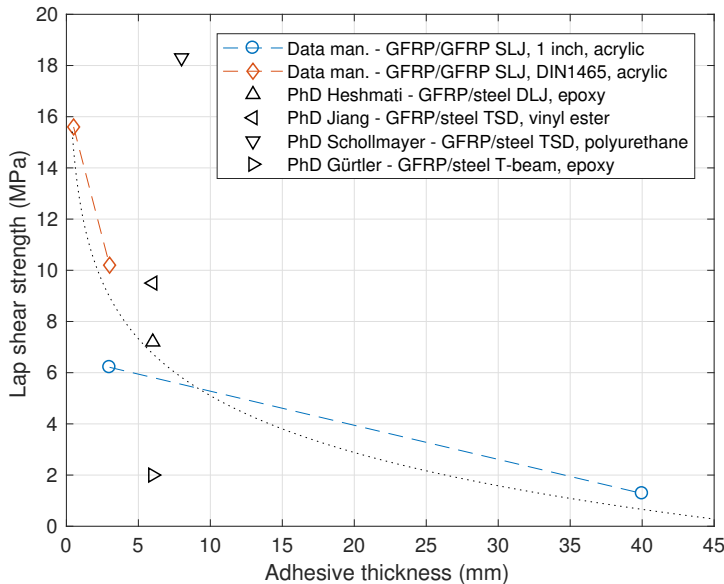


Figure 8.2: Lap shear strength versus adhesive thickness of bonded (GFRP/steel) joints. *Tensile-shear loading device

Lap shear strengths presented in Figure 8.2 are calculated dividing the ultimate load at failure by the bonded surface area, therefore averaged. Experimental strength results from PhD theses (Gürtler [8], Heshmati [9], Jiang [10] and Schöllmayer [14]) on bonded FRP/steel joints considered one adhesive thickness. Each having different material properties, geometry, surface treatment and loading conditions. As mentioned in the Chapter 2, there is a decreasing trend of lap shear strength for increasing adhesive thickness in bonded lap shear joints [13]. Also known as a thickness effect. It is therefore difficult to account for this effect with only one data point. The presented results from the PhD theses are still useful as indicative values for lap shear strengths of bonded FRP/steel joints.

The manufacturer of the acrylic based adhesive however, did perform single-lap joint (SLJ) tests for different adhesive thickness. The small scale specimens consisted of GFRP adherends, with polyester matrix, and the same acrylic based adhesive as considered in the case study. Exact testing setup, dimensions and material properties of the GFRP adherends are unfortunately unknown to the author. Adherend thickness is assumed to be 10-12 mm and adherend width 1-2 inch based on photo's of the setup. Overlap lengths considered in the tests are 1 inch. The first data set, seen in orange (Fig. 8.2), is performed with an adhesive thickness of 0.5 and 3 mm. The second data SLJ test set, also with GFRP adherends, is performed for 3 and 40 mm adhesive thickness is seen in blue (Fig. 8.2).

A trendline is plotted through the four data points from the manufacturer to have at least a reference value for the static strength to compare with the obtained (peak) stress levels from the structural analysis. A logarithmic trendline showed the best fit, namely $R^2 = 0.91$. **The static lap shear strength of the bonded GFRP/steel deck-to-girder connection is assumed to be 5 MPa considering the trendline at 10 mm adhesive thickness. Although the strength is in the approximate range of the obtained requirement, there are still uncertainties related to the strength prediction:**

1. All SLJ tests on the manufacturer failed by fibre-tear, meaning failure of the GFRP material. Trough-thickness stresses exceeded the interlaminar strength of the GFRP laminates. The bonded GFRP/steel deck-to-girder connection could have different failure mode(s).
2. Experimental results on the manufacturer are interpolated considering a logarithmic trendline. Actual relationship between strength and adhesive thickness should be tested.
3. Peak stress levels obtained from the structural analysis are compared with lap shear strengths averaged over the bonded surface, thus conservative.
4. Difference in geometry between small scale SLJ and large scale bonded GFRP/steel deck-to-girder connections results in different stress states and possibly different strength performance.
5. SLJ tests consisted of similar GFRP adherends. Dissimilar stiffness of adherends, such as in the bonded GFRP/steel deck-to-girder connections, results in increased peak stresses therefore

reducing strength performance.

6. Bonded deck-to-girder connections are multi-axially loaded, while the SLJ tests are uni-axially loaded. Complex stress states in the bonded FRP/steel deck-to-girder connection might show lower strength performance.

8.3. Recommendation for experimental program

Ideally, one would determine the strength of the bonded FRP/steel deck-to-girder connection in a large scale test to obtain the most accurate results and determine coupled global and local behaviour. The author suggest a more cost and time effective experimental program to determine the static and fatigue strength of a bonded FRP/steel deck-to-girder connection.

It includes static and fatigue tests on a bonded FRP/steel double-lap joint (DLJ) for various adhesive thickness, in which the inner adherend is steel and the outer adherends from FRP material. DLJ is considered because the stress state is somewhat similar to the one found in the deck-to-girder connection, i.e. dominant longitudinal shear stress. Single-lap joints (SLJ) show larger peeling stresses which reduce strength performance as explained in Chapter 2.

Material properties of the adhesive and adherends should be determined prior to the joint tests to obtain a detailed stress distribution in the bonded connection using FEA. This comprises elastic, strength and thermal properties. Emphasis should be put on the interlaminar (shear) strength of the FRP laminates as it is shown to be the governing parameter in the fatigue tests performed by the manufacturer.

Static strength tests of the DLJ should be performed for different under both tension and compression loading to account for different failure modes. Khabbaz [12] observed similar failure modes for corresponding fatigue loading, i.e. R-ratios. DLJ specimens with different overlap lengths would be needed to determine the asymptote that would lead to experimentally determined static peak strength. ASTM D3528 could be considered as standard for DLJ tests.

When it comes to fatigue strength, the author suggest to perform fatigue tests on the same DLJ at constant amplitude load ranges at 30, 50 and 70 % of the static strength determined from the static DLJ tests under various R-ratios, let's say $R=-1$, $R=0.1$ and $R=10$. And again for various adhesive thickness. Similar test setup is recommended as Khabbaz has used [12] (Fig. 2.6) or same setup as mentioned above. In this way, the load-life or S-N diagram can be constructed and be used for fatigue analysis depending on different adhesive thickness and R-ratio.

Lastly, it is recommended to experimentally determine the static and fatigue tensile strengths. Thereby the strength performance is covered for both mode 1 and mode 2 of the bonded connection. Ideally, mixed modes tests are performed considering the complex stress states in the deck-to-girder connections. Tensile-shear loading devices as used by Schollmayer [14] and Jiang [10] can be considered.

8.4. Conclusions

The following conclusions can be drawn from this chapter:

- The required static lap shear strength of the bonded GFRP/steel deck-to-girder connection is in the range of 4 to 5 MPa based on the fatigue analysis performed on the global model including the derived SCF.
- The predicted static lap shear strength is 5 MPa based on GFRP/GFRP SLJ tests with various adhesive thickness. Although the strength is in the approximate range of the obtained requirement, there are still uncertainties related to the laminate failure.
- Stresses from the local model should be determined at the FRP/adhesive interface, as failure of the SLJ specimens was governed by laminate failure.

Conclusions and recommendations

9.1. Main conclusions

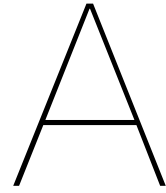
The following main conclusions can be drawn from this work:

1. **Bonded FRP/steel deck-to-girder connections are critical details in movable bridges.** The predicted lap shear strength of the bonded GFRP/steel connection with acrylic based adhesive (5 MPa) is in the approximate range of the required lap shear strength (4-5 MPa). However, there are uncertainties related to the laminate failure of the experimental results, hence the call for more detailed analysis of localised strength with various adhesive thicknesses.
2. **Stress concentrations occur along the edges and ends of the bonded FRP/steel deck-to-girder connections.** Longitudinal shear stress peaks (2.3 MPa) at the end of the bonded connection are approximately 8 times larger compared to the average stresses (0.3 MPa) in longitudinal direction under thermal loading. Stress peaks in transverse direction along the edge are approximately twice as large compared to stresses at level of the web of the girder.
3. **Stress results from the global model differ significantly from the local model, especially at the ends of the bonded connections.** Peak longitudinal shear stress levels from the local model under traffic loading, with 10 mm adhesive thickness and 0.6 GPa elastic modulus, are 1.6 times larger compared to the stresses from the global model due to longitudinal (Vierendeel) and transverse (local shear lag) effects.
4. **Stress concentration factors (SCF) are determined to relate the peak stress levels from the global to the local model.** The total SCF, SCF_{total} , is given by the multiplication of SCF_{long} and SCF_{trans} , corresponding to the longitudinal and transverse effects. Both dependent on adhesive thickness and elastic modulus. SCF_{trans} is independent of the considered loads, while SCF_{long} is. SCF_{total} ranges from 0.9 to 4.5 and is also highly dependent on modelling technique. Care should be taken using this SCF's for engineering purposes.
5. **Peak stress levels increase for lower adhesive thickness and higher adhesive elastic modulus.** This is caused by increased stiffness of the bonded connection. Longitudinal shear stress peaks increase by 351 % (1.5 to 6.8 MPa) for decreasing the adhesive thickness from 20 to 1 mm under thermal loading. Longitudinal shear stress peaks increase by 138 % (2.3 to 6.2 MPa) for increasing the adhesive elastic modulus from 0.6 to 7.1 GPa under thermal loading.
6. **Bonded FRP/steel deck-to-girder connections have sufficient shear stiffness to provide full composite action,** even for large adhesive thickness (20 mm) and low elastic modulus (0.6 GPa). Contribution of the top facing to the bending moment resistance of the composite girder is however low due to the low out-of-plane shear stiffness of the entire FRP deck in longitudinal direction.

9.2. Recommendations

Following aspects could be considered in future work:

- Improve modelling technique for global/engineering models to obtain a more detailed stress state in the bonded deck-to-girder connections, especially at the ends.
- Experimentally determine the static and fatigue strength of bonded FRP/steel joints under both tensile and shear loading conditions with various adhesive thickness.
- Determine the effects of geometrical imperfections on strength and stiffness performance of adhesively bonded FRP/steel connections.
- Include short-term, long-term and environmental effects on strength performance of bonded FRP/steel connections such as curing, ageing, creep, freeze-thaw cycles, temperature, moisture, etc.
- Determine recommendations/norms on thermal load cycles for composite FRP/steel bridges.



Figures

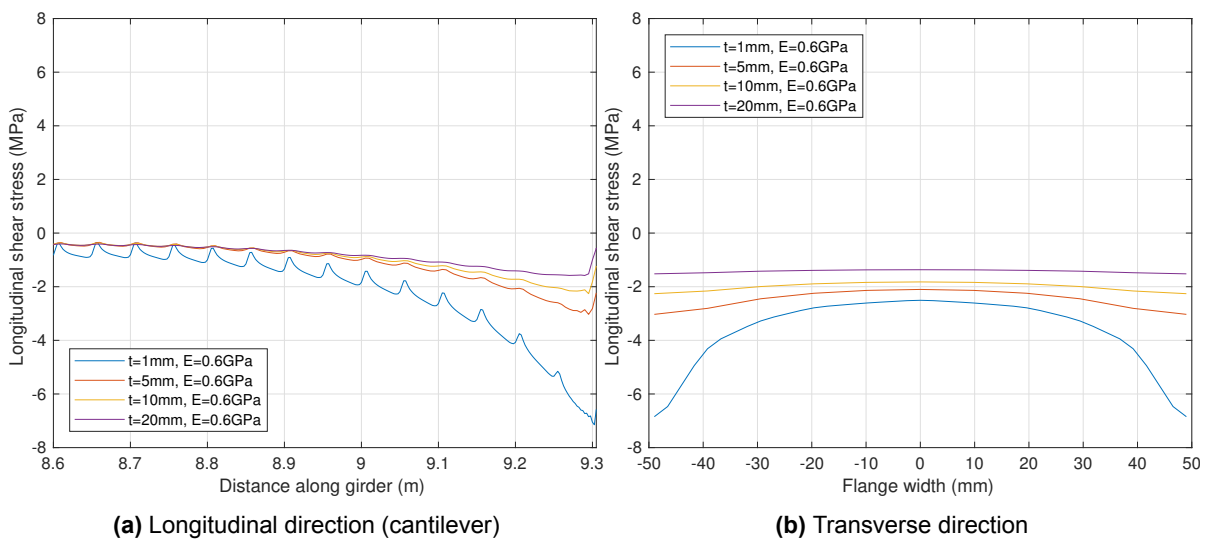


Figure A.1: Longitudinal shear stresses in adhesive layer for different thickness under thermal loading

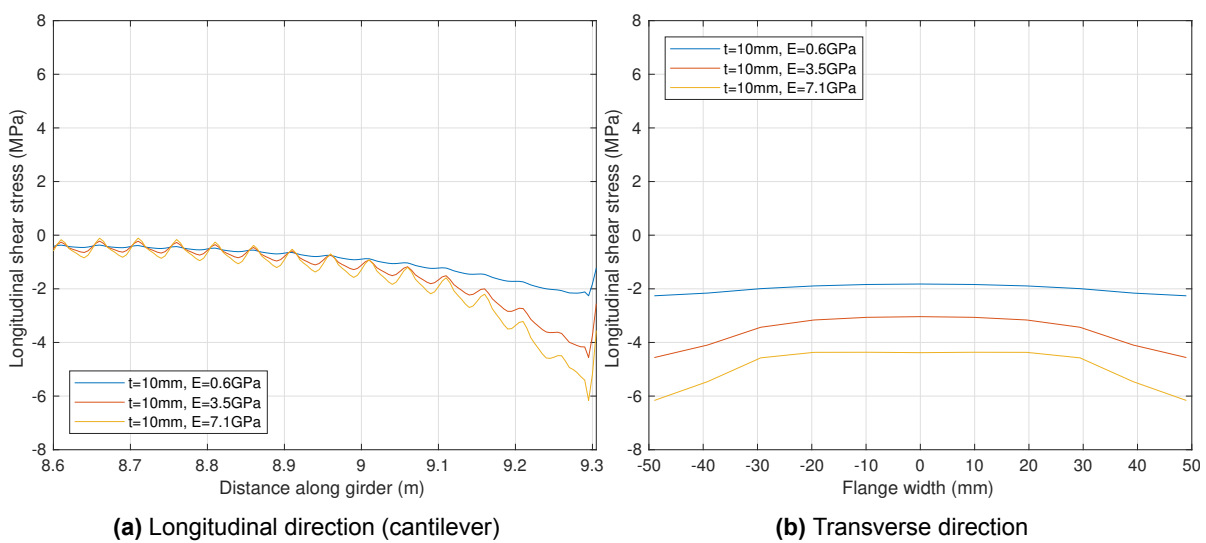


Figure A.2: Longitudinal shear stresses in adhesive layer for different modulus under thermal loading

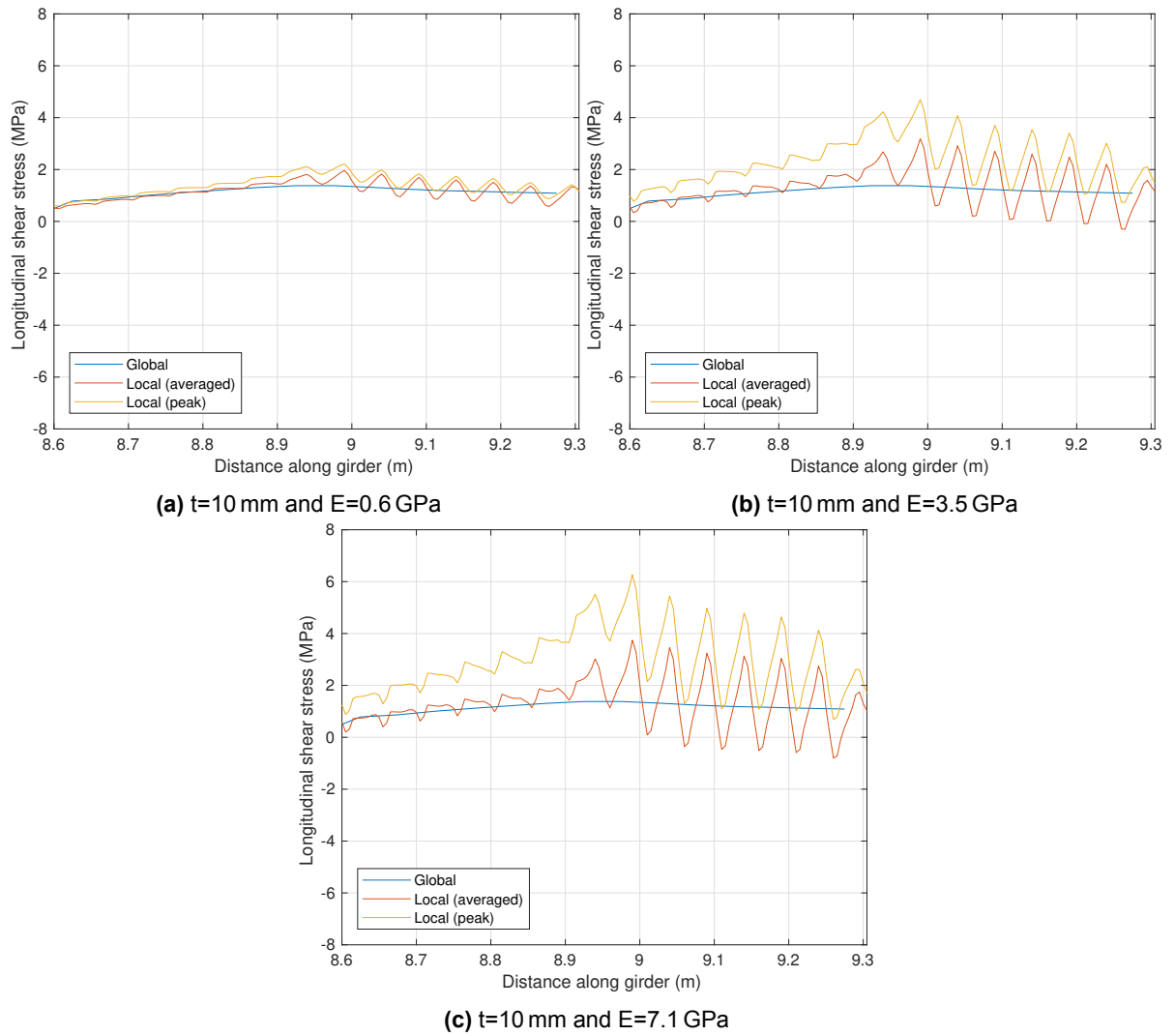


Figure A.3: Longitudinal shear stresses in longitudinal direction for different adhesive elastic modulus under traffic loading

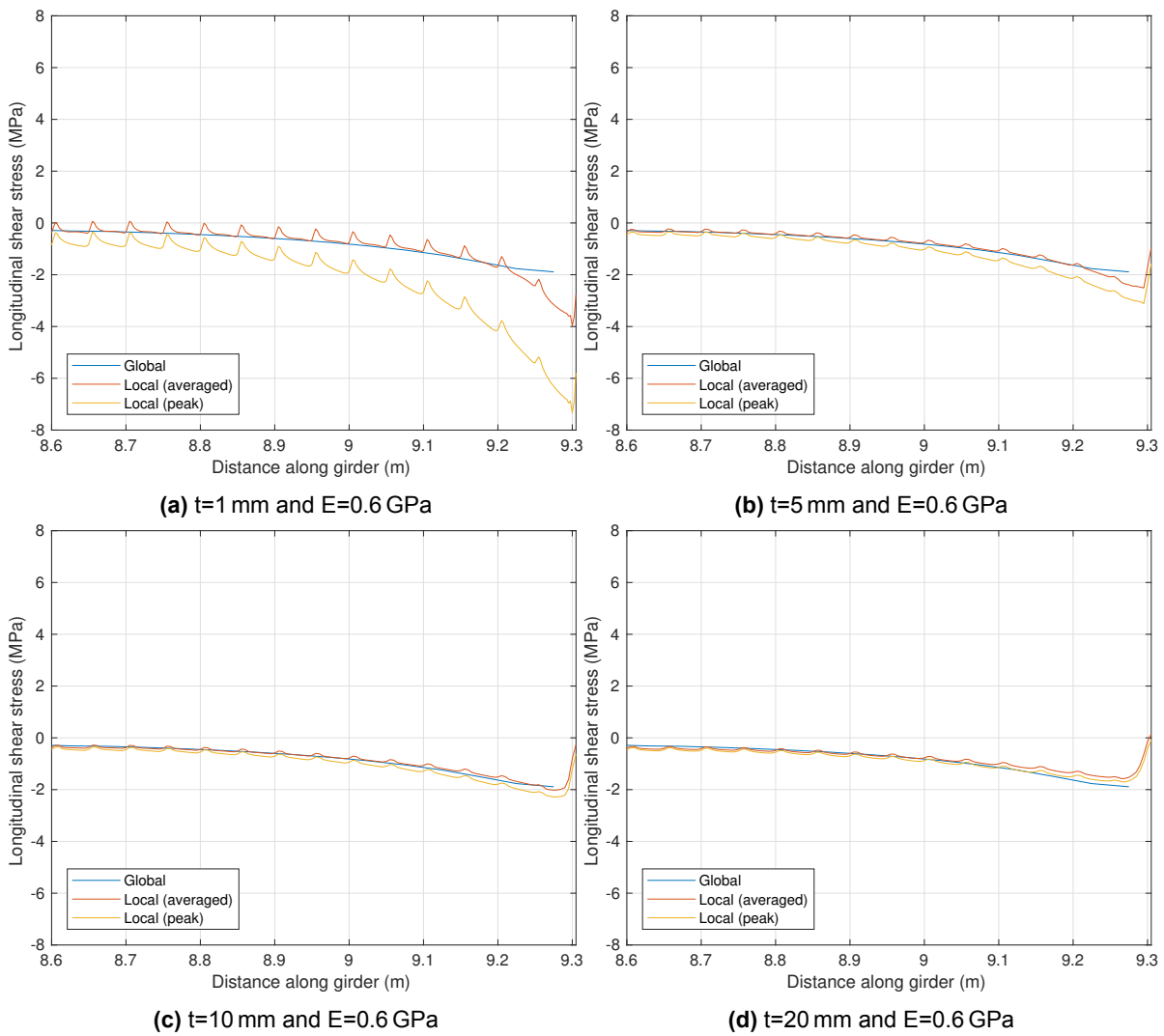


Figure A.4: Longitudinal shear stresses in longitudinal direction for different adhesive thickness under thermal loading

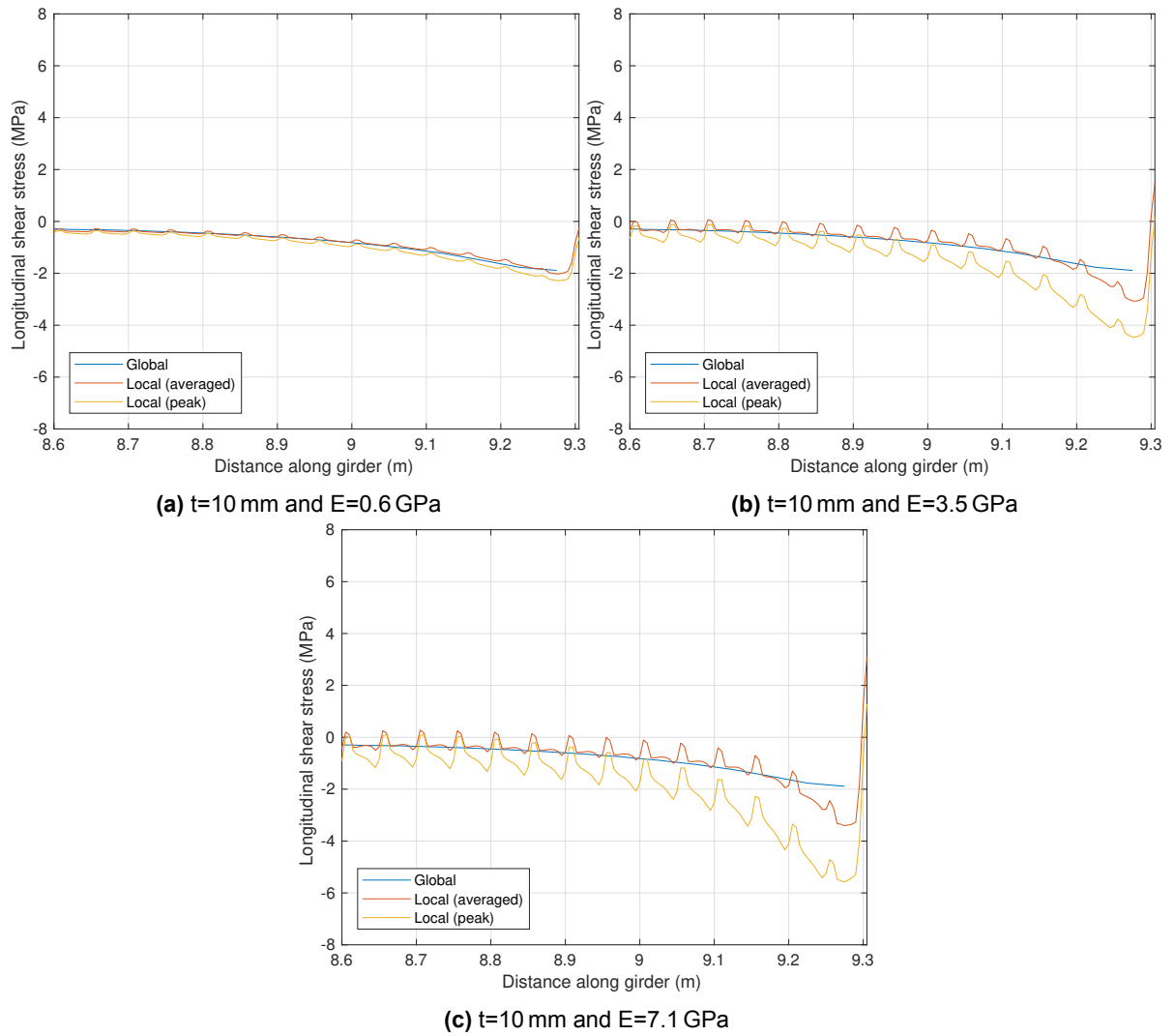


Figure A.5: Longitudinal shear stresses in longitudinal direction for different adhesive elastic modulus under thermal loading

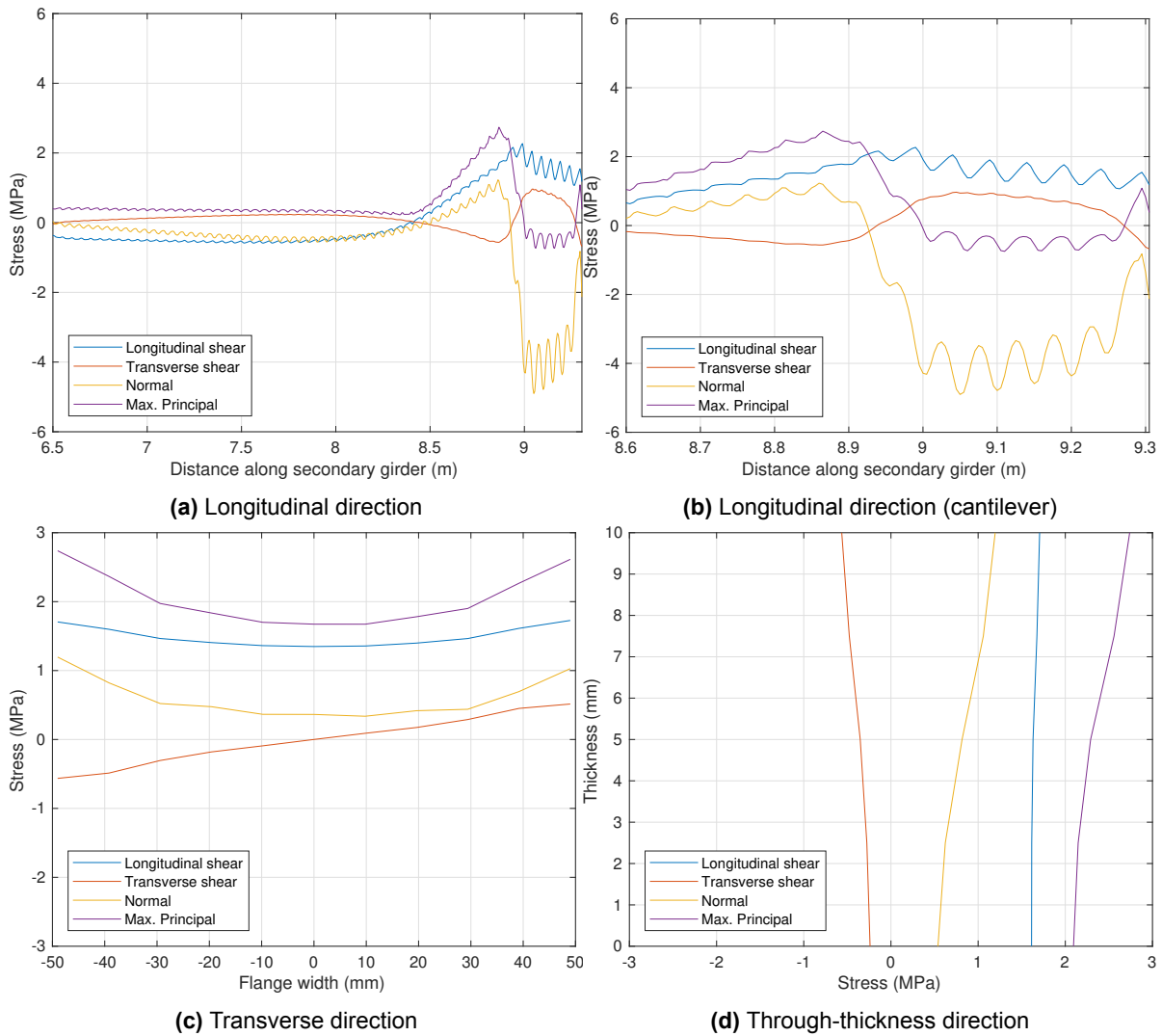


Figure A.6: Stress state in adhesive layer between secondary girder and FRP deck second to the main girder under traffic loading

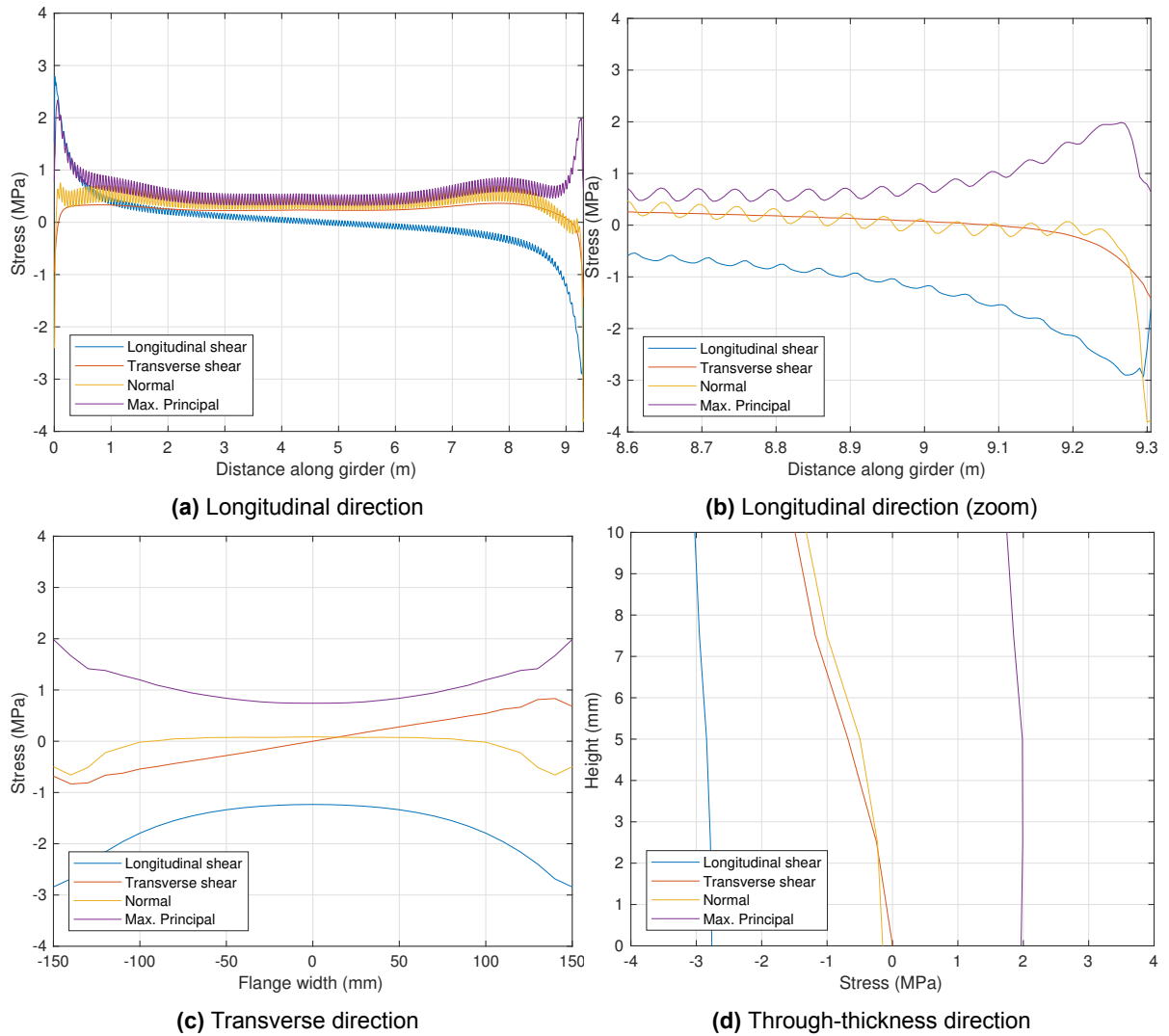


Figure A.7: Stress state in adhesive layer between main girder and deck under thermal loading

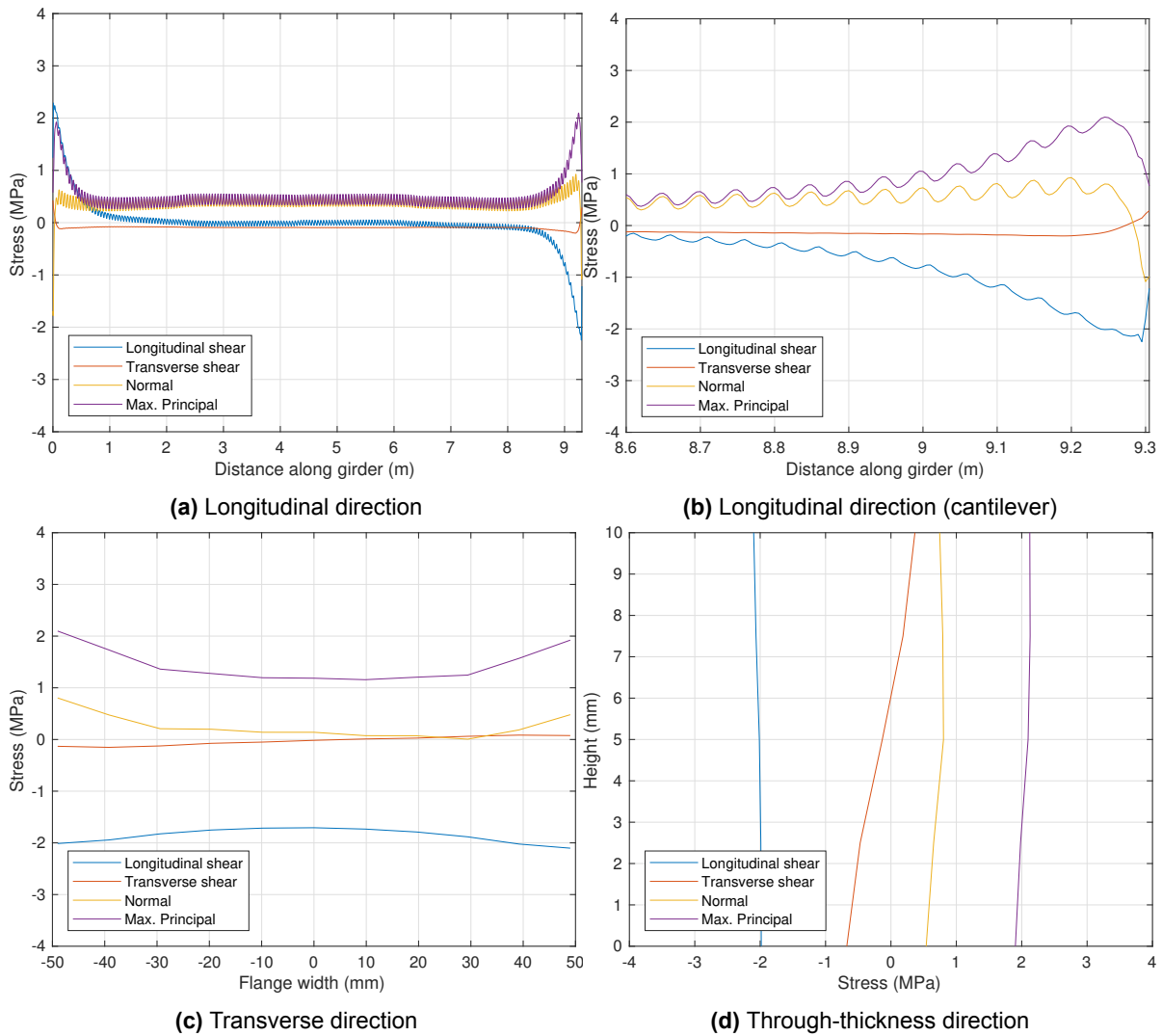


Figure A.8: Stress state in adhesive layer between secondary girder and deck adjacent to the main girder under thermal loading

Bibliography

- [1] Abaqus 6.14 documentation, 2014. URL <http://ivt-abaqusdoc.ivt.ntnu.no:2080/v6.14/books/usi/default.htm>.
- [2] Kwekersbrug, 2017. URL https://deskgram.org/p/1504987829817505663_1445028526.
- [3] Scia engineer composite design steel-concrete composite structures, 2017. URL https://help.scia.net/download/17.0/en/CompositeDesign_enu.pdf.
- [4] Scigrip technical datasheet sg230 hv methacrylate adhesive, 2017. URL <https://scigrip.com/assets/tds/SG230HV-TDS-US-0417.pdf>.
- [5] F. Csillag. Demountable deck-to-girder connection of frp-steel hybrid bridges. Master's thesis, Delft University of Technology, 2018.
- [6] Lucas F.M. da Silva et al. Analytical models of adhesively bonded joints-part 1: Literature survey. *International Journal of Adhesion Adhesives*, 2008.
- [7] Lucas F.M. da Silva et al. Analytical models of adhesively bonded joints-part 2: Comparative study. *International Journal of Adhesion Adhesives*, 2008.
- [8] H.W. Gürtler. *Composite Action of FRP Bridge Decks Adhesively Bonded to Steel Main Girder*. PhD thesis, ÉCOLE POLYTECHNIQUE FÉDÉRALE DE LAUSANNE, December 2004.
- [9] M. Heshmati. *Durability and Long-term Performance of Adhesively Bonded FRP/steel Joints*. PhD thesis, Chalmers University of Technology, 2017.
- [10] X. Jiang. *Mechanical Behaviour and Durability of FRP-to-steel Adhesively-bonded Joints*. PhD thesis, Delft University of Technology, 2013.
- [11] T. Keller and T. Tirelli. Fatigue behavior of adhesively connected pultruded gfrp profiles. *Composite Structures* 65, 2004.
- [12] R. Sarfaraz Khabbaz. *Fatigue Life Prediction of Adhesively-Bonded Fiber-Reinforced Polymer Structural Joints under Spectrum Loading Patterns*. PhD thesis, ÉCOLE POLYTECHNIQUE FÉDÉRALE DE LAUSANNE, December 2012.
- [13] Roy Aries P. Tarigan Kuncoro Diharjo, Miftahul Anwar and Ahmad Rivai. *Effect of Adhesive Thickness and Surface Treatment to Shear Strength on Single Lap Joint AL/CFRP Using Adhesive of Epoxy/Al-fine-powder*. PhD thesis, Sebelas Maret University, Indonesia, 2016.
- [14] M. Schollmayer. *Through-Thickness Performance of Adhesive Connections Between FRP Bridge Decks and Steel Main Girders*. PhD thesis, ÉCOLE POLYTECHNIQUE FÉDÉRALE DE LAUSANNE, February 2009.
- [15] A.P. Vassilopoulos and T. Keller. *Fatigue of Fiber-reinforced Composites*. Springer, 2011.
- [16] Y. Zhang. *Fracture and Fatigue of Adhesively-Bonded Fiber-Reinforced Polymer Structural Joints*. PhD thesis, ÉCOLE POLYTECHNIQUE FÉDÉRALE DE LAUSANNE, April 2010.